New Therapeutic Approaches for Cell Growth Inhibition of Acute Myeloid & Lymphoblastic Leukemia

Dissertation

der Mathematisch-Naturwissenschaftlichen Fakultät
der Eberhard Karls Universität Tübingen
zur Erlangung des Grades eines
Doktors der Naturwissenschaften
(Dr. rer. nat.)

vorgelegt von
Ann-Christin Krahl
aus Mühlacker

Tübingen
2018

Gedruckt mit Genehmigung der Mathematisch-Naturwissenschaftlichen Fakultät der Eberhard Karls Universität Tübingen.

Tag der mündlichen Qualifikation:	28.01.2019
Dekan:	Prof. Dr. Wolfgang Rosenstiel
1. Berichterstatter:	Prof. Dr. Rupert Handgretinger
2. Berichterstatter:	Prof. Dr. Hans-Georg Rammensee

“Well, Mortimer, for a gallon of elderberry wine, I take a teaspoonful of arsenic,

and add a half-teaspoon of strychnine, and then just a pinch of cyanide.”

Aunt Martha from the famous play ‘Arsenic and Old Lace’,

written by Joseph Kesselring, 1941

TABLE OF CONTENTS

TABLE OF FIGURES

LIST OF TABLES

1. SUMMARIES

1.1 Summary

Leukemia is a severe blood cell malignancy which is characterized by a high number of abnormal immature white blood cells, so-called leukemic blasts. Starting from the bone marrow, the infiltration into several organs like spleen, liver and lymph nodes leads to severe bleeding problems due to disseminated intravascular coagulation and thrombocytopenia as well as to increased risk of infections due to a lack of mature blood cells. Despite enormous improvement in cancer cell therapy, especially in targeted therapy strategies over the last decades, the two subtypes acute myeloid (AML) and acute lymphoblastic leukemia (ALL) are still life-threatening diseases for children and adults. Therefore, new therapeutic approaches for AML and ALL are urgently needed. The goal of the study is to establish a pharmacological-based therapy for AML and a CAR T cell-based approach for ALL.

Since successful therapeutic approaches for AML are still limited due to the high heterogeneity of AML subtypes, in the present study the combination of arsenic trioxide (ATO) and granulocyte-colony stimulating factor (G-CSF) was considered as a potential new pharmacological therapeutic approach for AML. The *in vitro* studies and the *in vivo* observations in a xenotransplantation mouse model shown in this study demonstrated that the combination of ATO and G-CSF has a synergistic anti-leukemic effect on AML cells potentially via a G-CSF-mediated upregulation of the main ATO transporter AQP9. Even G-CSF as a single agent displayed an anti-leukemic effectiveness *in vivo* rendering G-CSF to an important adjuvant in future AML therapy.

Despite the massive progress in targeted ALL therapy by introduction of chimeric antigen receptor (CAR) T cell therapy, severe therapy-associated complications like cytokine release syndrome and ‘on target off tumor’ toxicities demand further optimization of CAR T cell therapy. For that, bispecific CAR T cells as well as universal adapter anti-biotin CAR T cells are promising tools and need to be validated for their efficacy and specificity in leukemia therapy. Both methods were tested in this study and demonstrated good effectiveness in killing B cell-ALLs *in vitro* and *in vivo*. Bispecific CAR T cells seem to be a good approach to prevent specific escape strategies of leukemic blasts during therapy like antigen loss, while the modularity of the adapter anti-biotin CAR T cells allows to target any antigen which is accessible to a biotinylated antibody. Therefore, adapter CAR T cells might be the future method of choice for targeting a wide range of tumors.

In conclusion, two therapeutic approaches for two types of acute leukemia resulted in a therapeutic success. The high heterogeneity among acute leukemia requires a development of a wide spectrum of treatment possibilities.

1.2. Zusammenfassung

Leukämie ist eine ernsthafte Erkrankung des blutbildenden Systems und zeichnet sich durch eine hohe Anzahl an abnormalen, unreifen weißen Blutzellen aus, die sogenannten leukämischen Blasten. Ausgehend vom Knochenmark infiltrieren sie mehrere Organe wie Milz, Leber und Lymphknoten. Dies führt zu einer Verdrängung der gesunden Zellen und folglich zu einer erhöhten Blutungsneigung, sowie Infektionen aufgrund eines Mangels an ausgereiften und funktionellen Blutzellen. Die letzten Jahrzehnte brachten große Fortschritte in der Krebszelltherapie, vor allem bei gezielten Immuntherapien. Dennoch stellen die Formen der akuten myeloischen (AML) und akuten lymphoblastischen Leukämie (ALL) immer noch eine lebensbedrohliche Krankheit für Kinder und Erwachsene dar. Deshalb sind neue Therapieansätze von hoher Dringlichkeit. Das Ziel dieser Studie ist es, eine pharmakologisch-basierte Therapie für AML und ein CAR-T-Zell-basierter Ansatz für ALL zu etablieren.

Da aufgrund starker Heterogenität innerhalb der AML-Untergruppen Therapierfolge begrenzt sind, sollte in dieser vorliegenden Arbeit die Kombination aus Arsentrioxid (ATO) und dem Granulozyten-Kolonie-stimulierende Faktor (engl. ‘granulocyte-colony stimulating factor‘, G-CSF) als möglicher neuer pharmakologischer Therapieansatz für die AML getestet werden. Sowohl die *In-vitro*- als auch die mithilfe eines Xenotransplantation-Mausmodells generierten *In-vivo*-Ergebnisse demonstrierten, dass die Kombination aus ATO und G-CSF eine synergistisch anti-leukämische Wirkung auf die AML-Zellen ausübt, womöglich über eine G-CSF-vermittelte Hochregulierung des primären ATO-Transporters AQP9. Selbst G-CSF als Einzelmedikament zeigte dabei eine anti-leukämische Wirkung *in vivo*. Daher liegt es nahe, dass G-CSF in zukünftigen Therapieansätzen der AML eine wichtige Rolle spielen könnte.

Trotz großer Verbesserungen in der ALL-Immuntherapie durch die Einführung der ’Chimeric Antigen Receptor’ (CAR)-T-Zell-Therapie, kommt es zu schweren Therapie-assoziierten Komplikationen wie das ‘Cytokine Release Syndrome‘ und die ‘On-Target-Off-Tumor’-Toxizität, die eine weiterführende Optimierung der CAR-T-Zell-Therapie bedürfen. Hierfür stellen die bispezifischen und universalen Adapter-CAR-T-Zellen vielversprechende Werkzeuge dar, die jedoch noch auf ihre Effektivität und Spezifität in der Leukämie-Therapie untersucht werden müssen. Beide in der vorliegenden Arbeit getesteten Methoden bewiesen eine effiziente Wirksamkeit beim Abtöten von B-Zell-Leukämien *in vitro* und *in vivo*. Bispezifische CAR-T-Zellen stellen einen guten Ansatz dar, um spezifische Fluchtstrategien von leukämischen Blasten, wie zum Beispiel der Verlust von Antigenen, während der Therapie zu verhindern. Die Modularität der Adapter-anti-Biotin-CAR-T-Zellen ermöglicht es hingegen, jedes Antigen anzugehen, das für einen biotinylierten Antikörper zugänglich ist.

Daher könnten die Adapter-CAR-T-Zellen die Methode der Wahl sein, um zukünftig verschiedenartige Tumore zu behandeln.
Abschließend lässt sich sagen, dass die Behandlung von AML und ALL anhand zwei gänzlich verschiedener therapeutischer Ansätze zu einem Erfolg führte. Die Heterogenität unter den akuten Leukämien ist hoch und fordert daher die Entwicklung eines breiten Behandlungsspektrums.

2. INTRODUCTION

2.1 Leukemia

Cancer is one of the foremost causes of morbidity and mortality worldwide. The number of new cases is expected to increase in the next decades due to a higher life expectancy (Jemal *et al.*, 2011; WHO, 2017). Leukemia represents 3.7% of all new cancer cases in the United States and it is the seventh most common cancer leading to death. In the year 2017, 62.130 people developed leukemia with 24.500 fatal cases (NIH, 2017). In Germany, 13.700 new cases of leukemia were registered in 2014, 7.743 with fatal outcome (Robert Koch-Institut, 2014). Leukemia is a severe blood cell malignancy which is characterized by a high number of abnormal immature white blood cells. Starting from the bone marrow, the so-called leukemic blasts eliminate the healthy blood cells and infiltrate into spleen, liver and lymph nodes leading to an impairment of the intruded organs. This blood formation disorder results in anemia, bleeding problems and increased risk of infections due to a lack of mature blood cells. As known for cancer in general, the disease pathogenesis is based on chromosomal aberrations and gene mutations. However, the exact trigger of leukemia initiation is unknown, but both inherited and environmental factors are believed to be involved, including smoking, ionizing radiation and some chemicals as well as prior chemotherapy (Radivoyevitch *et al.*, 2015). Also an abnormal immune response to (viral) infections is supposed to be an important causal factor in developing leukemia (Greaves, 2006). There are four main types of leukemia which are divided by their form (acute versus chronic) and derivation (lymphoblastic versus myeloid lineage) of the disease: acute lymphoblastic leukemia (ALL), acute myeloid leukemia (AML), chronic lymphoblastic leukemia (CLL) and chronic myeloid leukemia (CML) (Hunger and Mullighan, 2015; De Kouchkovsky and Abdul-Hay, 2016). Chronic leukemia is characterized by slowly growing abnormal white blood cells and due to improved targeted therapies their prognosis is quite good (Nowell, 2007; National Cancer Institute, 2013; Mahon, 2015). Whereas the acute leukemia exhibit a rapid expansion of immature aberrant cells and eventually result in an early death if left untreated (Roboz, 2012). Therefore, new therapeutic strategies should particularly focus on the acute forms of leukemia, which will be the pivot of this work.

2.2 The concept of the leukemic stem cell

The initiation of leukemia formation, also known as leukemogenesis, is based on an aberrant hematopoiesis. In this process, hematopoietic stem cells (HSCs) are differentiated into manifold mature blood cells. HSCs are located in the bone marrow and embedded within a

complex regulatory unit called the bone marrow niche, which includes vascular endothelial cells, mesenchymal stromal progenitor cells and a range of mature hematopoietic cells such as macrophages, neutrophils and megakaryocytes. HSCs are characterized by their self-renewal ability and are normally quiescent, spending most of the time in the G0 phase of the cell cycle (Dean *et al.*, 2005; Birbrair and Frenette, 2016; Tay *et al.*, 2017). They can be separated into a long-term subset (LT-HSC), capable of unlimited self-renewal and sustainment of the stem cell pool, and a short-term subset (ST-HSC), which has a limited time to self-renew and undergoes differentiation to produce mature hematopoietic cells (Passegué *et al.*, 2003; Challen *et al.*, 2010). An important marker to characterize and identify HSCs is their drug-transporting capacity which is mediated by membrane-bound transport proteins termed ATP-binding cassette (ABC) transporters. High expression levels of ABC transporters, e.g. ABCB1, ABCG2 and ABCC1, are responsible for an ATP-dependent efflux of drugs or dyes and therefore important for the multidrug resistance ability of HSCs (Goodell *et al.*, 1996; Wulf *et al.*, 2001). Most cells cannot extrude a fluorescent dye like Hoechst 33342 or rhodamine 123, but stem cells can actively do it. Hence, they show a low level of fluorescent dye in fluorescence-activated cell sorting (FACS) analysis and reside in the so-called ‘side population’ (SP) (Goodell *et al.*, 1996; Passegué *et al.*, 2003; de Jonge-Peeters *et al.*, 2007). The drug resistance and an active DNA-repair capacity are basic requirements for a long lifespan of HSCs (Dean *et al.*, 2005).

HSCs are constantly exposed to stress and carcinogens, which can cause DNA damage leading to an accumulation of mutations and over the time to malignant transformation (Welch *et al.*, 2012; Schepers *et al.*, 2015). These transformed malignant HCSs retain many characteristics of normal HSCs, like self-renewal, niche dependence and differentiation to mature but dysregulated clonogenic progenitor cells, and behave as disease-initiating leukemic stem cells (LSCs) (Passegué *et al.*, 2003; Schepers *et al.*, 2015). Based on this model, the concept of a LSC that initiates leukemia has been proposed (FIGURE 1). J. Dick and colleagues showed that LCSs can initiate and serially propagate diseases upon transplantation into immune-deficient mice, thereby recreating the primary malignancy with its full heterogeneity. In terms of AML, they thought that only cells with an immature phenotype, characterized by cluster of differentiation (CD) markers $CD34^+CD38^-$, were capable to expand the disease in the recipient mice, not mature $CD34^+CD38^+$ cells. However, new studies elucidated that LSCs are no longer restricted to the HSC compartment and can also emerge from transformed progenitors (Bonnet and Dick, 1997; Cozzio *et al.*, 2003; Passegué *et al.*, 2003; Eppert *et al.*, 2011; Schepers *et al.*, 2015). It was also shown for ALL that both immature $CD34^+CD19^-$ and mature $CD34^-CD19^+$ cells can repopulate and propagate the leukemia in immune-deficient mice (Bomken *et al.*, 2010). As well as normal

HSCs, LSCs are naturally resistant to chemotherapy agents through an ABC-transporter-mediated efflux of drugs. In addition, LSCs can also acquire drug resistance by genetic changes for example mutations or overexpression of drug targets before or after chemotherapy (Dean *et al.*, 2005). Therefore, LSCs have different properties than the bulk leukemic population and are most responsible for relapse after therapy. Because of the genetic diversity of LSCs, therapy options targeting LSCs as well as the therapeutic success are limited. Treatment approaches are often very specific and target only definite properties of LSC clones, such as ABC transporters, mutations in embryonic stem cell signaling or tissue differentiation pathways, for example the Hedgehog, Notch or wingless-related integration site (Wnt) signaling. Even the inhibition of antigens that are strongly expressed on LSCs, like CD123, CLL-1, CD44, CD47 or c-Kit, targets only a small portion of LSCs (Dean *et al.*, 2005; Van Rhenen *et al.*, 2007; Pollyea *et al.*, 2014; Schepers *et al.*, 2015). To overcome these limitations, new strategies should be proposed and pursued like testing drug response of genetically diverse LSCs (Pollyea *et al.*, 2014; Shlush *et al.*, 2017).

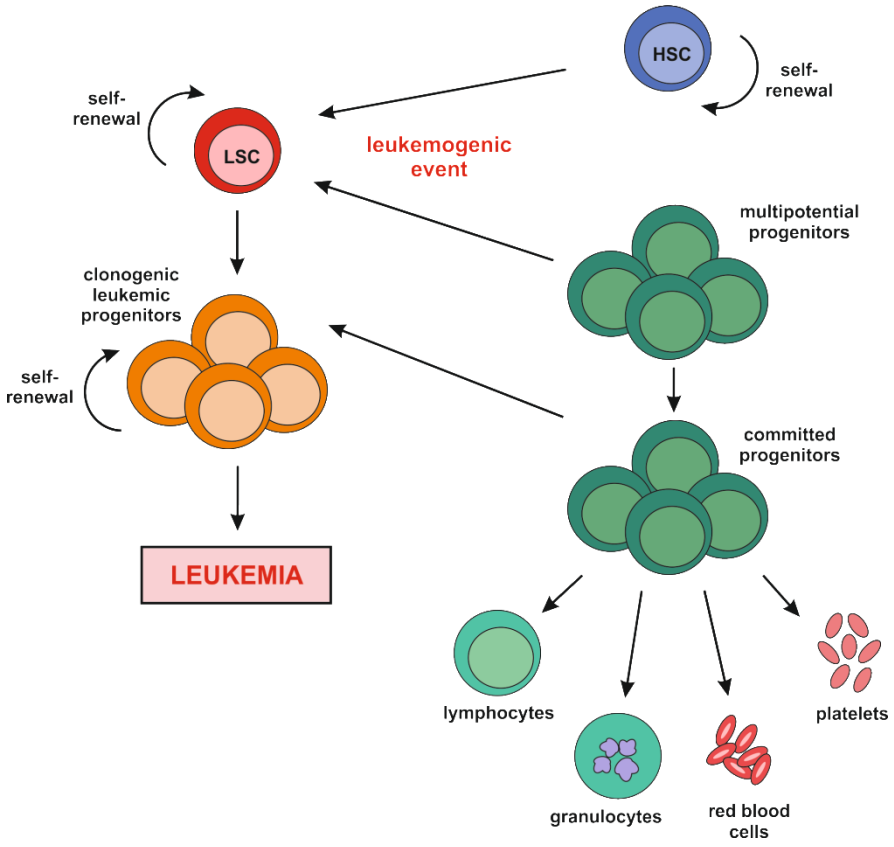

Figure 1: The concept of the leukemia initiating stem cell.

Leukemogenic mutations may occur within long-term hematopoietic stem cells (HSC) or in multipotential/ committed downstream progenitors giving rise to a pre-leukemia state with unlimited self-renewal. As a hierarchical structure the leukemic stem cell (LSC) at the apex produces both the clonogenic leukemic progenitors and the non-clonogenic blast cells, which built up the bulk of the leukemia. Figure based on Huntly and Gilliland, 2005; Lane and Gilliland, 2010.

2.3 Acute myeloid leukemia

The acute myeloid form of leukemia is characterized by an impaired myeloid differentiation and accumulation of malignant immature progenitor cells of the myeloid origin in the bone marrow. The diversity of progenitor cells that are susceptible to malignant transformation leads to a high heterogeneity among AMLs (Fernandes *et al.*, 2014). The concept of the leukemia initiating stem cell was primarily investigated and well characterized in AML. LSCs are able to initiate, maintain and serially propagate leukemia *in vivo* while they keep their capacity to produce both the clonogenic leukemic progenitors and the non-clonogenic blast cells which constitute the bulk of the leukemia (Huntly and Gilliland, 2005; Lane and Gilliland, 2010). AML is the most common acute leukemia in adults with a poor outcome and median age of 66 years at diagnosis. Even less than 10% of elderly patients can be cured. The outcome for younger patients are more favorable, but still two-thirds of them die from relapse (Roboz, 2012; Pollyea *et al.*, 2014). There are several differences in childhood and adult AML in terms of incidence, cytogenetic pattern and molecular aberrations. The majority of childhood AML occurs *de novo*, while AML in adults develops often from antecedent myeloid disorders such as myelodysplastic syndromes (MDS) (de Rooij *et al.*, 2015). Also, a higher frequency of cytogenetic abnormalities creating fusion genes (for example RUNX1-RUNX1T1 and NUP98-NSD1) or specific chromosomal translocations (for example t(1;22)(p13;q13)/RBM15-MKL1, t(7;12)(q36;p13)/ETV6-MNX1 and t(11;12)(p15;p13)/NUP98-KDM5A) distinguish childhood from adult AML. In adult AML, many patients have a normal karyotype with increasing numbers of driver mutations in the RUNX1, TP53, IDH1/2 and NPM1 genes. These distinctions between adult and childhood AML imply an age-dependent difference in pathogenesis (de Rooij *et al.*, 2015; Laing *et al.*, 2017).
Further, an unexplained high risk of AML has been found in families who inherited driver mutations like TP53, GATA2, RUNX1 and CEBPA suggesting a familial predisposition to develop AML or MDS/AML (Owen *et al.*, 2008; de Rooij *et al.*, 2015). Also several congenital conditions increase the risk of developing leukemia like Down-syndrome or congenital and cycling neutropenia (Zwaan *et al.*, 2010; Klimiankou *et al.*, 2016).

2.3.1 Classification of AML

Two of the main systems that have been used to classify AML into subtypes are the French-American-British (FAB) and the World Health Organization (WHO) classification. The basic FAB classification system relies on cytomorphological and cytochemical studies and defines eight subtypes (FAB M0 through M7). The modern WHO classification systems are based on cytomorphology, cytochemistry, immunophenotyping, immunogenetics and molecular cytogenetics, hence, combining the earlier classification methods with the newer ones

(Segeren and Van 't Veer, 1996; Szczepański *et al.*, 2003). The WHO classification defines six major disease entities which are listed with genetic abnormalities (if present) in TABLE 1 (Segeren and Van 't Veer, 1996; Vardiman *et al.*, 2009; De Kouchkovsky and Abdul-Hay, 2016). Knowing the subtype of AML is important for the therapeutic approach and prognosis of the patients.

Table 1: Classification of AML.

TYPES	**FURTHER DESCRIPTION**
AML with recurrent genetic abnormalities	- AML with t(8:21)(q22;q22); RUNX1-RUNX1T1 - AML with inv(16)(p13.1q22) or t(16;16)(p13.1;q22); CBFB-MYH11 - APL with PML-RARα (**FAB M3**) - AML with t(9;11)(p21.3;q23.3); MLLT3-KMT2 - AML with t(6;9)(p23;q34.1); DEK-NUP214 - AML with inv(3)(q21.3q26.2) or t(3;3)(q21.3;q26.2); GATA2, MECOM - AML (megakaryoblastic) with t(1;22)(p13.3;q13.3); RBM15-MKL1 - AML with BCR-ABL1 (provisional entity) - AML with mutated NPM1 - AML with biallelic mutations of CEBPA - AML with mutated RUNX1 (provisional entity)
AML with myelodysplasia-related changes	n/a
Therapy-related myeloid neoplasms	n/a
AML, not otherwise specified	- AML with minimal differentiation (**FAB M0**) - AML without maturation (**FAB M1**) - AML with maturation (**FAB M2**) - Acute myelomonocytic leukemia (**FAB M4**) - Acute monoblastic/monocytic leukemia (**FAB M5**) - Acute erythroid leukemia (**FAB M6**) - Acute megakaryoblastic leukemia (**FAB M7**)
Myeloid sarcoma	n/a

Myeloid proliferation related to Down syndrome	- Transient abnormal myelopoiesis - AML associated with Down syndrome

2.3.2 Standard and alternative therapies for AML

A first-line treatment of AML is the induction chemotherapy, a combination of the cytostatic agents anthracycline, such as daunorubicin, which intercalates into DNA/RNA and inhibits the topoisomerase II enzyme, and a high dose of cytarabine, also known as cytosine arabinoside (Ara-C), which acts as a nucleoside analogue. The treatment with both agents impairs the replication of the rapidly growing tumor cells leading to cell cycle and cell growth arrest (Ellison *et al.*, 1968; Minotti, 2004; van Dalen *et al.*, 2014). The induction chemotherapy is followed by either a consolidation chemotherapy or allogeneic hematopoietic stem cell transplantation (HSCT), depending on the treatment outcome of chemotherapy alone. So far, HSCT remains the most successful therapy for prevention of relapse in non-favorable risk AML and in young AML patients. However, relapse after allogeneic HSCT does occur. Moreover, the vast majority of elderly patients are not even qualified for HSCT or cannot tolerate the high toxicity of the standard therapy scheme (Roboz, 2012; Fernandes *et al.*, 2014; Lichtenegger *et al.*, 2017). Aside from age, the classification of AML in different prognostic-risk groups based on cytogenetic and molecular profile also help to predict the susceptibility and outcome of the standard therapy (Roboz, 2012; De Kouchkovsky and Abdul-Hay, 2016). Because of the very poor prognosis of patients which are not eligible for the intensive standard therapy as well as patients with relapsed or refractory disease, new innovative therapeutic approaches are urgently needed, especially targeted therapeutics which specifically target leukemic cells and minimize off-target effects. For that, many immunotherapy approaches have been developed using monoclonal antibody (mAb) conjugates, T cell-recruiting antibody constructs or reprogrammed T cells (Tettamanti *et al.*, 2013).

Since conventional, unconjugated mAbs are not efficient enough to eradicate the disease, the fragment crystallizable (Fc) part of mAbs were conjugated with cytotoxic drugs or toxins to induce DNA damage or cell cycle arrest in tumor cells. A common target antigen for mAb-conjugate therapy is CD33, a transmembrane cell surface receptor expressed on cells from myeloid lineage, but also on some lymphoid cells. CD33 is expressed with a high density on AML cells and LSCs (Hamann *et al.*, 2002; Lichtenegger *et al.*, 2017). The first antibody-drug conjugate was Gemtuzumab Ozogamicin (GO, Mylotarg®), an anti-CD33 antibody linked with the antitumor antibiotic calicheamicin (Bernstein, 2000). In the year 2000, the Food and Drug Administration (FDA) approved GO as a promising mAb conjugate. However, ten years

later, GO was voluntarily withdrawn from the market because it did not prolong the survival and increased the rate of early death (Petersdorf *et al.*, 2013). A common problem of mAb conjugates may be their limited effect on resting, low proliferative cells or quiescent LSCs that may express CD33 at low levels (Walter *et al.*, 2012; Krupka *et al.*, 2014). Nevertheless, different clinical trials with relapsed or untreated AML patients have been performed in the last years to evaluate the benefit of adding GO in low doses to chemotherapy. Their results suggested an improvement in survival with GO in selected patients (Burnett *et al.*, 2011; Castaigne *et al.*, 2012; Walter *et al.*, 2014).

Another immunotherapeutic approach for AML is a T cell-recruiting antibody construct, composed of two single-chain variable fragments (scFv) of two antibodies with different specificities connected by a short peptide linker. This bispecific antibody simultaneous binds a tumor-associated antigen and CD3ε in the T cell receptor (TCR) complex leading to activation and expansion of cytotoxic T cells for cancer cell lysis without the requirement of co-stimulatory signals (Baeuerle and Reinhardt, 2009). A bispecific antibody for AML is AMG 330, which recognizes CD33 as a tumor-associated antigen. Preclinical studies have shown that AMG 330 is effective against CD33-expressing blasts even in extremely low doses or at a low effector-to-target (E:T) cell ratio. Besides, it has been demonstrated *in vitro* that both AMG 330's activity and cytotoxicity are increased proportionally to the expression level of CD33 and are not altered by drug efflux capability of ABC transporters. However, the use of bispecific antibodies leads to a strong T cell activation and production of proinflammatory cytokines, which might trigger tumor cells to escape the antibody-mediated tumor cell lysis by immunosuppressive strategies. Clinical trials are now in progress to investigate the safety and efficacy of AMG 330 in patients with AML (Krupka *et al.*, 2014; Laszlo *et al.*, 2014; Harrington *et al.*, 2015; Laing *et al.*, 2017).

It is reported that some AML patients have $CD34^{+}CD33^{-}$ LSCs, hence, targeting CD33 antigen alone would not be effective enough for all the heterogeneous AML subtypes. CD123, an often targeted LSC antigen, or CD135 (FLT-3), the most frequently acquired alterations identified in AML, are additional targets for novel immunotherapeutic approaches (Walter *et al.*, 2012; Tettamanti *et al.*, 2013).

A novel highly promising approach for targeted immunotherapy of cancer are chimeric antigen receptor (CAR) T cells. CAR T cells are engineered T cells consisting of extracellular tumor antigen-recognition domains, most commonly antibody-derived scFvs, linked through a transmembrane domain to T cell-triggering intracellular domains. This enables both a major histocompatibility complex (MHC) independent antigen binding and a highly potent cytotoxic effector cell function. Hence, recognition of an antigen leads to T cell activation, expansion and resultant cancer cell death (Barrett *et al.*, 2015; June *et al.*, 2015). The major advantage of CAR T cells is their ability to target any molecule which is accessible to an antibody-like

recognition (paragraph 2.4.3). To date, several antigens for AML CAR T cell therapy are under preclinical investigation. CD33 and CD123 are the most prominent ones showing an efficient lysis of AML blasts in xenotransplanted NSG mice (Mardiros *et al.*, 2013; O'Hear *et al.*, 2015; Lichtenegger *et al.*, 2017). However, significant 'on-target off-leukemia' toxicity with reduction of myeloid lineage and hematopoietic stem cells was observed. To circumvent this myelotoxicity, new strategies have been followed such as a transient CD33-CAR expression (Kenderian *et al.*, 2015) or a new engineered anti-CD123 CAR T cell receptor, using V_H and V_L chains derived from different CD123-specific mAbs (Thokala *et al.*, 2016), showing reduced lysis of normal hematopoietic stem cells.

In addition to the other immunotherapeutic approaches described so far, mAbs against checkpoint molecules has also been proven to be a highly effective tool in cancer immunotherapy. In normal cells, cell cycle checkpoint kinases act as tumor suppressors and are crucial for the maintenance of genetic stability. In cancer, however, they have been found to protect tumor cells from different stresses and, consequently, to promote tumor progression. MAbs against these checkpoint molecules were primarily confirmed for solid tumors but they are also in the ascendant for hematologic malignancies (R. Berger *et al.*, 2008; Alatrash *et al.*, 2016). Currently ongoing clinical trials are studying the effect of the most prominent checkpoint inhibitors, programmed cell death 1 (PD-1) and cytotoxic T lymphocyte-associated antigen 4 (CTLA-4), as a monotherapy for various malignancies including AML. Furthermore, the combination of checkpoint inhibitors with hypomethylating agents (Yang *et al.*, 2014), such as azacytidine and guadecitabine - which are in combination with low-dose Ara-C good alternatives for AML patients who are ineligible for conventional cytotoxic induction chemotherapy (Stein and Tallman, 2016) -, or with the bispecific antibody AMG 330 showed an increased tumor cell lysis compared to the agents alone, encouraging future studies to test combinatorial treatments (Krupka *et al.*, 2016).

Many potential drugs for AML therapy targeting mutant or overexpressed driver proteins, for example mutant Fms-related typrosine kinase 3 (FLT3) and isocitrate dehydrogenase (IDH), or upregulated polo-like kinase 1 (PLK1) were developed. FLT3 is expressed on hematopoietic progenitors and on most leukemic myeloblasts. An internal tandem duplication of FLT3 (FLT3-ITD) is found in approximately 30% of patients with *de novo* AML and is associated with a poor prognosis (Kottaridis *et al.*, 2001; Fröhling *et al.*, 2002). The contribution of FLT3-ITD to the pathogenesis of leukemia is generally thought to be due to a gain-of-function of the FLT3 receptor, leading to a ligand-independent auto-phosphorylation and constitutive activation of the receptor (Lagunas-Rangel and Chávez-Valencia, 2017). Several FLT3 inhibitors were developed and some of them, such as midostaurin, quizartinib and crenolanib, are currently under clinical trial. Mutations in IDH1 (protein is localized in the

cytoplasm) and IDH2 (protein is predominantly located in the mitochondria) are found in 5% and 10% of adult AML patients, respectively. The wild type function of IDH enzymes of catalyzing the conversion of isocitrate to α-ketoglutarate is altered to a conversion of α-ketoglutarate into β-hydroxyglutarate in AML patients with IDH mutations. This causes a hypermethylation of target genes and consequently an impaired myeloid differentiation (Figueroa *et al.*, 2010; Richarson *et al.*, 2016). First results of currently ongoing clinical trials with inhibitors of mutant IDH1 and IDH2 have shown an encouraging efficacy and a low toxicity in patients with relapsed AML (Stein *et al.*, 2014). PLKs are a family of five conserved serine/threonine kinases which are important for many processes involved in cell cycle control, DNA replication and in stress response to DNA damage checkpoint regulation. Inhibition of the overexpressed PLK1 leads to a disorganized spindle assembly and cellular apoptosis of AML cells (Gjertsen and Schöffski, 2015). Clinical studies with the PLK1 inhibitor volasertib in combination with low-dose Ara-C showed promising results for treating patients with relapsed/refractory or previously untreated AML, who were considered to be unsuitable for intensive conventional therapy (Döhner *et al.*, 2014).

In general, the agents of the so-called targeted therapy have a limited efficacy as single drugs. However, they do demonstrate biologic activity with a tolerable toxicity making them attractive for combination with other agents for newly diagnosed and relapsed/refractory AML patients ineligible for conventional chemotherapy.

2.3.3 New therapeutic approaches for AML

2.3.3.1 Arsenic trioxide

Arsenic is a naturally occurring substance and one of the oldest drugs, in both Western and traditional Chinese medicine used for treatment of periodic fever, chronic myelogenous leukemia and other diseases (Haller, 1975; Zhu *et al.*, 2002). Arsenic trioxide (ATO) is an inorganic form of arsenic. Its modern history started in the 1970s with studies in China which demonstrated its efficiency as a therapeutic agent for APL patients by the achievement of clinical remissions. APL is morphologically defined as a FAB M3 AML-subtype and is cytogenetically characterized by a balanced reciprocal translocation between chromosomes 15 and 17, which results in the fusion of the genes encoding the promyelocytic leukemia protein (PML) and retinoic acid receptor α (RARα) (Bennett *et al.*, 1976; Litzow, 2008). The chimeric PML-RARα protein disrupts the retinoic acid signaling pathway, which is essential for granulocytic differentiation (Zheng *et al.*, 2005). The efficacy of conventional chemotherapy with anthracycline and Ara-C for treating APL is relatively poor, leading to an aggravation of the bleeding syndrome and, thus, to an early death. In 1985, the combination

of all-*trans* retinoic acid (ATRA) and chemotherapy significantly improved the clinical outcome of APL patients by inducing the differentiation of leukemic cells. However, some patients developed an APL syndrome associated with a severe hyperleukocytosis due to an acquired resistance of leukemic cells to ATRA (Fenaux *et al.*, 2007; Litzow, 2008; Wang and Chen, 2008). To overcome these limitations, the introduction of ATO in the early 1990s further optimized the ATRA-based therapies by a profound degradation of the PML-RARα protein which led to a longer survival of refractory/relapsed and newly diagnosed APL patients (Niu *et al.*, 1999; Shen *et al.*, 2004). Furthermore, a recent Italian-German study (APL0406 trial) demonstrated a superior and more sustained anti-leukemic efficacy of ATRA in combination with ATO compared with ATRA and chemotherapy in low- and intermediate-risk APL patients (Platzbecker *et al.*, 2017). ATO is currently regarded as the most effective single agent in APL and was approved by the FDA in 2000 for treatment of refractory/relapsed APL as a second-line therapy (Y. Zhang *et al.*, 2016; Platzbecker *et al.*, 2017).

Since the discovery of its efficacy in treating APL, many studies tried to elucidate ATO's mechanism of action, not only for treatment of APL but also for other AML subtypes and moreover for other forms of cancer (Jiao *et al.*, 2015; Leung *et al.*, 2017). At the cellular level, ATO exerts dose-dependent dual effects on APL cells by inducing apoptosis through activation of the mitochondria-mediated intrinsic apoptotic pathway at high concentrations and promoting cell differentiation with a longer treatment at low concentrations (Wang and Chen, 2008; Chen *et al.*, 2011). Aside from the degradation of the PML-RARα fusion protein in APL, ATO also causes inhibition of transcription factors like Gli1 in the Hedgehog signaling pathway (Kim *et al.*, 2010; Beauchamp *et al.*, 2011) as well as reduction of other AML oncoproteins such as AML1/MDS1/EVI1 (Shackelford *et al.*, 2006), thereby inducing growth arrest, differentiation and apoptosis of leukemia cells. Furthermore, a study of Halicka *et al.* demonstrated that ATO treatment of different leukemia cell lines leads to a cell cycle arrest in the G2/M phase and consequently to a cell growth inhibition, regardless of the PML-RARα status (Halicka *et al.*, 2002). In 2014, S. Kumar and colleagues confirmed that ATO induces the mitochondrial pathway of apoptosis in AML HL-60 cells, as well as in APL cells, via oxidative stress, DNA damage and changes in mitochondrial membrane potential (Kumar *et al.*, 2014). Similar observations were made in ATO-treated human chondrosarcoma (Jiao *et al.*, 2015), hepatocellular carcinoma (Lin *et al.*, 2007; Zhang *et al.*, 2014) and lung carcinoma cells (Leung *et al.*, 2017), suggesting that ATO is also a promising agent for other hematological malignancies and other types of cancer. However, despite ATO's encouraging efficacy in many forms of cancer, its myocardial toxicity and other side effects, such as the APL syndrome with its severe hyperleukocytosis and increased cytokine expression, as well

as the increased risk of secondary malignancies due to chronic arsenic exposure, need to be considered (Litzow, 2008; Mathews *et al.*, 2013).

2.3.3.2 Granulocyte-colony stimulating factor

Colony-stimulating factors are glycoproteins essential for proliferation, differentiation and survival of hematopoietic cells. One of its members is the granulocyte-colony stimulating factor (G-CSF), a hematopoietic cytokine whose major function is to regulate granulopoiesis by stimulating the bone marrow to produce neutrophils from committed myeloid precursor cells. In year 1985, K. Welte and colleagues isolated and purified G-CSF from the human bladder carcinoma cell line 5637 and identified its capability of stimulating growth of progenitor cells and differentiation of promyelocytic leukemia cell lines *in vitro* (Welte *et al.*, 1985). Furthermore, Nagata *et al.* and Souza *et al.* isolated the cDNA and determined the amino acid sequence of the purified G-CSF protein (Nagata *et al.*, 1986; Souza *et al.*, 1986). In response to the need of highly purified G-CSF for clinical use, a glycosylated (lenograstim, synthesized in Chinese hamster ovary cells) and a non-glycosylated form (filgrastim, synthesized in *Escherichia coli*) of the human protein have been manufactured. These both recombinant human G-CSF (rhG-CSF) variants exhibit the same pharmacokinetics and pharmacological effects (Tanaka *et al.*, 1997). Nowadays, it is known that G-CSF is produced by stromal cells, macrophages, neutrophils, endothelial cells and fibroblasts, as well as by tumors (Nagata *et al.*, 1986; Mendoza *et al.*, 1990; Baba *et al.*, 1995). After secretion, G-CSF binds with high affinity to the G-CSF receptor (G-CSFR), which is expressed on myeloid precursor cells in the bone marrow, and induces neutrophilic precursors to proliferate and differentiate into mature neutrophils. To the signaling pathways involved in the G-CSF signal transduction upon binding to G-CSFR belongs the Janus tyrosine kinase (JAK)/ signal transducer and activator of transcription protein (STAT) signaling cascade, mitogen-activated protein kinase (MAPK), phosphoinositide 3-kinase (PI3K) and Wnt signaling pathway (Marino and Roguin, 2008; Skokowa *et al.*, 2017). Dysregulation in the G-CSFR signaling pathway at the level of downstream effector proteins leads to severe defects in myeloid cell proliferation and differentiation. The protein lymphoid enhancer-binding factor 1 (LEF-1), generally collaborates with β-catenin as a transcriptional complex downstream of the canonical Wnt signaling pathway, can also act independently of β-catenin and is known to be crucial for correct G-CSF-mediated neutrophil granulopoiesis (Van de Wetering *et al.*, 2002; Skokowa *et al.*, 2006). Myeloid cells with a reduction of LEF-1 protein levels, along with a hyperactivated JAK2 and a constitutively active STAT5A, show a maturation arrest of granulopoiesis at the level of promyelocytes, which is causative for severe congenital neutropenia (CN) (Skokowa *et al.*, 2006; Gupta *et al.*, 2014). Due to the

impaired differentiation and therefore reduced number of neutrophilic granulocytes, CN patients suffer from severe bacterial infections starting shortly after birth and, without proper treatment with rhG-CSF, throughout lifetime (Dale *et al.*, 2006; Welte *et al.*, 2006). In patients with CN, compensatory mechanisms of granulopoiesis can be induced by increasing the G-CSF signaling via G-CSF administration, rendering G-CSF a qualified drug for neutropenia.

With the clinical use of the pharmaceutical rhG-CSF forms, not only febrile neutropenia in patients with non-myeloid malignancies under chemotherapies can be reduced, but also bone marrow recovery after HSCT can be accelerated and the onset of severe myelosuppression prevented. Moreover, G-CSF is clinically used as bone marrow mobilizer to increase the number of circulating CD34-positive progenitor cells in the blood for further HSCT (To *et al.*, 1997; Crobu *et al.*, 2014). Besides, G-CSF has also been shown to improve cardiac function after myocardial infarction by bone marrow cell mobilization (Deindl *et al.*, 2006) as well as act neuroprotective in stroke models (Schäbitz and Schneider, 2007).

Growth factors have also been used for treatment of leukemia. For AML therapy, G-CSF can be applied after induction therapy to handle neutropenia and reduce the incidence of infections, especially for elderly AML patients who are susceptible to infection-related mortality (Von Lilienfeld-Toal *et al.*, 2007). G-CSF has also been investigated in several combinations for treating AML with genetic abnormalities or relapsed/refractory AML such as fludarabine + high-dose Ara-C + G-CSF (FLAG) or cladribine + Ara-C + G-CSF (Visani *et al.*, 1994; Borthakur *et al.*, 2008; Roboz, 2012). The so-called FLAG therapy could also be a good alternative for induction treatment of poor risk AML (Burnett *et al.*, 2013). Aside from reducing the toxicity of standard therapy, G-CSF also induces the quiescent AML cells into the cell cycle and, thus, increases their sensitivity to Ara-C (Nakayama *et al.*, 2017). Also, Kitagawa *et al.* showed that the combination of G-CSF with Ara-C and the cytostatic agent etoposide is superior regarding its AML cytotoxicity when compared to the therapy with Ara-C and etoposide alone. By adding G-CSF, reduced cell viability and cell number, as well as an increased level of apoptotic cells were observed. Moreover, G-CSF mobilized resting G0/G1 phase cells into S phase suggesting a priming effect of G-CSF on AML cells (Kitagawa *et al.*, 2010). However, despite promising results for G-CSF as an adjuvant for AML therapy, the application of G-CSF for leukemia treatment is still controversial. G-CSFR is also expressed on leukemic cells what can sensitize them to proliferate upon G-CSF stimulus (Budel *et al.*, 1989; Kita *et al.*, 1993).

2.3.3.3 Combinatorial ATO-G-CSF treatment – a new therapeutic approach for AML by stimulating the aquaglyceroporin 9 channel?

The revival of the notorious and likewise life-giving 'poison' arsenic for treating APL is a unique story in cancer research. It also highlights some of the essential concepts in pharmacology regarding the cytotoxicity of compounds: the achievement of a favorable therapeutic ratio between normal healthy and malignant target cells. As the specificity of compounds for malignant cells is mostly not given, the development of combinatorial treatments is mandatory to reduce off-target effect, which may harm healthy cells. Indeed, for APL the combination ATO-ATRA has exhibited an enhanced therapeutic efficacy compared with either single agent. In treating other hematological diseases, several combinations can improve the clinical outcome like arsenic sulfide in combination with imatinib for treating 'breakpoint cluster region/Abelson murine leukemia viral oncogene homolog 1' (BCR/ABL)-associated CML, whereby arsenic sulfide potentiates the efficacy of imatinib to decrease the constitutive activity of BCR/ABL (Zhang *et al.*, 2009; Chen *et al.*, 2011). Arsenic can not only act as a potentiator in therapeutic approaches, but it can also be amplified in its function by several agents such as vitamin D3, which enhances the anti-tumorigenic effects of ATO in human HL-60 leukemia cells through induction of nucleosomal DNA fragmentation (Rogers *et al.*, 2014). Also, ATRA and the hypomethylating agent azacytidine augment the cytotoxic effect of ATO in AML cells by upregulating the main arsenic transporter aquaglyceroporin 9 (AQP9) (Iriyama *et al.*, 2012; Chau *et al.*, 2015).

Aquaglyceroporins are members of the major intrinsic protein superfamily, which allow the passage of not only water – like the true aquaporins – but also glycerol and other neutral solutes. Thirteen aquaporin (AQP) subtypes (AQP0 – 12) have been identified in mammals, but only AQP3, AQP7, AQP9, and AQP10 are members of the aquaglyceroporin family. They are expressed in almost all tissues, even though their distribution pattern is tissue-specific (Saito *et al.*, 1292; Bhattacharjee *et al.*, 2004). AQP3 is present among others at the basolateral membrane of kidney, colon and skin, whereas AQP7 is found in testes, adipose tissue and heart. Human AQP10 is expressed only in small intestine (Ishibashi *et al.*, 2002). AQP9 transcript is found in humans in liver, lung, spleen, brain and peripheral leukocytes and is therefore the only known AQP expressed in the hematopoietic system (Tsukaguchi *et al.*, 1999; Elkjær *et al.*, 2000). The *AQP9* gene is located on chromosome 15q22.1-22.2 and has a size of 25 kb. It encodes a protein monomer of 295 amino acids, which contains six full- and two half-transmembrane stretching α-helices. Together with three further monomers it forms an AQP9 tetramer. The pore for transportation of solutes is formed within the helices of each monomer, hence, the tetrameric AQP9 comprises four independent pores (FIGURE 2) (Tsukaguchi *et al.*, 1999; Viadiu *et al.*, 2007).

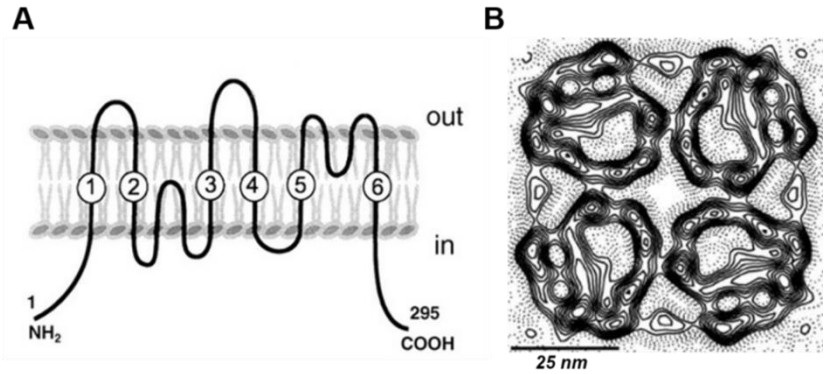

Figure 2: Structure of the AQP9 channel.
(A) The AQP9 monomer is constituted of 295 amino acids and contains six full- and two half-transmembrane stretching α-helices. (B) The projection map shows the rat AQP9 tetramer constituted of four helix-clusters and featuring oval pores with an approximate dimension of 7 Å by 12 Å. The large pores of AQP9 allow the passage of bulkier solutes. Figures adapted from Tsukaguchi *et al.*, 1999; Viadiu *et al.*, 2007.

AQP9 has the broadest specificity among the AQP family and transports water, glycerol, urea, carbamides, polyols, purines and pyrimidines, as well as arsenic. However, transportation of arsenic was shown to be additionally mediated by AQP3 and AQP7 (Liu *et al.*, 2002; Lee *et al.*, 2006). Many studies with cell lines cultures revealed that an increased AQP3 or AQP9 expression leads to an enlarged arsenic influx and sensitivity and, thereby, to an accumulation of arsenic within the cells (Bhattacharjee *et al.*, 2004; Lee *et al.*, 2006; Leung *et al.*, 2007). On the other hand, experiments with mice lacking an AQP9 expression demonstrated that AQP9 is not only responsible for the uptake but also for the elimination of arsenic. These results suggest that AQP9 may also act as a protector against arsenic poisoning (Carbrey *et al.*, 2009).
In respect of therapeutic approaches for leukemia, AQP9 is widely expressed on the plasma membranes of leukemic cells and plays a crucial role for arsenic uptake. AQP9 is also assumed to be a promising candidate biomarker for predicting the efficacy of ATO treatment in APL patients (Iriyama *et al.*, 2013). By upregulating AQP9 with agents like ATRA or azacytidine the arsenic level and, thereby, the cytotoxicity can be increased. Another AQP9-stimulating candidate may be G-CSF. G-CSF as well as ATO are already known to be efficient agents for promoting cycling of dormant HSCs and LSCs (Essers and Trumpp, 2010). Iriyama *et al*. also showed that G-CSF in addition to ATO and ATRA has an enhanced anti-leukemic effect on HT93A APL cells by potentiating the ATO-ATRA-induced differentiation and rendering them more sensitive to ATO. Even though Iriyama *et al*. could not directly detect an upregulation of AQP9 expression upon G-CSF addition, increased intracellular ATO levels were observed when compared to ATRA/ATO treatments alone. This

led to the assumption that G-CSF has a stimulating effect on AQP9 protein expression or stability (Iriyama *et al.*, 2012).

2.4 Acute lymphoblastic leukemia

Acute lymphoblastic leukemia (ALL) is the most common childhood malignancy in developed countries. The malignant transformation and subsequent clonal expansion of immature lymphoid lineage-derived progenitors can arise during B cell- (B-ALL) or T cell development (T-ALL). 85% of childhood and adolescence ALL are B-ALL and 15% T-ALL, while 75% of adulthood ALL are B-ALL and 25% T-ALL (Chiaretti and Foà, 2009; Kunz *et al.*, 2015). Over the last decades, massive improvements in survival have been achieved in children, but less for adolescents and adults. More than 80% of children with standard risk ALL can be cured, whereas just 30 – 45% of adolescents and adults show an event-free survival (Pui and Evans, 2006; Smith *et al.*, 2010). There are several reasons for this disparity of outcomes: Adolescents and adults show an increased prevalence of specific genetic alterations (for example BCR-ABL1 or MLL translocation), unspecified chromosomal abnormalities and treatment-related toxicities, including higher rates of infections, steroid-induced osteonecrosis and hyperglycemia, when compared with younger children (Harrison, 2009; Mullighan and Downing, 2009; Gramatges and Rabin, 2013). Moreover, drug metabolism and response to chemotherapy may also differ in adolescent and adult ALL patients leading to a poor prognosis for these patients (Friend and Schiller, 2017).
Further, children with down syndrome or familial history of autoimmune thyroid disease have an higher risk to develop ALL (Hasle *et al.*, 2000; Perillat-Menegaux *et al.*, 2003).

2.4.1 Classification of ALL

ALL was firstly divided into three groups by the FAB classification based on cytomorphological studies: FAB L1 (B-/T-ALL with small uniform cells), FAB L2 (B-/T-ALL with large varied cells) and FAB L3 (B-ALL large varied cells with vacuoles, also called Burkitt leukemia). In 2008, the WHO classification categorized ALL in distinct subgroups based on their cytomorphology, immunophenotyping and immunogenetics, which consider also the type (B or T cell) and the maturity of the malignant lymphocyte (TABLE 2). These groups have largely replaced the FAB classification (Vardiman *et al.*, 2009; Loghavi *et al.*, 2015). Additionally, B- and T-ALLs are also divided in classes based on their expressing of maturation level-specific CD markers (immature → mature): pro-B-ALL → common B-ALL → pre-B-ALL → mature ALL; pro-T-ALL → pre-T-ALL → cortical T-ALL → mature T-ALL.

Table 2: Classification of ALL

TYPES	FURTHER DESCRIPTION
(Precursor) B lymphoblastic leukemia/lymphoma, not otherwise specified (FAB L1/2)	n/a
(Precursor) B lymphoblastic leukemia/lymphoma with recurrent genetic abnormalities (FAB L1/2)	- B-ALL with t(9;22)(q34;q11.2); BCR-ABL 1 - B-ALL with t(v;11q23); MLL rearranged - B-ALL with t(12;21)(p13;q22) TEL-AML1 (ETV6-RUNX1) - B-ALL with hyperdiploidy - B-ALL with hypodiploidy - B-ALL with t(5;14)(q31;q32) IL3-IGH - B-ALL with t(1;19)(q23;p13.3); TCF3-PBX1
(Precursor) T lymphoblastic leukemia/lymphoma (FAB L1/2)	n/a
Burkitt's leukemia/lymphoma (FAB L3)	n/a

2.4.2 Standard and alternative therapies for ALL

The first-line treatment of ALL is a remission-induction chemotherapy, which constitutes a combination of an antiinflammatory glucocorticoid (prednisone, prednisolone or dexamethasone), the cytostatic agent vincristine, and usually the asparagine-degrading enzyme asparaginase together with an anthracycline such as daunorubicin, to rapidly eradicate most tumor cells and to restore normal hematopoiesis. When ALL patients achieve remission, the consolidation chemotherapy, which includes the cytostatic agents mercaptopurine, cyclophosphamide and cytarabine, high-dose asparaginase (generally given only to children for an extended period) followed by the maintenance therapy (repetition of the initial induction therapy) further eliminate tumor burden (Schrappe *et al.*, 2000; Pui and Evans, 2006; Stock *et al.*, 2008). For patients with a poor response to the remission-induction chemotherapy, especially adults, relapsed or very high-risk ALL, HSCT is the ultimate form of consolidation treatment (Hunault *et al.*, 2004). Since ALL cells can also enter

the central nervous system (CNS), CNS therapy already starts in the remission-induction phase by administration of the CNS-penetrating cytarabine, the immunosuppressive drug methotrexate as well as cranial irradiation. For eliminating residual leukemic cells as a final step, a combination of weekly-administered methotrexate and daily-given mercaptopurine forms the basis of most maintenance therapy regimens (Pui *et al.*, 2002; van der Werff ten Bosch *et al.*, 2005). It should be mentioned that the effect of the individual agents within the therapy regimens depends on the dosage and schedule of administration (Pui and Evans, 2006). The response to therapy is also influenced by the genetics of leukemia cells and the pharmacogenetics of the host. Both parameters can be further used as prognostic markers. Regarding this, the measurement of minimal residual disease (MRD) during and after remission-induction therapy using FACS or polymerase-chain-reaction (PCR) analysis, helps to anticipate and consequently combat relapses. Moreover MRD assessment can be utilized as a surrogate marker for clinical outcome (Chung *et al.*, 2006; Ebinger *et al.*, 2010). In this context, it has been shown that low or undetectable levels of MRD appear to result in improved clinical outcome of ALL patients, while rising MRD levels after HSCT seem to predict hematological relapses (Bader *et al.*, 2015).

In contrast to the increasingly improved outcome of patients with newly diagnosed and standard-risk ALL upon chemotherapy, little progress has been made in the treatment of refractory and relapsed ALL. Compared to the good survival rate of standard-risk ALL, refractory and especially relapsed ALL after HSCT are still associated with a poor prognosis due to a resistance of malignant cells to chemotherapy (Bhojwani and Pui, 2013). Therefore, new and efficient therapeutic strategies, which specifically target leukemic cells and minimize off-target effects, are urgently needed. Similar to AML immunotherapy approaches, targeted therapeutics such as unconjugated or conjugated mAbs against cell surface marker and bispecific T cell-recruiting antibody constructs are becoming increasingly important. ALL blasts express a variety of lineage-specific antigens which can be used as targets for mAb (-conjugate) therapy such as CD19, CD20, CD22 and CD52 (Hoelzer, 2011; Raponi *et al.*, 2011).

CD19 appears during the early stages of B cell maturation and development and is thusly expressed in almost all precursor B-ALLs (BCP-ALL) or mature B-ALLs. Although the unconjugated mAbs can directly induce cytotoxicity through inhibition of proliferation, triggering of cell death pathways or indirectly via antibody-dependent cell-mediated cytotoxicity (ADCC), their efficacy is limited. Therefore, the Fc part of mAbs can be either conjugated with cytotoxic drugs or optimized by specific modifications to increase the clinical effectiveness (Kantarjian, Thomas, Wayne, *et al.*, 2012; Lichtenegger *et al.*, 2017). Two Fc-optimized CD19 mAbs are already used in (pre-) clinical trials, MEDI-551, which features a

genetic modification of its glycosylation pattern, and MOR208, which carries an exchange of two amino acids in the CH2 domain of the human Fc-part of IgG1 (SDIE modification). Both antibodies have demonstrated a markedly superior efficiency compared to the non-Fc-optimized counterparts by increased ADCC cytotoxicity and effectiveness of recruiting immune cells like natural killer (NK) cells or macrophages (Lang *et al.*, 2004; Kellner *et al.*, 2013; Matlawska-Wasowska *et al.*, 2013). Another therapeutic approach for targeting CD19-positive B-ALL is blinatumomab (Blincyto®), a bispecific T cell-recruiting antibody which simultaneously binds the tumor-associated antigen CD19 and CD3ε in the T cell receptor complex. It consists of two scFv, each formed by a pair of variable domains from heavy and light immunoglobulin chains binding CD3 and CD19, which are connected by a flexible 25 amino acid-long linker. In the first clinical trials, blinatumomab was evaluated in adult patient cohorts with primary resistant or relapsed B-ALL, who had a detectable MRD. Most patients showed a rapid response within the first cycle of treatment with a tolerable toxicity (Topp *et al.*, 2011; Queudeville *et al.*, 2017). Blinatumomab also achieved a molecular remission in childhood relapsed ALL with tolerable side effects (Handgretinger *et al.*, 2011). More recently, Kantarjian *et al.* compared blinatumomab with conventional second-line standard chemotherapy in patients with refractory/relapsed ALL showing that treatment with blinatumomab resulted in a significantly longer overall survival than with chemotherapy (Kantarjian *et al.*, 2017). For future therapeutic strategies, blinatumomab may be used as a monotherapy during the consolidation or maintenance phase or for elderly frail patients, who are not eligible to chemotherapy.

Another candidate for mAb therapy is CD20 which functions as a calcium channel and influences cell cycle progression and differentiation. CD20 is heterogeneously expressed on 20 - 50% of normal and malignant precursor B lymphocytes as well as most commonly on mature ALL or Burkitt's leukemia/lymphoma, but not on normal HSC and plasma cells (Raponi *et al.*, 2011; Kantarjian, Thomas, Wayne, *et al.*, 2012). A CD20-targeting therapeutic antibody is the unconjugated chimeric mAb rituximab (Rituxan®), an IgG1 immunoglobulin that contains murine variable region sequences and human constant κ and Fc region sequences. It was already approved by the FDA in 1997 as the first mAb for therapeutic treatment of cancer (Leget and Czuczman, 1998; Binder *et al.*, 2006). The efficacy of rituximab was firstly described in CLL patients who received either rituximab alone or in combination with chemotherapy. Surprisingly, rituximab had minimal anti-CLL activity as single-agent, whereas the addition of rituximab to chemotherapy demonstrated a benefit in overall survival (Robak *et al.*, 2010; Elter *et al.*, 2011). Several studies combined rituximab with chemotherapy in CD20-positive B-ALL subsets which led to an improved outcome particularly in younger adults. However, clinical data for rituximab administration in children is still limited (Griffin *et al.*, 2009; Hoelzer *et al.*, 2010; Thomas *et al.*, 2010). Moreover, some

studies showed that the low expression level of CD20 on precursor B lymphocytes can be stimulated with corticosteroids, which may further improve the sensitivity of low CD20-expressing cells to rituximab (Gaipa *et al.*, 2005; Dworzak *et al.*, 2008).

Another B-lineage-specific antigen is CD22, which is a member of the sialoglycoprotein family of adhesion molecules and regulates B cell activation as well as interaction of B cells with T cells and antigen-presenting cells. Expression of CD22 has been demonstrated in more than 90% of patients with BCP-ALL and mature B-ALL (Raponi *et al.*, 2011). The unconjugated mAb epratuzumab has been explored only in few studies so far. Even though in one pediatric relapsed ALL study, the administration of epratuzumab showed an enhanced response to chemotherapy compared to chemotherapy alone (Raetz *et al.*, 2008). Also studies with inotuzumab ozogamicin (CMC-544), an humanized anti-CD22 mAb conjugated to the cytotoxic antibiotic calicheamicin, revealed as single-agent antitumor activity in patients with refractory/relapsed B-ALL by inducing double-strand DNA cleavage with subsequent apoptosis (DiJoseph *et al.*, 2004; Kantarjian, Thomas, Jorgensen, *et al.*, 2012). Lately, Kantarjian *et al*. further evaluated CMC-544 in combination with chemotherapy showing a prolonged progression-free and overall survival (Kantarjian *et al.*, 2016)

CD52 is a B- and T cell lineage antigen, a cell-surface glycoprotein which is involved in T cell activation and expressed on up to 70% of more mature B and T cells, but not on HSCs (Hale and Waldmann, 2000). An antibody against CD52 is alemtuzumab, an unconjugated, genetically engineered, humanized IgG1 mAb, which is currently used for second-line therapy of CLL and for the prevention of graft-versus-host disease (GvHD) in allogeneic HSCT. Alemtuzumab has also been evaluated in patients with de novo CD52-positive ALL after induction chemotherapy, however with little anti-leukemic efficacy. Moreover, alemtuzumab was associated with an increased risk of CMV viremia and developing neutropenia (Stock *et al.*, 2009; Wei *et al.*, 2017). Hence, Gorin *et al*. tested alemtuzumab in combination with G-CSF in refractory/relapsed ALL to increase the neutrophil-mediated ADCC, but again with modest results. The further clinical use of alemtuzumab in treatment of ALL has not been clarified yet (Gorin *et al.*, 2013). It must be mentioned that B- and T-ALL subtypes show individual antigen expression patterns during different maturation steps und may therefore respond differentially to mAb therapy. Additionally, target antigens are not expressed exclusively on malignant cells, so the cytotoxic effects are less selective and may lead to mAb-specific side effects like B or T cell lymphopenia with related clinical consequences, which are mostly infections (Hoelzer, 2011).

Like in AML therapy, checkpoint inhibitors also play a role in immunotherapy approaches of ALL, albeit to a lesser extent. Several studies tested different checkpoint inhibitors for potentiating the efficacy of different anti-neoplastic drugs and to increase the cytotoxicity of standard therapies against B- and T-ALL. Using checkpoint inhibitors like PD-1, CTLA-4 and

checkpoint kinase 1 and 2 is a highly promising approach to increase antitumor T cell activity as a treatment of hematological malignancies (Shimauchi *et al.*, 2007; Feucht *et al.*, 2016; Ghelli Luserna Di Rorà *et al.*, 2016; Knaus *et al.*, 2017).
Another approach for targeted therapy of ALL is focusing on genetic abnormalities such as BCR-ABL1 or MLL translocations. Preclinical studies demonstrated that BCR-ABL1-positive ALLs responded to ABL1 tyrosine kinase inhibitors, like imatinib mesylate (Gleevec®), while those with BCR-JAK2 fusion protein expression were sensitive to JAK2 inhibitors (Maude *et al.*, 2012; Roberts *et al.*, 2012). Gene expression studies showed that FLT3, a receptor tyrosine kinase, which plays a role in promoting cell proliferation and transformation, is overexpressed in MLL-rearranged ALL. Targeting FLT3 with an FLT3-inhibitor like midostaurin, which is also highly effective in the therapy of FLT3-ITD AML, is a possible therapeutic approach for MLL-rearranged ALL (Armstrong *et al.*, 2003; Stam *et al.*, 2005).

Analogous to AML-targeted immunotherapy approaches, many agents have a limited efficacy as a single drug, but in combination with other therapeutics they may improve the clinical outcome of ALL patients, who are ineligible for conventional chemotherapy.

2.4.3 CAR T cell-based therapy – a new therapeutic approach for ALL

In the last twenty years, several experimental and clinical studies indicated that *ex vivo*-cultivated and re-administered patient-derived tumor-infiltrating lymphocytes (TILs) can identify and kill cancer cells by triggering an acute inflammatory reaction. The adoptive transfer of TILs has been proven as an effective therapy for metastatic melanoma patients. It has also been extensively studied as a treatment for other cancer types, but only with elusive success because of the difficult identification and expansion of TILs (Rosenberg *et al.*, 1988; Morgan *et al.*, 2006). The adoptive transfer of genetically engineered autologous CAR T cells, however, has proven to be extremely effective against cancer. Like already mentioned for AML therapy, redirected CAR T cells are a novel highly promising approach for targeted immunotherapy of hematological malignancies, especially for ALL. CARs are chimeric transgenes which are usually composed of a scFv specific for a tumor-associated antigen and fused to a transmembrane (TM) domain via an extracellular spacer domain, such as the immunoglobulin (Ig)G Fc hinge region. The TM domain is linked to intracellular signaling components, which are capable of activating the cell and triggering the immune response (FIGURE 3A) (Marcus and Eshhar, 2014; Park and Brentjens, 2015). Since CARs combine the binding domain of an antibody and T cell signaling moieties, they can redirect T cell specificity to the tumor in a MHC-independent manner and activate the CAR-modified T lymphocytes to lyse targeted tumor cells (Chmielewski *et al.*, 2013). The formation of the

intracellular signaling components changed during evolution of CAR T cells. In the first-generation CAR, TM domain is linked to a single signaling domain which is most commonly the intracytoplasmic CD3ζ domain of the TCR complex (FIGURE 3B). These basic CAR T cells can effectively prevent tumor growth *in vivo* by sufficient cytotoxicity and interferon-γ production. However, T cell proliferation is limited and they fail to persist in the long term. Thus, the implementation of an additional co-stimulatory signaling domain, like CD28, 4-1BB or CD134 (OX-40), further improved signaling, proliferation and survival of the so-called second-generation CAR T cells and promotes interleukin (IL)-2 production. The third-generation CAR contains tandem cytoplasmic signaling domains from two co-stimulatory receptors like CD28 – 4-1BB or CD28 – OX40 for optimal co-stimulation (Finney *et al.*, 1998; Bridgeman *et al.*, 2010).

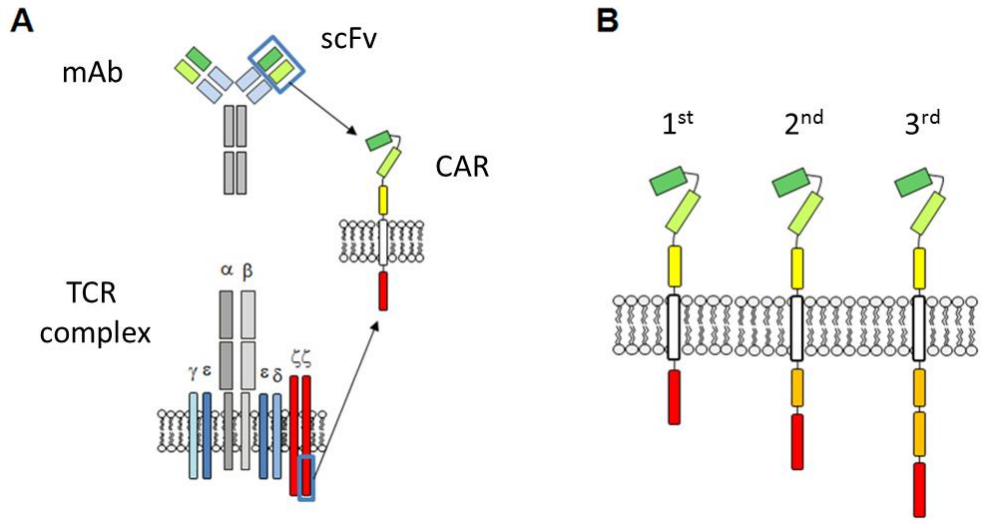

Figure 3: Formation and evolution of chimeric antigen receptors.
A) Chimeric antigen receptors consist of a single-chain variable fragment (scFv) specific for a tumor-associated antigen, which is fused to a transmembrane (TM) domain via a spacer domain. The TM domain is further linked to intracellular signaling components of the T cell receptor (TCR) complex. B) In the first-generation CAR, TM is linked to a cytoplasmic signaling domain of the TCR, such as CD3-ζ or Fc receptor γ chains. With the evolution of CAR T cells, the second-generation CAR was developed with an additional co-stimulatory signaling domain, for example CD28, 4-1BB or OX-40. The third-generation CAR contains tandem cytoplasmic signaling domains from two co-stimulatory receptors like CD28-4-1BB or CD28-OX40. Figure taken from http://www.discoverymedicine.com and adapted based on Park and Brentjens, 2015.

Primary clinical experiences with first-generation CAR T cells showed limited efficacy, whereas second-generation CAR T cells targeting CD19 displayed significantly enhanced expansion and strong antitumor efficacy in patients with low-grade and aggressive B cell malignancies, including B-CLL and relapsed B-ALL (Porter *et al.*, 2011; Brentjens *et al.*,

2013; Davila *et al.*, 2014). Cumulative data reported a 60% complete remission rate in patients with CLL and ALL (Kalos *et al.*, 2013). These results demonstrated that adoptive CAR T cell therapy can eradicate advanced hematological malignancies and provided clinical proof of concept for the CAR approach. The third-generation CAR was successfully tested in several mouse experiments, but clinical experiences are still limited (Carpenito *et al.*, 2009; Till *et al.*, 2012). Very recently, the FDA approved two CAR T cell therapies (second-generation CAR) for treatment of hematological cancer: Kymriah™ (CTL019) for the treatment of patients with BCP-ALL which is refractory or in second or later relapse up to 25 years of age, and Yescarta™ for adult patients with large B cell lymphoma after at least two other failed treatment approaches (U.S. Food & Drug Administration, 2017).

It has been shown that the optimal CAR design, such as the sequence of the signaling domains, have an impact on the CAR function. For example the CD28 co-stimulatory domain is not effectively functional when placed downstream of the CD3ζ domain (Marr *et al.*, 2012). Although both 4-1BB- and CD28-CAR models have shown to be clinically effective, some studies demonstrated that 4-1BB is superior to CD28 in terms of enhancing anti-leukemic CAR efficacy in a xenograft mouse model (Carpenito *et al.*, 2009; Milone *et al.*, 2009). Moreover, a study from Long *et al.* indicated that CD28 co-stimulation augments, whereas 4-1BB co-stimulation reduces, exhaustion which is induced by persistent CAR signaling (Long *et al.*, 2015). Frigault *et al*. confirmed this observation and further indicated that CD28-based endodomains can mediate constitutive signaling which leads to terminal differentiation of effector T cells (Frigault *et al.*, 2015). This concludes that the third-generation CAR with CD28 – 4-1BB as tandem cytoplasmic signaling domains may promote effective and persistent CAR T cells for clinical application. Furthermore, several studies showed that even the length and composition of IgG-derived extracellular spacer domains can have an influence on the CAR function. CAR T cells with a short spacer length were superior to CAR T cells with a long spacer length *in vivo* regarding their cytokine secretion, proliferation and function. CD19 CAR T cells with a long spacer exhibited antitumor activity only *in vitro*, as under *in vivo* conditions, the interaction between the Fc domain within the spacer and the Fc receptor-bearing myeloid cells led to activation-induced CAR T cell death (Hudecek *et al.*, 2013, 2015; Almåsbak *et al.*, 2015).

The major issue for clinical application is that there is no standard accepted CAR configuration. This makes it difficult to compare the results effectively from the wide number of currently ongoing clinical trials.

Also, the composition of the CAR T cell product has been demonstrated to influence on CAR function. In initial CAR T cell therapy studies, only highly differentiated CD8-positive CAR T cells were administered, but they did not have sufficient replicative capacity after infusion

and a poor persistence in patients. Therefore, the administration of a mixture of CD4-positive and CD8-positive T cells is often preferred, probably because the CD4-positive T cells provide growth factors and other signals to maintain the function and survival of the infused CD8-positive T lymphocytes, as well as can eliminate tumor cells in a direct manner to a certain extent (Hombach *et al.*, 2006; Barrett *et al.*, 2015).

Furthermore, also the state of differentiation of CAR T cell is important for the efficient CAR function. Studies with mice and primates indicated that naïve (CD62L-positive) or central memory T cells are preferable for adoptive immunotherapy because of their capability of an extensive replication and establishment of a persistent T cell memory pool (Maus *et al.*, 2004; C. Berger *et al.*, 2008). The observation that naïve $CD62L^{high}$-positive antigen-specific T cells are more persistent than differentiated $CD62L^{low}$ cells implied a linear developmental model of T cell differentiation. This concept states that naïve or less differentiated memory cell types, which express CD62L, give rise to effector cells and not vice versa (FIGURE 4) (Klebanoff *et al.*, 2006; Youngblood *et al.*, 2013; Stemberger *et al.*, 2014; Restifo, 2015). The two isoforms of CD45, namely CD45RA and CD45RO, are important to further characterize the differentiation status of T cells. CD45RA is expressed on naïve and effector T cells, while CD45RO is expressed on memory T cells (Mahnke *et al.*, 2013). Studies of leukemia patients treated with CD19 CAR T cells indicated that the presence of persistent central memory T cells is the most important predictive biomarker of therapy success (Kalos *et al.*, 2011; Barrett *et al.*, 2015). In addition, Chan *et al*. showed that persistent CD45RO-positive memory T cells are important for the anti-leukemic CAR T cell activity as well as for the pathogen memory response (Chan *et al.*, 2015). To promote the maintenance of a less differentiated population of naïve and central memory T cells, cells have to be cultured under special conditions with specific co-stimulatory signals, such as CD28 or 4-1BB stimulation (Thomas *et al.*, 2002; Kawalekar *et al.*, 2016) or addition of cytokines like IL-2, IL-7 and IL-15 (Kaneko *et al.*, 2009; Barrett *et al.*, 2014).

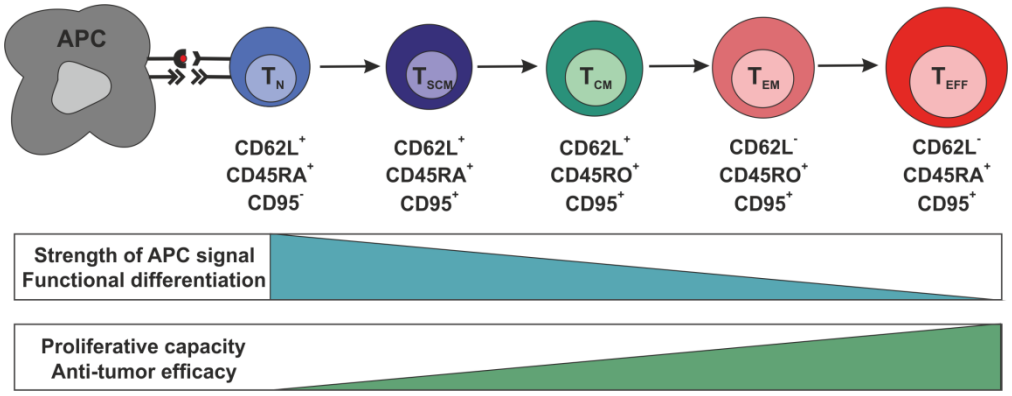

Figure 4: Current model of central and effector memory T cell generation.
This model of T cell differentiation is also known as the "linear" or "developmental" model. It indicates that naïve or less differentiated memory cell types that express CD62L give rise to effector cells, and not vice versa. CD45RA is expressed on naïve and effector cells, CD45RO on memory cell. The Fas receptor (CD95) describes the activation status. APC, antigen-presenting cell; T_{CM}, central memory T cell; T_{EFF}, effector T cell; T_{EM}, effector memory T cell; T_N, naive T cell; T_{SCM}, T memory stem cell. Figure based on Restifo, 2015s.

While efficacy of generating genetically engineered T cells has improved in the field of adoptive immunotherapy, accompanying toxicities for patients have also increased. The most prominent toxicity of CAR T cells for bone marrow-derived tumors is the cytokine release syndrome (CRS). Highly proliferative T cells can induce proinflammatory cytokine release, such as IL-6 and interferon gamma (IFN-γ), which in turn activates further immune cells leading to high fever and myalgia or up to unstable hypotension and respiratory failure (Morgan *et al.*, 2010; Kochenderfer *et al.*, 2012; Davila *et al.*, 2014). Positively, the anti-IL-6 receptor mAb tocilizumab has been shown to effectively decrease the IL-6 level and quickly reverse CRS (Lee *et al.*, 2014; Maude *et al.*, 2014). Moreover, CD19 CAR therapy is also accompanied by 'on-target off-tumor' toxicities which can lead to acute B cell aplasia. The depletion of the patients' B cells induces a profound hypogammaglobulinemia which must be treated intravenously with immunoglobulin replacement (Davila *et al.*, 2014; Barrett *et al.*, 2015). To prevent off-tumor toxicities and achieve strict safety requirements, various approaches to induce apoptosis of genetically modified T cells have been proposed. With the incorporation of a so-called 'suicide gene', for example inducible caspase 9, it is possible to quickly eliminate the infused cells in case of adverse events (Di Stasi *et al.*, 2011; Gargett and Brown, 2014).

A major problem of CAR T cell therapy is the obtainability of suitable cells for transplantation: on the one hand, using autologous T cells may bear the risk of a contamination with residual malignant T cells. On the other hand, employing MHC-matched allogeneic T cells may cause

GvHD in immunocompromised patients. Despite the risk of alloreactivity, many clinical studies showed that allogeneic CD19 CAR T cells have a limited propensity to induce GvHD in B cell malignancy patients (Davila *et al.*, 2014; Lee *et al.*, 2015; Ghosh *et al.*, 2017). Several approaches to circumvent the issue of GvHD reactivity have been proposed, such as the transfer of T cell precursors in combination with autologous HSCT. Hereby, infused cells differentiate into mature T cells in the host thymus and, thereby, lose their GvHD reactivity (Zakrzewski *et al.*, 2008). Another approach to prevent GvHD is to use genome editing techniques like zinc finger nucleases to knockout the endogenous TCR (Torikai *et al.*, 2012; Philip *et al.*, 2015). Moreover, using not MHC-restricted γδ T cells or NK cells for CAR cell therapy can also avoid GvHD reactivity (Deniger *et al.*, 2013; Oberoi and Wels, 2013).

While there are several trials currently ongoing targeting B cell malignancies, clinical studies for CAR T cell therapy of solid tumors are limited due to tumor histopathological structure and strong immunosuppressive environment as well as the lack of ideal targets. CAR T cell therapy studies for targeting HER2/neu-positive large solid tumors demonstrated promising results (Textor *et al.*, 2014), although Morgan *et al*. showed that a patient experienced fatal CRS shortly after infusion of HER2/neu-specific CAR T cells, which was attributed to low-level expression of HER2/neu on lung epithelial cells (Morgan *et al.*, 2010). As well, several clinical trials for treatment of GD2-positive neuroblastoma or FRα-positive ovarian and breast cancer patients are currently ongoing (Singh *et al.*, 2014; H. Zhang *et al.*, 2016).

2.4.3.1 Mechanisms for targeted activation of CAR T cells to reduce toxicities

Aside from targeting CD19, further promising targets for CAR T cell therapy of B cell malignancies are CD20, CD22 and the receptor tyrosine kinase-like orphan receptor 1 (ROR-1), which is a tumor-associated molecule expressed in B-lymphoid cancer but not on normal mature B cells (Müller *et al.*, 2008; Haso *et al.*, 2013; Hudecek *et al.*, 2013). Relapsed B cell malignancies are often accompanied with an antigen-loss on tumor cells likewise observed upon therapy with therapeutic antibodies (Davis *et al.*, 1999; Ruella and Maus, 2016). These patients have a very poor prognosis and novel approaches to treat and ideally prevent antigen-loss are strongly needed. Due to a large heterogeneity in the antigen pattern of leukemia, one strategy is to target two leukemic blast antigens simultaneously rendering CAR T cells more specific for tumor cells and consequently reducing ‘on-target off-tumor’ toxicities. Basically, there are at least three options to redirect T cells by CARs for targeting two antigens concurrently and preventing specific escape strategies of leukemic blasts:
First, administration of a mixture of two CAR T cell products, for example anti-CD19 and anti-CD22 CAR T cells. Second, infusion of T cells which co-express two independent CARs,

each of them competent to trigger T cell activation. Third, administration of T cells engineered with one bispecific CAR construct which is composed of two single-chain antibody fragments specific for two tumor antigens (Hegde *et al.*, 2013; Anurathapan *et al.*, 2014). The feasibility of targeting two antigens by a bispecific CAR was previously shown by Qin *et al.* for CD19- and CD22-positive B-ALLs (Qin *et al.*, 2015) and by Zah *et al*. for CD19 and CD20-positive B-ALLs (Zah *et al.*, 2016).

Another mechanism to functionally control CAR T cell intensity or off-tumor toxicity is based on the integration of an 'on-switch' molecule. Different to the strategy of inducing apoptosis and hence eradication of the engineered T cells, the 'on-switch' strategy implements a non-lethal control of CAR T cells by separating T cell activation signals or adding a switch molecule to enable T cell activation (Kloss *et al.*, 2012; Wu *et al.*, 2015; Juillerat *et al.*, 2016). Some studies confirmed an improved control of T cell activation by using antibody-based switch molecules, whereby tumor-targeting antibodies are specifically modified with a conjugate, such as fluorescein isothiocyanate (FITC) or biotin (FIGURE 5). CAR T cells are then redirected against this conjugate (Cao *et al.*, 2016; Ma *et al.*, 2016; Rodgers *et al.*, 2016). Ma et al. demonstrated a potent tumor antigen-specific efficacy of universal CAR T cells *in vitro* and *in vivo*, targeting CD19- and CD22-positive B cell malignancies (Ma *et al.*, 2016). Cao *et al*. confirmed this observation for targeting HER2-positive breast cancer *in vitro* and *in vivo* (Cao *et al.*, 2016). The modularity of this approach allows universal CAR T cells to target a wide range of tumor antigens or even T cell malignancies. CAR T cell therapy of T-ALL remains a challenge due to the shared surface antigen pool between normal and malignant T cells which could result in self-targeting and compromising the therapeutic ability. To circumvent autolysis of CAR T cells, Chen *et al*. demonstrated that genetically engineered NK cells can be used instead of T cells to target T cell malignancies. When targeting CD3 and CD5, a potent tumor-directed cytotoxicity of CAR NK cells was observed (K. H. Chen *et al.*, 2016; Chen *et al.*, 2017). Instead of using other competent immune cells, universal adapter CAR T cells could help to overcome the limitations of CAR T cell therapy for T cell malignancies. Therefore, the 'on-switch' mechanism of universal adapter CAR T cells represents an important progress to further improve the CAR T cell technology and its safety for clinical application.

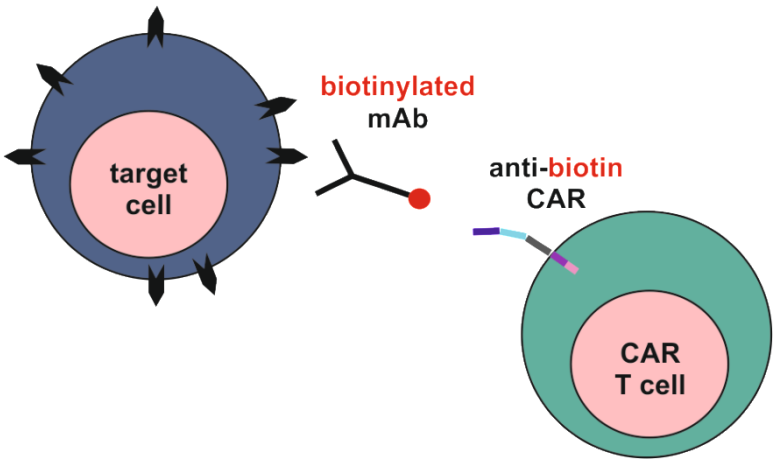

Figure 5: Universal adapter CAR system.

An adapter CAR system allows functional control over CAR T cell intensity via addition of an 'on-switch' molecule to initiate T cell activation. Antibody-based switch molecules are specifically modified with a conjugate, such as biotin or fluorescein isothiocyanate, and CAR T cells are redirected against this conjugate. The modularity of this universal system enables targeting of a wide range of tumor antigens and, hence, several cancer cell types. Figure based on Cao *et al.*, 2016; Ma *et al.*, 2016.

3. OBJECTIVES OF THE STUDY

Despite the enormous progress in cancer cell therapy over the last decades, AML and ALL are still two life-threatening diseases for children and adults. Therefore, new therapeutic approaches for AML and ALL are urgently needed.

Successful therapeutic approaches for AML are still limited due to the high heterogeneity of AML subtypes. Since malignant and normal myeloid cells share the same surface antigen pool, targeting of AML cell markers may also compromise hematopoiesis of normal blood cells. Hence, new pharmacological strategies with less off-tumor effects have to be proposed. In this study, a synergistic anti-leukemic effect of ATO and G-CSF was considered as a potential new pharmacological therapeutic approach for AML, since both drugs have been already studied for cancer cell therapy. The impact of ATO alone and in combination with G-CSF on AML cells and LSCs should be analyzed *in vitro* and *in vivo*. Based on previous findings that G-CSF might have an AQP9-stimulating effect, a resulting increased ATO sensitivity had to be further determined.

The improved outcome of newly diagnosed and relapsed ALL patients is not only due to a solid standard therapy but also to a massive progress in targeted therapy strategies. Especially the implementation of CAR T cells promises further improvements in future ALL therapy. However, heterogeneous tumor antigen pattern and severe therapy-associated complications demand further optimization of CAR T cell therapy. In this study, bispecific CAR T cells targeting CD19 and CD20 should be analyzed for eliminating a CD19-CD20-positive B-ALL patient sample *in vivo*. Furthermore, universal adapter CAR T cells targeting biotin-conjugated mAbs and mAb fragments should be tested for the capability of killing a CD19-positive B-ALL cell line *in vitro* and *in vivo*. In addition, adapter CAR T cells had to be analyzed for differentiation and exhaustion markers upon co-culture experiments *in vitro*. Universal CAR T cells should also be studied for their ability to kill γδ-TCR and CD231 (Talla-1)-positive T-ALL cell lines *in vitro*.

4. MATERIAL

4.1 Cell lines

Table 3: Cell lines

Cell line	Cell type/ DSMZ number	Media
HEK 293T	Embryonal kidney/ ACC 635	Complete DMEM GlutaMAX + 10 % fetal calf serum (FCS)
HL-60	Acute myeloid leukemia/ ACC 3	Complete RPMI 1640 media + 10 % FCS
Jurkat	T cell leukemia/ ACC 282	Complete RPMI 1640 media + 10 % FCS
Kasumi-1	Acute myeloid leukemia/ ACC 220	Complete RPMI 1640 media + 20 % FCS
KG-1a	Acute myeloid leukemia/ ACC 421	Complete RPMI 1640 media + 20 % FCS
Molt-14	T cell leukemia/ ACC 437	Complete RPMI 1640 media + 10 % FCS
Nalm-6	B cell precursor leukemia/ ACC 128	Complete RPMI 1640 media + 10 % FCS
U-937	Histiocytic lymphoma/ ACC 5	Complete RPMI 1640 media + 10 % FCS

4.2 Patient-derived primary leukemia and healthy donor cells

The patient-derived primary leukemia and the healthy donor (HD) cells were obtained from the University Children's Hospital Tübingen and the University Department of Medicine Tübingen with the informed consent and Institutional Review Board approval of the University Hospital Tübingen (#27/2008B01, 213/2014BO2).

Table 4: Patient-derived primary leukemia cells

Anonymous Patient ID	Cell type	Media
P17R	Pediatric acute myeloid Leukemia	Complete RPMI 1640 media + 10 % FCS
P18R	Pediatric acute myeloid leukemia	Complete RPMI 1640 media + 10 % FCS

P49S	Pediatric acute myeloid Leukemia, FAB M5	Complete RPMI 1640 media + 10 % FCS
P84D	Pediatric acute myeloid Leukemia, FAB M2	Complete RPMI 1640 media + 10 % FCS
P93A	Pediatric acute myeloid Leukemia, FAB M4	Complete RPMI 1640 media + 10 % FCS
P94H	Pediatric acute lymphoid leukemia	Complete RPMI 1640 media + 10 % FCS
1035	Adult acute myeloid leukemia	Complete RPMI 1640 media + 10 % FCS
1067	Adult acute myeloid leukemia	Complete RPMI 1640 media + 10 % FCS

4.3 NSG mice

The NOD.Cg-Prkdc^{scid}IL2rg$^{tmWjl/SzJ}$ (NSG) mice were obtained from The Jackson Laboratory (Bar Harbor, USA) and maintained under specific pathogen-free conditions in the research animal facility of the University of Tübingen, Germany, according to German federal and state regulations (Regierungspräsidium Tübingen, K4/13, K4/15 and §10a, 1.10.2012).

4.4 Cell culture media, sera, supplements

Table 5: Cell culture media, sera, supplements

Medium/serum/supplement for cell culture	Manufacturer
DMEM GlutaMAX™	Invitrogen Life Technologies, Karlsruhe, Germany
Fetal bovine serum (FCS)	Biochrom AG, Berlin, Germany
HEPES buffer (1M)	Sigma-Aldrich, Saint Louis, MO, USA
L-glutamine (200 mM)	Biochrom AG, Berlin, Germany
MACS buffer (Clini-MACS)	Miltenyi Biotec, Bergisch Gladbach, Germany
Opti-MEM® I Reduced Serum Medium	Invitrogen Life Technologies, Karlsruhe, Germany
Penicillin/Streptomycin	Biochrom AG, Berlin, Germany
RPMI 1640	Biochrom AG, Berlin, Germany

Stem line medium II	Invitrogen Life Technologies, Karlsruhe, Germany
Tex-MACS	Miltenyi Biotec, Bergisch Gladbach, Germany

4.5 Media and buffers

Table 6: Media and buffers

Medium/buffer	Composition
4 x LDS sample buffer	1 M Tris base pH 8.5 2 mM EDTA 8 % LDS 40 % glycerol 0.075 % CBB G 0.025 % phenol red
Bicine/Bis-Tris transfer buffer	25 mM Bicine 25 mM Bis-Tris pH 7.2, 1 mM EDTA 15 % methanol
Blocking buffer	5% SlimFast in TBS
Complete Dulbecco's Modified Eagle Medium (DMEM) GlutaMAX medium	DMEM GlutaMAX medium 10 % FCS 100 U/ml Penicillin 100 U/ml Streptomycin 2 mM L-Glutamine
Complete RPMI 1640 medium	RPMI 1640 medium 10 % FCS 100 U/ml Penicillin 100 U/ml Streptomycin 2 mM L-Glutamine 20 mM HEPES buffer
Complete stem line medium II	Stem line medium II 10 % FCS 100 U/ml Penicillin 100 U/ml Streptomycin 2 mM L-Glutamine
Dilution solution	distilled deionized water 0.1% Ultrapure HNO_3 0,2% Triton X-100

FACS buffer	PBS 5 % FCS 2 mM EDTA
Freezing medium	20 % DMSO 80 % human albumin 1:1 with cell culture media
MES buffer	50 mM MES 50 mM Tris base pH 7.3 0.1 % SDS 1 mM EDTA
RIPA buffer	50 mM Tris base pH 7.5 150 mM NaCl 1% (v/v) Triton X-100 0.1% (w/v) sodium dodecylsulfate 0.5% (w/v) sodium deoxycholate Complete Protease Inhibitor Cocktail EDTA-free, PhosStop phosphatase inhibitor
TBS-T buffer	TBS with 0.1 % Tween 20
Tex-MACS medium	Tex-MACS medium 10 µg/ml IL7 25 µg/ml IL15 1% P/S

4.6 Chemicals, reagents, solutions and cytokines

All general chemicals were attained by Sigma-Aldrich, Saint Louis, MO, USA; Carl Roth GmbH & Co. KG, Karlsruhe, Germany; AppliChem GmbH, Darmstadt, Germany; Merck KGaA, Darmstadt, Germany and VWR International GmbH, Darmstadt, Germany.

Table 7: Chemicals, reagents, solutions and gels

Chemical/reagent/solution/cytokine	Manufacturer
4x Annexin V buffer	eBioscience, San Diego, CA, USA
7-Aminoactinomycin D staining solution (7-AAD)	BD Biosciences, San Jose, CA, USA
Ampuwa® Water	Fresenius Kabi Deutschland GmbH, Bad Homburg, Germany
Annexin V 647 (1:20)	BioLegend, San Diego, CA, USA

Arsenic trioxide (Trisenox®) (1 mg/ml)	Teva Pharmaceutical Industries Ltd., Petach Tikva, Israel
Biocoll Separating Solution	Biochrom AG, Berlin, Germany
Bradford reagent	Bio-Rad Laboratories, Hercules, CA, USA
D-Luciferin synthetic	Sigma-Aldrich, Saint Louis, MO, USA
FACS Clean®	BD Biosciences, San Jose, CA, USA
FACS Flow®	BD Biosciences, San Jose, CA, USA
FACS Rinse®	BD Biosciences, San Jose, CA, USA
Granocyte® (G-CSF) (13/34 Mio. IE/ml)	Chugai Pharmaceutical Co., Ltd., Tokio, Japan
Hoechst 33342 (bisBenzimide H 33342 trihydrochloride)	Sigma-Aldrich, Saint Louis, MO, USA
Human serum albumin (HSA; 20 % solution for infusion)	CSL Behring GmbH, King of Prussia, PA, USA
IL15 (10 µg/ml)	Miltenyi Biotec, Bergisch Gladbach, Germany
IL7 (10 µg/ml)	Miltenyi Biotec, Bergisch Gladbach, Germany
Oligo(dT)18 Primer (SO131)	Thermo Fisher Scientific, Rockford, IL, USA
Phosphate buffered saline (PBS)	Sigma-Aldrich, Saint Louis, MO, USA
Random Hexamer Primer (SO142)	Thermo Fisher Scientific, Rockford, IL, USA
SlimFast	Unilever, London, UK
TransAct™	Miltenyi Biotec, Bergisch Gladbach, Germany
Trypan blue	Sigma-Aldrich, Saint Louis, MO, USA
XenoLight D-Luciferin	PerkinElmer, Waltham, MA, USA

4.7 Reaction Kits

Table 8: Reaction Kits

Reaction Kit	Manufacturer
BD Cytofix/Cytoperm™ Kit	BD Biosciences, San Jose, CA, USA
LightCycler® 480 SYBR Green I Master Kit	F. Hoffmann-La Roche AG, Basel, Switzerland
Lipofectamine® 3000 Transfection Reagent Kit	Thermo Fisher Scientific, Rockford, IL, USA
Omniscript Reverse Transcription (RT) Kit (200)	Qiagen, Hilden, Germany
RNeasy® Micro Kit	Qiagen, Hilden, Germany
Two-step cell cycle analysis Kit	ChemoMetec, Allerod, Denmark
WesternBright Sirius HRP substrate	Advansta Inc., Menlo Park, CA, USA
Zombie Aqua™ Fixable Viability Kit	BioLegend, San Diego, CA, USA

4.8 MACS® cell separating reagents

Table 9: MACS® cell separating reagents

Separation Kit	Manufacturer
CD33 MicroBeads, human	Miltenyi Biotec, Bergisch Gladbach, Germany
CD34 MicroBeads, human	Miltenyi Biotec, Bergisch Gladbach, Germany
CD4 MicroBeads, human	Miltenyi Biotec, Bergisch Gladbach, Germany
CD8 MicroBeads, human	Miltenyi Biotec, Bergisch Gladbach, Germany
LNGFR MicroBeads, human	Miltenyi Biotec, Bergisch Gladbach, Germany

4.9 Antibodies

4.9.1 Antibodies for FACS

Table 10: Antibodies for FACS

Antibody	Dilution	Clone	Isotype	Manufacturer
Anti-human CD10 PE-CF594	1:50	HI10A	Mouse BALB/c IgG1, κ	BD Biosciences, San Jose, CA, USA
Anti-human CD114 (G-CSFR) APC	1:25	LMM741	Mouse IgG1, κ	BioLegend, San Diego, CA, USA
Anti-human CD19 PE-Cy7	1:50	HI30	Mouse IgG1, κ	BioLegend, San Diego, CA, USA
Anti-human CD20 APC	1:20	2H7	Mouse IgG2b, κ	BioLegend, San Diego, CA, USA
Anti-human CD25 BUV737	1:20	2A3	Mouse BALB/c IgG1, κ	BD Biosciences, San Jose, CA, USA
Anti-human CD271 (LNGFR) FITC	1:10	ME20.4-1.H4	Mouse IgG1, κ	Miltenyi Biotec, Bergisch Gladbach, Germany
Anti-human CD279 (PD-1) APC	1:10	PD1.3.1.3	Mouse IgG2b, κ	Miltenyi Biotec, Bergisch Gladbach, Germany
Anti-human CD3 Brilliant Violet 711	1:25	SK7	Mouse IgG1, κ	BioLegend, San Diego, CA, USA
Anti-human CD3 Violet-Blue	1:10	BW264/56	Mouse IgG2a, κ	Miltenyi Biotec, Bergisch Gladbach, Germany
Anti-human CD33 APC	1:25	P67.6	Mouse IgG1, κ	BioLegend, San Diego, CA, USA
Anti-human CD34 PE-Cy7	1:50	8G12	Mouse IgG1, κ	BioLegend, San Diego, CA, USA
Anti-human CD4 BUV395	1:20	SK3	Mouse BALB/c IgG1, κ	BD Biosciences, San Jose, CA, USA
Anti-human CD45 PE-Cy7	1:50	HIB19	Mouse IgG1, κ	BioLegend, San Diego, CA, USA
Anti-human CD45 APC-H7	1:20	2D1	Mouse IgG1, κ	BD Biosciences, San Jose, CA, USA
Anti-human CD45 APC	1:25	REA747	Recombinant human IgG1	Miltenyi Biotec, Bergisch Gladbach, Germany

Anti-human CD45RA Brilliant Violet 785	1:20	HI100	Mouse IgG2b, κ	BioLegend, San Diego, CA, USA
Anti-human CD45RO PE	1:10	UCHL1	Mouse IgG2a, κ	Miltenyi Biotec, Bergisch Gladbach, Germany
Anti-human CD62L APC	1:10	145/15	Mouse IgG1, κ	Miltenyi Biotec, Bergisch Gladbach, Germany
Anti-human CD69 Brilliant Violet 785	1:20	FN50	Mouse IgG1, κ	BioLegend, San Diego, CA, USA
Anti-human CD8 APC-Vio770	1:10	BW135/80	Mouse IgG2a, κ	Miltenyi Biotec, Bergisch Gladbach, Germany
Anti-human CD95 PE-Vio770	1:10	DX2	Mouse IgG1, κ	Miltenyi Biotec, Bergisch Gladbach, Germany
Anti-human/mouse AQP9 AF350	1:50	polyclonal	Rabbit IgG	Bioss Antibodies, Woburn, MA, USA
Anti-mouse CD34 AF647	1:25	RAM34	Rat IgG2b	BD Biosciences, San Jose, CA, USA
Anti-mouse CD45 FITC	1:500	30-F11	Rat IgG2b, κ	BioLegend, San Diego, CA, USA
Anti-mouse CD45 APC-eFluor780	1:50	30-F11	Rat IgG2b	eBioscience, San Diego, CA, USA

4.9.2 Antibodies for Western blot

Table 11: Antibodies for Western blot

Antibody	**Dilution**	**Clone**	**Isotype**	**Manufacturer**
Anti-human AQP9 mAb, purified	1:25	G-3	Mouse IgG2a	Santa Cruz Biotechnology, Inc., Dallas, USA
Anti-human Caspase 3 polyclonal antibody (pAb)	1:200		Rabbit IgG	Santa Cruz Biotechnology, Inc., Dallas, USA
Anti-human Spectrin alpha chain mAb	1:1000	AA6	Mouse IgG1	Merck, Darmstadt, Germany

Anti-human Vinculin XP® mAb, purified	1:1000	E1E9V	Rabbit IgG	Cell Signaling Technology, Inc., Danvers, MA, USA
Anti-mouse IgG, pAb, HRP	1:5000		Goat IgG	Jackson ImmunoResearch, West Grove, PA, USA
Anti-rabbit IgG, pAb, HRP	1:10 000		Goat IgG	Abcam, Cambridge, UK

4.9.3 Antibodies for cell culture and mouse experiments

The working concentration of each antibody for *in vitro* experiments was 100 ng/ml, for mouse experiments see below.

Table 12: Antibodies for cell culture and mouse experiments

Antibody	Dose	Species/Clone	Isotype	Manufacturer
Anti-human γδ-TCR Biotin		REA591	Recombinant human IgG1	Miltenyi Biotec, Bergisch Gladbach, Germany
Anti-human CD19 4G7SDIE mAb Biotin	5-50 µg/mouse	Chimeric mouse/human Fc-optimized	IgG1	SYNIMMUNE GmbH, Tübingen, Germany
Anti-human CD19 4G7SDIE mAb unconjugated	5-50 µg/mouse	Chimeric mouse/human Fc-optimized	IgG1	SYNIMMUNE GmbH, Tübingen, Germany
Anti-human CD19 4G7SDIE Fab Biotin	15 µg/mouse	Chimeric mouse/human Fc-optimized	IgG1	SYNIMMUNE GmbH, Tübingen, Germany
Anti-human CD19 Biotin	50 µg/mouse	REA675	Recombinant human IgG1	Miltenyi Biotec, Bergisch Gladbach, Germany
Anti-human CD231 Biotin		SN1a	Mouse IgG1κ	Miltenyi Biotec, Bergisch Gladbach, Germany

4.10 Primer

All Primers were achieved from Eurofins, Ebersberg, Germany.

Table 13: Primer

Primer	Sequence 5'-3'
AQP9-V4 forward	AGCCACCTCTGGTCTTGCTA
AQP9-V4 reverse	ATGTAGAGCATCCCCTGGTG
β-actin forward	TTCCTGGGCATGGAGTC
β-actin reverse	CAGGTCTTTGCGGATGTC
Gli1 forward	CCAACTCCACAGGCATACAGGAT
Gli1 reverse	CACAGATTCAGGCTCACGCTTC
Gli2 forward	AAGTCACTCAAGGATTCCTGCTCA
Gli2 reverse	GTTTTCCAGGATGGAGCCACTT
TATA box binding protein (TBP) forward	TGCACAGGAGCCAAGAGTGAA
TBP reverse	CACATCACAGCTCCCCACCA

4.11 Provided Material

4.11.1 Mono- and bispecific CAR T cells

Anti-CD19-, anti-CD20- and anti-CD20-CD19 bispecific CAR T cells were provided by Prof. Dr. Hinrich Abken from the Center for Molecular Medicine Cologne, University of Cologne, Cologne, Germany as a part of a collaboration project. The monospecific CAR T cells were engineered as follows: anti-CD19scFv-Fc-CD28-CD3ζ and anti-CD20scFv-Fc-CD28-CD3ζ. The bispecific anti-CD20-CD19 CAR was obtained by linking the anti-CD19 and anti-CD20 scFvs by a $(glycin_4serin)_4$ linker. The anti-CD19 and anti-CD20 CARs, as well as the retroviral expression cassettes for the scFv-Fc-CD28-CD3ζ CARs were previously described in detail (Hombach *et al.*, 2001; Cooper *et al.*, 2003; Müller *et al.*, 2008; Koehler *et al.*, 2012).

4.11.2 Effluc-leukemia cell lines/ -vector

The enhanced firefly luciferase (effluc)-leukemia cell lines Nalm-6-effluc-mCherry, Molt-14-effluc-mCherry and Jurkat-effluc-GFP, all transduced with an effluc pCDH-EF1-MCS-T2A-copGFP or mCherry vector, and the effluc-vector itself were kindly provided and described in detail by Prof. Dr. Irmela Jeremias from the Department of Gene Vectors, Helmholtz Zentrum München, German Research Center for Environmental Health, Munich, Germany (Vick *et al.*, 2015).

4.11.3 Plasmids

All CAR plasmids were provided by Miltenyi Biotec (Bergisch Gladbach, Germany). CAR plasmids are engineered as follows: anti-CD19scFv-**SPACER**-TM-4-1BB-CD3ζ-F2A-LNGFR. #7-, #9- and #10 CARs differ in the spacer domain. #7 CAR has a long spacer: **hinge-C_H2-C_H3**; #9 CAR has a very short spacer composed of only the **hinge** region; #10 CAR has also a short spacer: **hinge-CD8**. Low-affinity nerve growth factor receptor (LNGFR) serves as a transduction marker. The envelope and packing (gag/pol) plasmids were also obtained by Miltenyi Biotec.

4.12 Equipment

Table 14: Equipment

Equipment	Manufacturer
ABX Micros CRP Cell Counter	Horiba Medical, Kyoto, Japan
Arsenic hallow cathode lamp	Thermo Fischer Scientific, Ulm, Germany
BD LSR II cytometer	BD Biosciences, San Jose, CA, USA
Bolt™ Mini Gel Tank	Thermo Fischer Scientific, Ulm, Germany
Caliper Life Science IVIS Spectrum imaging system	PerkinElmer, Waltham, MA, USA
Clean bench HERAsafe	Heraeus Holding GmbH, Hanau, Germany
Incubator HERA cell	Heraeus Holding GmbH, Hanau, Germany
LI-COR ODYSSEY® FC	LICOR Biosciences, Lincoln, NE, USA
LightCycler® 480 PCR machine	F. Hoffmann-La Roche AG, Basel, Switzerland
Mastercycler® nexus X2 PCR machine	Eppendorf AG, Hamburg, Germany
Mouse injection cage type B 32 mm 100680	G&P Kunststofftechnik, Kassel, Germany
Mouse injection cage type C 25 mm 100690	G&P Kunststofftechnik, Kassel, Germany
NanoDrop™ 2000	Thermo Fischer Scientific, Ulm, Germany
NucleoCounter® NC-3000™	ChemoMetec, Allerod, Denmark

Olympus IX50 inverse microscope	Olympus GmbH, Shinjuku, Tokio
Rotina 420R centrifuge	Hettich AG, Bäch, Switzerland
SOLAAR M Series AA Spectrometer	Thermo Fischer Scientific, Ulm, Germany
TE22 transfer tank	Hoefer, Holliston, MA, USA
Ultrasonic Homogenizer Sonopuls	Bandelin, Berlin, Germany
Wallac Victor 2 1420 Multilabel counter	PerkinElmer, Waltham, MA, USA

4.13 Consumables

Table 15: Consumables

Consumable	**Manufacturer**
Amersham™ Protran™ Premium 0.2 µm nitrocellulose membrane	GE Healthcare, Little Chalfont, UK
BD Plastipak™ 1 ml single syringe with cannula 45 x 12,7 mm (26 G)	BD Biosciences, San Jose, CA, USA
Capillary, natrium-heparin	Hirschmann GmbH & Co. KG, Eberstadt, Germany
C-Chip® Neubauer improved counting chamber	NanoEnTek Inc, Pleasanton, USA
Cell culture flasks	Greiner Bio-One GmbH, Frickenhausen, Germany
Cell culture plates	Greiner Bio-One GmbH, Frickenhausen, Germany
Cell strainer 45 µM	BD Biosciences, San Jose, CA, USA
Cryopreservation tubes	Corning GmbH, Kaiserslautern, Germany
LightCycler® 480 adhesive foil	F. Hoffmann-La Roche AG, Basel, Switzerland
LightCycler® 480 multi-well plate (96-well plate)	F. Hoffmann-La Roche AG, Basel, Switzerland
MACS® Columns (LS and MS Columns)	Miltenyi Biotec, Bergisch Gladbach, Germany
Microvette 500 potassium-EDTA	Sarstedt AG & Co., Nümbrecht, Germany

NC-Slide A8™	ChemoMetec, Allerod, Denmark
Pipette tips (10 µl)	Abimed GmbH, Langenfeld, Germany
Pipette tips (200 µl, 1 ml)	Sarstedt AG & Co., Nümbrecht, Germany
Polypropylene tubes (15 ml, 50 ml)	Greiner Bio-One GmbH, Frickenhausen, Germany
Polystyrene FACS tubes	BD Biosciences, San Jose, CA, USA
BD Microlance cannula 27G x ¾“ 0,4 x 19 mm	BD Biosciences, San Jose, CA, USA
Graphite cuvette	Thermo Fischer Scientific, Ulm, Germany
Safe-Lock tubes (0.5 ml, 1.5 ml, 2 ml)	Eppendorf, Hamburg, Germany
Bolt™ 4-12% Bis-Tris Plus gels, 15-well	Thermo Fisher Scientific, Rockford, IL, USA

4.14 Software

Table 16: Software

Software	**Manufacturer**
BD FACSDiva Software 6.1.3	BD Biosciences, San Jose, CA, USA
CorelDRAW X6	Corel GmbH, Munich, Germany
Graph Pad Prism 5.0	GraphPad Software
LightCycler® 480-Software	Roche, Basel, Switzerland
Living Image 4.5.2	PerkinElmer, Waltham, MA, USA
Microsoft Word, Excel, Power Point	Microsoft
NucleoView™ NC-3000 Software	ChemoMetec, Allerod, Denmark
ODYSSEY® image studio software version 4.1	LICOR Biosciences, Lincoln, NE, USA
Wallac 1420 manager component version 2.00.0.13	PerkinElmer, Waltham, MA, USA

5. METHODS

5.1 Isolation of peripheral blood mononuclear cells (PBMCs)

PBMCs were isolated from 1:1 diluted peripheral blood or bone barrow with PBS by Ficoll-Hypaque density gradient centrifugation. For that, two volume fractions of diluted blood or bone marrow were layered above one volume fraction of Ficoll-Hypaque and centrifuged at 500 *g* for 30 min at 20 °C without brake. Subsequently, the mononuclear cell layer was transferred into a new tube and washed twice with PBS. The isolated PBMCs were resuspended in PBS and kept on ice until further use.

5.2 MACS® immunomagnetic cell separation

Cells were MACS® immunomagnetic separated according to the manufacturer's protocol. Briefly, cells for separation were transferred into precooled MACS buffer prior to incubation with microbeads for 15 min on ice. After a washing step, cells were positively selected with a LS column and MidiMACS separator.

5.3 Determination of cell number

Cell numbers and vitality were determined using disposable C-Chip® Neubauer improved counting chambers and trypan blue. Trypan blue negative vital cells were counted in the four main squares. The cell concentration was calculated as indicated in the following formula:

$$\frac{\text{number of cells}}{\text{ml}} = \frac{\text{number of counted cells}}{\text{number of main squares}} \times \text{dilution factor} \times 10.000$$

5.4 Cell culture treatment with ATO/ G-CSF

Cells were plated in a concentration of 0.5x 10^6 cells/ml and treated with 10 ng/ml G-CSF, 0.5 – 2 µM ATO or with the combination of both for 24 – 120 h. For long incubation times, media were changed after 72 h and pharmaceuticals were freshly added. Cells were subsequently analyzed for cell viability (paragraph 5.8.3), for inhibition of the side populations as a model of AML-derived LSCs (paragraph 5.8.4), for cell cycle (paragraph 5.9), for proliferation (paragraph 5.10) as well as for AQP9 stimulation by FACS (paragraph 5.8.2) and by western blot (paragraph 5.11).

5.5 Lentivirus production

5x 10^6 HEK293T cells were plated in a 10 cm Petri dish one day before transfection with Lipofectamin®3000 according to the manufacturer's protocol with Opti-MEM® I reduced serum medium and 30 µg of the transgene (#7, #9, #10), 15 µg of the envelope (VSV-G) and 30 µg of the packing (gag/pol) plasmid. After two days, supernatants containing the produced lentiviruses were harvested and run through a 0.45 µM cell strainer prior to centrifugation at 4 °C, 20 000 *g* for 4 h and following snap freezing. Viruses were stored at -80 °C until use.

5.6 CAR T cell production

PBMCs from healthy volunteers were isolated (paragraph 5.1) and MACS® immunomagnetic separated for CD4/CD8-positive cells (paragraph 5.2). After transfer into Tex-MACS medium (1x 10^6 cells/ml), cells were stimulated with 1:100 TransAct™ according to the manufacturer's protocol. The next day, cells were transduced with thawed transgene containing lentivirus (paragraph 5.5) by spin inoculation at 32 °C, 800 *g* for 30 min. CAR T cells were expanded for six days until they were MACS® immunomagnetic separated for LNGFR positivity or directly used for experiments.

5.7 Co-cultivation of CAR T and leukemia cells

5.7.1 FACS-based cytotoxicity assay

CAR T cells and leukemia cells were co-cultivated with an E:T ratio of 1:1 with or without the addition of 100 ng/ml biotinylated mAb or mAb fragment. After 48 h, CAR T cells were analyzed by FACS for activity, exhaustion and differentiation surface markers as well as leukemia cells for viability (paragraph 5.8.1).

5.7.2 Luciferase activity-based cytotoxicity assay

CAR T cells and effluc-leukemia cells were co-cultivated with E:T ratios of 10:1 – 1:1 with or without the addition of 100 ng/ml biotinylated mAb as well as with 3 µg/ml/well D-luciferin. After 24 h, the luciferase activity in effluc-leukemia cells was measured based on luminescence signal detection with a Wallac victor2 1420 multilabel counter and an acquisition time of 1 s/ well at 37 °C.

5.8 FACS analyses

Samples were measured on a 14-colours LSR II cytometer, equipped with 4 lasers (488 nm blue, 640 nm red, 405 nm violet, 355 nm ultraviolet), and analyzed by using BD FACSDiva™ software. In any FACS analysis, vital mononuclear cells were selected, and doublets excluded based on scatter characteristics.

5.8.1 Immunofluorescent staining of cell surface antigens

For cell surface staining, 0.1 – 1x 10^6 cells were transferred into FACS tubes and washed once with FACS buffer. Fluorochrome-labelled antibodies were added to a final concentration of 1 – 5 µg/ml and incubated in the dark at 4 °C for 30 min. After that, cells were washed twice with FACS buffer. A subsequent additional staining with the live/dead discrimination marker Zombie Aqua (1:400) was performed for 30 min at 4 °C, followed by two washing steps with FACS buffer. All centrifugation steps were conducted at 400 *g* for 5 min.

5.8.2 Intracellular staining of AQP9

G-CSF-treated human healthy donor (HD) cells, mouse samples and ATO/G-CSF-treated AML cells were stained for intracellular AQP9 using BD Cytofix/Cytoperm™ kit according to the manufacturer's protocol. First, 0.5 – 1x 10^6 cells were stained for cell surface markers (CD33 APC, CD34 PE-Cy7, CD45 PE-Cy7 or mCD45-AF647) (paragraph 5.8.1) prior to the permeabilization/ fixation step using Cytofix/Cytoperm™ solution for 20 min at 4 °C in the dark, followed by two washing steps with Cytofix/Cytoperm™ wash buffer. Cells were subsequently stained with 1 µg anti-AQP9-AF350 for 30 min on 4 °C. After cells were washed twice with Cytofix/ Cytoperm™ wash buffer, a fixation prior to analysis was performed. All centrifugation steps were conducted at 400 *g* for 5 min.

5.8.3 Viability assay of ATO and G-CSF treated AML cells

For cell viability determination after ATO/ G-CSF treatment, 2.5x 10^5 cells were washed twice with freshly diluted 1x Annexin V buffer. Subsequently, cells were stained with 1:20 Annexin V AF647 in 1x Annexin V buffer for 20 min at room temperature in the dark according to the manufacturer's protocol. Without a previous washing step, 7-AAD was added in a final dilution of 1:50 and the cells were directly analyzed. All centrifugation steps were conducted at 400 *g* for 5 min. The data were analyzed as follows: viable cells are defined as 7-AAD$^-$/Annexin V$^-$, early apoptotic cells as 7-AAD$^-$/Annexin V$^+$ and late apoptotic cells as 7-AAD$^+$/Annexin V$^+$.

5.8.4. Hoechst 33342 staining for detection of stem cell-like side population

4x 10^6 of ATO-treated patient-derived AML cells (1x 10^6 cells/ml) were stained with 5 µg/ml Hoechst 33342 in DMEM medium at 37 °C for 2 h, while shaking every 20 min. After a centrifugation step at 2 °C, 400 *g* for 5 min, cells were stained for surface markers (CD45 PE-Cy7, mCD45 FITC) on ice for 30 min. Two more washing steps (2 °C, 400 *g*, 5 min) were performed before cells were analyzed by FACS.

5.9 Cell cycle analyses

Cell cycle analysis of ATO/ G-CSF-treated AML cells was performed with a NucleoCounter® NC-3000™, equipped with the NucleoView™ NC-3000 Software, and the two-step cell cycle analysis kit according to the manufacturer's protocol. 0.5x 10^6 cells were washed once with PBS, followed by a combined cell lysis and DAPI staining step (mixture of solution 12 and 10) for 5 min at 37 °C. A subsequent stabilization step was performed by adding solution 11. Measurement of DAPI fluorescence intensity, which correlates with the DNA content of the cells, allows the determination of G0/G1, S and G2/M cell cycle phases. Sub-G1 phase represents apoptotic/necrotic cells.

5.10 Proliferation assay

Proliferation analysis of ATO/ G-CSF-treated AML cells was performed using a ^{3}H-thymidin incorporation assay. For that, 5x 10^4 cells/ well were treated in a 96-well plate for 72 h and afterwards incubated with 14.8 kBq ^{3}H-thymidin/ well for 16 h. After washing three times with VE-water in vacuo, cells were dried for 24 h and resolved with a scintillation solution before measuring proliferation in counts per minute (cpm) with a MicroBeta LumiJET Microplate Counter.

5.11 Protein extraction and western blot analyses

All ATO/ G-CSF-treated samples were harvested, washed with precooled PBS and centrifuged at 300 *g* for 5 min. Cell pellets were homogenized in RIPA buffer by using ultrasonication for 10 s at 10% intensity. Subsequently, homogenates were incubated for 25 min on ice and mixed with glycerol to a final concentration of 10 %. Protein concentrations were measured spectrophotometrically using Bradford reagent. Western blotting was performed as follows: 30 µg of protein, mixed with 4x LDS sample buffer and 100 mM DTT, was heat denatured for 10 min at 70 °C prior to electrophoretic separation using Bolt™ 4-12% Bis-Tris Plus gels and MES running buffer. Proteins were transferred on 0.2 µm

Amersham™ Protran™ Premium nitrocellulose membranes using Bicine/Bis-Tris transfer buffer at 80 V for 2 h. Afterwards, membranes were blocked for 1 h with 5% SlimFast in TBS at room temperature and incubated overnight at 4 °C with primary antibodies diluted in TBS-T with 0.02% NaN_3. On the next day, membranes were washed with TBS-T and incubated with the respective horseradish peroxidase (HRP)/ fluorochrome-conjugated secondary antibodies diluted in TBS-T at room temperature for 1 h. For chemiluminescence detection, membranes were incubated for 2 min with HRP substrate. Chemiluminescence and fluorescence signals were detected using the LI-COR ODYSSEYFC® and quantified with ODYSSEY® image studio software version 4.1.

5.12 Quantitative real-time PCR

Total RNA was extracted from ATO/ G-CSF-treated AML cells by using the RNeasy® Micro Kit. RNA concentration was measured with a NanoDrop™ 2000. Complementary cDNA was synthesized from 500 ng of RNA with the Omniscript Reverse Transcription (RT) Kit (200). Quantitative RT-PCR (qRT-PCR) for AQP9, Gli1 and Gli2 was performed using LightCycler® 480 SYBR Green I Master Kit and LightCycler® 480 PCR-Cycler, the housekeeper genes β-actin or TBP served as controls. The results were analyzed with the comparative C_T ($\Delta\Delta C_T$) method.

5.13 Microarray studies of G-CSF-treated healthy volunteers

PBMC's RNA from healthy volunteers – either treated with 5 µg/kg recombinant human G-CSF for 3 days or not treated – was extracted using the RNeasy® Micro Kit. RNA concentration was measured with a NanoDrop™ 2000. Complementary cDNA was synthesized from 500 ng of RNA with the Omniscript Reverse Transcription (RT) Kit (200). Microarray studies were performed in cooperation with PD Dr. Gunnar Cario, Christian-Albrechts University Kiel.

5.14 Determination of ATO in murine peripheral blood by atomic absorption spectroscopy

The murine EDTA blood samples were stored at -20 °C before use. Inhomogeneous blood samples were treated with ultrasound for 10x 60 s. Samples were vortexed and diluted 1:10 with a dilution solution. The measurements were performed with an atomic absorption spectrometer (AAS) equipped with a graphite furnace and a FS95 furnace auto sampler. In the graphite furnace, samples were reduced to ashes at 1400 °C and atomized at 2400 °C.

An arsenic hollow cathode lamp operated at 193.7 nm and at 9 mA with a monochromatic spectral band pass of 0.5 nm. For the measurements, pyrolytically coated Omega Platform Extended Lifetime graphite cuvette and an argon carrier gas (purity of 99.998%) were used. 8 µl from the diluted sample was injected into the graphite atomizer to get the analytical signal. All results were obtained in peak height measurement mode using the method of standard addition. The results were obtained as mean values from 2-3 batches and each single value consists of a double determination from one batch.

5.15 Adoptive transfer and following treatment of AML cells in NSG mice

5.15.1 ATO treatment for inhibition of LSCs and AML cell growth

For the adoptive cell transfer, 2x 10^6 patient-derived AML cells were injected intravenously (i.v.) into 8-12 weeks old unirradiated NSG mice. When leukemia engraftment exceeded 1% in peripheral blood, mice were randomized to the treatment groups and daily intraperitoneally (i.p.) injected with 0.15 – 5 mg/kg ATO or PBS as a control (each group n = 2-7). Three weeks after starting the treatment, mice were euthanized, and the bone marrow and spleen were analyzed for leukemia burden and inhibition of side population by FACS (paragraph 5.8).

5.15.2 ATO/ G-CSF treatment for AML cell growth inhibition

2x 10^6 AML cells were injected i.v. into 8-12 weeks old, unirradiated NSG mice. Four days after leukemia inoculation, mice were randomized to the treatment groups and daily injected i.p. with 4 mg/kg ATO, 250 µg/kg G-CSF or with the combination of both (each group n = 6). Mice treated with PBS served as control. Three weeks after starting the treatment, mice were euthanized, and the bone marrow, spleen and peripheral blood were analyzed for leukemia engraftment, AQP9 expression and viability markers by FACS (paragraph 5.8) and western blot (paragraph 5.11).

5.16 G-CSF stimulation of AQP9 in NSG mice

For G-CSF stimulation of murine AQP9, mice were injected i.p. with 300 µg/kg G-CSF three times per week. After one week, mice were euthanized, and the bone marrow was analyzed for AQP9 by FACS (paragraph 5.8.2).

5.17 Analysis of CD19-CD20-positive ALL- and mono-/bispecific CAR T cell-transplanted NSG mice

For the *in vivo* study, 2x 10^6 B-ALL blasts, positive for CD19 and heterogeneous for CD20, were injected i.v. into unirradiated 8-12 weeks old NSG mice. Before starting the treatment, CAR T cells were thawed and cultivated in RPMI 1640 medium for 48 h at 37 °C. Mice were randomized to the treatment groups with n = 4-5 animals per group. Ten days after leukemia inoculation, mice were injected i.v. with either 2x 10^7 CAR T cells (each group n = 5) or served as controls (leukemia without CAR T cells, n = 4). Seven weeks after leukemia induction, mice were euthanized, and bone marrow and peripheral blood were analyzed for leukemia burden and CAR T cell expansion by FACS (paragraph 5.8). Additionally, paraffin sections of bone marrow from tibia were performed by Prof. Dr. Hinrich Abken, Univeristy of Cologne. Sections were stained by haematoxylin and eosin stain (H&E) and for human CD10 by immune histology. Microscope magnification for H&E staining is 20-fold, for human CD10 40-fold.

5.18 Bioluminescence imaging and analysis of ALL-effluc cells and adapter CAR T cell-transplanted mice

For bioluminescence imaging of mice, 0.5x 10^6 ALL-effluc cells were injected i.v. into 8 – 12 weeks old, unirradiated NSG mice. Mice received i.p. injections of 1.5 mg/mouse luciferin substrate resuspended in PBS. Afterwards, mice were anesthetized with isoflurane and imaged using a Caliper Life Science IVIS Spectrum imaging system. Five minutes after luciferin injection, unsaturated images with an acquisition time of 1 – 60 s were obtained. Luciferase activity was analyzed using Living Image Software. Six days after leukemia inoculation, mice were randomized to the treatment groups, transplanted i.v. with 1 – 25x 10^6 CAR T cells or/and daily injected i.p. with 15 – 50 µg/mouse biotinylated antibody or antibody fragment three times or once a week (each group n = 5). Two or three weeks after CAR T cell transplantation, mice were imaged again and afterwards euthanized to isolate bone marrow and peripheral blood. Analysis for leukemia and CAR T cell engraftment/activity were performed by FACS (paragraph 5.8).

5.19 Statistical analysis

Statistical analysis was performed with GraphPad Prism 6.00 for Windows. Statistical significance of data sets obtained by FACS, cell cycle, qRT-PCR and western blot analyses was determined by using one-way-ANOVA. P-values < 0.05 were considered as statistically significant with * $p < 0.05$, ** $p < 0.01$, *** $p < 0.001$.

6. RESULTS

6.1 Pharmaceutical-based therapy of AML cells with ATO *in vitro* and *in vivo*

Since effective AML therapy is still limited because of the heterogeneous subtypes of AML, new therapeutic approaches are urgently needed. In this study, ATO, which is an already FDA-approved drug for APL, was considered as a good drug candidate for different AML subtypes not only for APL therapy (Litzow, 2008). First, ATO needed to be tested *in vitro* for its effectiveness against different AML cell lines. For that, the pediatric cell line Kasumi-1 and the adult cell line KG-1a were cultivated with different concentrations of ATO (0.5 – 2 µM) for 72 h and analyzed for cell viability using 7-AAD/ Annexin V staining. KG-1a cells were further examined for side population modifications, as a model of AML-derived LSCs, by a FACS-based Hoechst 33342 staining. The results demonstrated that both cell lines were susceptible to ATO treatment, which led to a decreased cell viability in a dose-dependent manner (FIGURE 6A). Interestingly and in contrast to the reduced cell viability, a massive and dose-dependent increase of diploid (SP 2n) and tetraploid (SP 4n) side populations in KG-1a cells were observed indicating an expansion of the AML-derived LSCs upon ATO treatment (FIGURE 6B). Kasumi-1 cells were further analyzed for alterations of the Hedgehog signaling pathway by using qRT-PCR after 24 – 48 h of ATO incubation. Analyzing the transcription factors Gli1 (FIGURE 6C) and Gli2 (FIGURE 6D), results demonstrated that ATO treatment led to a slightly downregulation of both transcription factors after 48 h of incubation.

To further confirm the *in vitro* observed ATO cytotoxicity *in vivo*, $2x10^6$ previously *in vivo* expanded patient-derived AML cells were injected intravenously into unirradiated NSG mice, followed by daily intraperitoneal injections with 0.15 – 5 mg/kg ATO. Two anonymous patient-derived AML cells P84D (FIGURE 7) and P17R (FIGURE 9) were selected due to their fast engraftment kinetics *in vivo* and the existence of good-detectable stem cell-like side populations. Owing to difficulties in finding the right ATO dose for mice, a low dose of 0.15 mg/kg (human dose) and a high but good tolerable dose of 2.5 mg/kg were tested in the first *in vivo* experiment using the patient-derived AML cells P84D. After three weeks of treatment, mice were sacrificed and the ATO-dependent effect on leukemia cell growth (hCD45-positive cells) as well as on side populations (SP 2n/SP 4n) was determined in bone marrow and spleen by FACS. Compared to PBS-treated control mice, ATO did not demonstrate a beneficial anti-leukemic effect on leukemia burden in the bone marrow (FIGURE 7A) and showed just a slightly leukemia reduction in the spleen (FIGURE 7D). Similar to the *in vitro* results (FIGURE 6B), but with a much fewer intensity, ATO stimulated the proliferation of the splenic LSCs that resided within the side populations (FIGURE 7E+F),

whereas in the bone marrow, no differences were detectable between the treatment groups (FIGURE 7B+C).

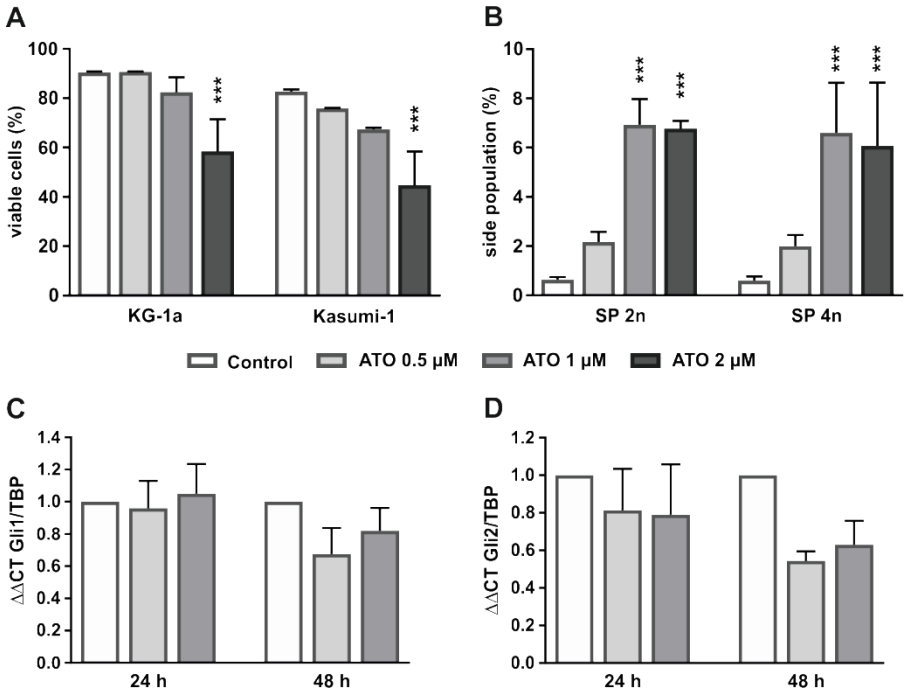

Figure 6: Anti-leukemic effect of ATO on AML cell lines KG-1a and Kasumi-1 *in vitro*.
AML cell lines KG-1a and Kasumi-1 were treated with ATO for 72 h and analyzed for cell viability. KG-1a cells were also screened for the percentage of side cell population and Kasumi-1 for alterations of the Hedgehog signaling pathway. Data are shown as means ± SD, n = 3. * $p < 0.05$, ** $p < 0.01$, *** $p < 0.001$ compared to control. (A) Cell viability of treated AML cells were measured by FACS analysis using 7-AAD/Annexin V staining. Viable cells were defined as 7-AAD/Annexin V double negative cells. B) ATO-dependent effects on KG-1a side populations (SP 2n/ SP 4n) were analyzed by FACS using Hoechst 33342 staining. (C+D) ATO-treated Kasumi-1 cells were screened for regulations of the Hedgehog signaling pathway analyzing the mRNA expression of the transcription factors Gli1 (C) and Gli2 (D) in relation to the TATA box binding protein (TBP) by qRT-PCR. Data were analyzed with the ΔΔCT method.

Because of the little impact of 0.15 mg/kg and 2.5 mg/kg ATO on P84D AML cell growth *in vivo* (FIGURE 7), non-transplanted mice were treated with different ATO doses (0.15 – 5 mg/kg) for seven days to find the right dosage for further mouse experiments. To evaluate the ATO bioactivity, peripheral blood of mice treated with 0.15 – 5 mg/kg was collected post-mortem and analyzed for their ATO content by atomic absorption spectrometer (AAS). The analysis showed that the ATO blood concentration in mice treated with 0.15 mg/kg of ATO was below the ATO detection level of AAS, while the treatment with 2.5 mg/kg and 5 mg/kg of ATO resulted in ATO blood concentrations of 76.38 µg/l (± 9.67 SEM) and 129 µg/l (± 10.15 SEM), respectively (FIGURE 8). The ATO concentration in peripheral blood of ATO-

treated patients is about 100 µg/l (internal control, not published) rendering 2.5 – 5 mg/kg ATO a good dose for further mouse experiments.

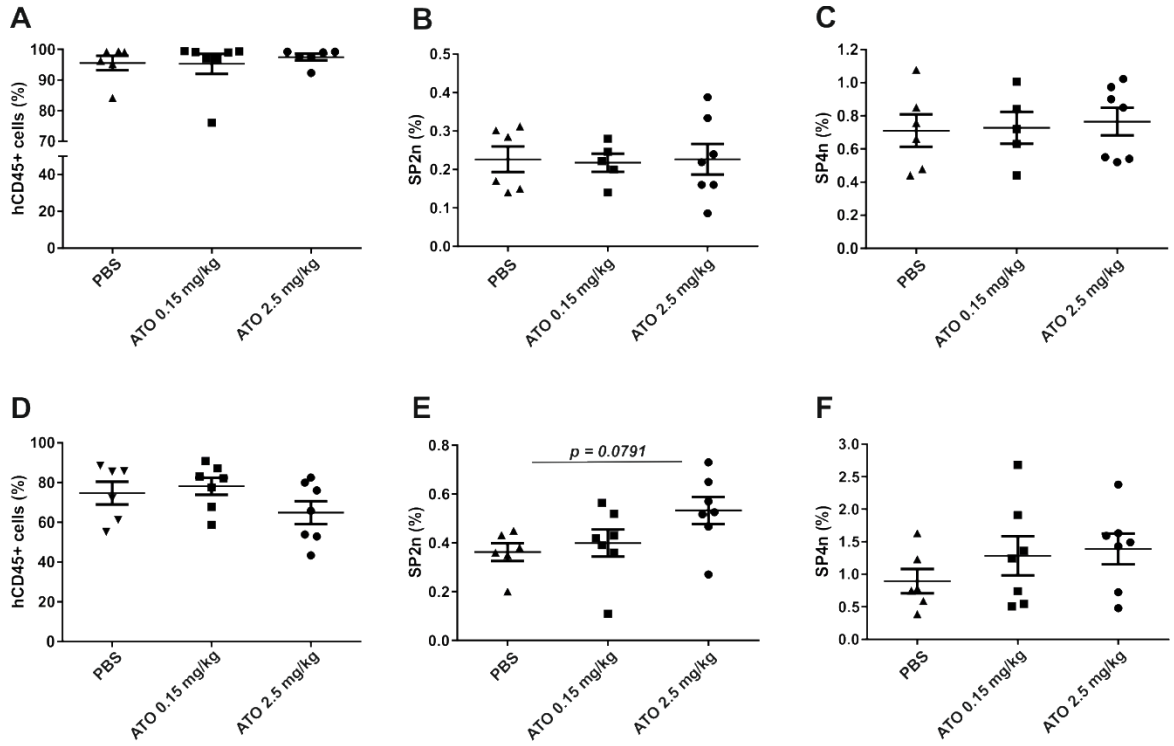

Figure 7: ATO treatment has no effect on AML patient sample P84D cell growth *in vivo*.
2x 10^6 AML patient cells (P84D) were injected intravenously into NSG mice. After leukemia burden exceeded 1% in peripheral blood, mice were daily injected intraperitoneally with 0.15 mg/kg or 2.5 mg/kg of ATO for three weeks. PBS treated mice served as controls. After euthanization, bone marrow (A–C) and spleen (D–F) were screened for leukemia cells (hCD45-positive cells) (A+D) and for inhibition of the diploid (SP 2n) (B+E) and tetraploid side population (SP 4n) (C+F) by FACS using Hoechst 33342 staining. Data are presented as means ± SEM of n = 6-7 per group.

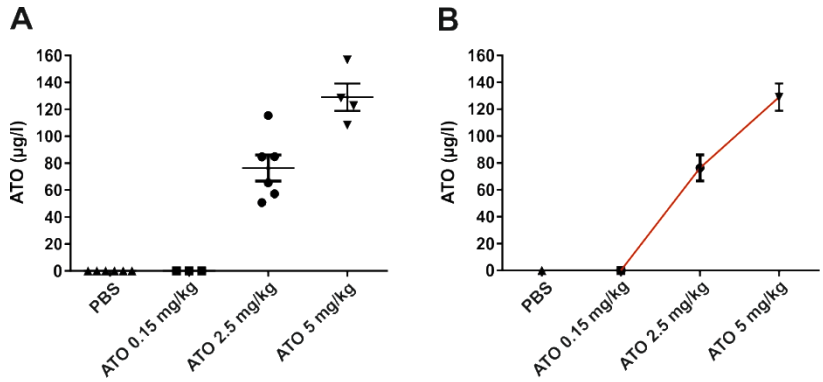

Figure 8: ATO concentration in murine peripheral blood.
Peripheral blood of PBS or 0.15 – 5 mg/kg ATO-treated mice were analyzed for ATO concentrations (µg/l) by AAS. Data are shown as means ± SEM of n = 3-6 per group.

In the second *in vivo* experiment, the patient-derived sample P17R was treated with ATO doses of 2.5 mg/kg and 5 mg/kg for three weeks. FACS-based analysis of the bone marrow demonstrated an obvious ATO dose-dependent decrease of the leukemia burden (hCD45-positive cells) (FIGURE 9A), whereas no differences were observed regarding the side populations (SP 2n/SP 4n) (FIGURE 9B+C). Despite successful leukemia reduction, treatment with the high dose of 5 mg/kg ATO caused severe side effects, such as apathy and disturbed escape response of the mice as well as local hyperkeratosis at the ATO injection site in two of three mice (FIGURE 9D). However, the ATO dose of 2.5 mg/kg was well tolerated. Therefore, in the following mouse experiments an ATO dosage between 2.5 – 4 mg/kg was used.

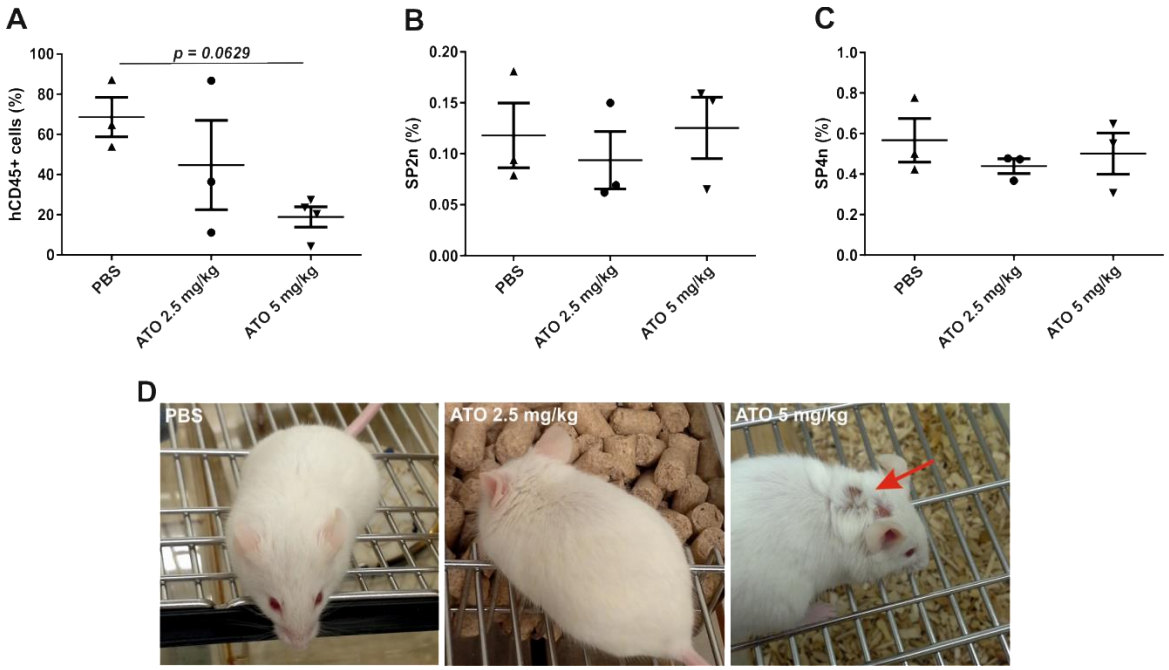

Figure 9: High dose ATO inhibits cell growth of AML patient sample P17R *in vivo*.
NSG mice were injected intravenously with 2x 10^6 AML patient cells (P17R). After leukemia burden exceeded 1% in peripheral blood, mice were daily injected intraperitoneally with 2.5 mg/kg or 5 mg/kg ATO for three weeks. PBS treated mice served as controls. Mice were sacrificed, and the bone marrow was analyzed for leukemia burden (hCD45-positive cells) (A) and for inhibition of the side population SP 2n (B) and SP 4n (C) by FACS using Hoechst 33342 staining. (D) ATO 5 mg/kg treatment caused severe side effects resulting in a local hyperkeratosis. Data are presented as means ± SEM of n = 3 per group.

6.2 Pharmaceutical-based targeting of AML cells with ATO and G-CSF

6.2.1 Synergistic effect of ATO and G-CSF induces apoptosis, cell cycle arrest and reduces proliferation in vitro

To increase the ATO sensitivity of AML cells and to reduce the ATO dose and accompanied side effects, combinatorial ATO treatment studies needed to be established. The cytokine G-CSF was considered as a good candidate because of its ability to potentiate differentiation, to promote quiescent AML cells for entering the cell cycle, as well as to increase ATO sensitivity potentially by stimulating the ATO transporter AQP9 (Kitagawa *et al.*, 2010; Iriyama *et al.*, 2012, 2013). Initially, to test a potential enhanced cytotoxic effect of ATO and G-CSF *in vitro*, the adult AML cell line U-937 and the pediatric AML cell line Kasumi-1 were incubated with 0.5 – 2 µM ATO, 10 ng/ml G-CSF and with a combination of both for 24 – 120 h. Cells were subsequently analyzed for cell viability using 7-AAD/Annexin V staining by FACS (FIGURE 10A+B) and for cell cycle progression with DAPI staining using a NucleoCounter® NC-3000™ (FIGURE 10C+D). Moreover, treated cells were examined for proliferation capacity by ^{3}H-thymidin incorporation assay using a MicroBeta LumiJET Microplate Counter (FIGURE 10E+F). Cell viability results demonstrated that ATO had a cytotoxic effect on both cell lines which led to a reduced number of viable cells after 48 h of treatment. Compared to control, the ATO-G-CSF combination showed a significantly increased cytotoxic effect after 72 h, compared to ATO alone after 96 h of treatment (FIGURE 10A+B). Consequently, the synergistic anti-leukemic effect of ATO and G-CSF was superior to ATO alone in inducing apoptosis of AML cell lines in a long-term *in vitro* treatment.

Cell cycle analyses after 72 h of treatment demonstrated that ATO affected all cell cycle phases (G0/G1, S, and G2/M), especially the S phase in both AML cell lines. In comparison to the control and ATO groups, a highly significant reduction of the S phase was detected upon combinatorial treatment with ATO and G-CSF. As a consequence, the sub-G1 phase (apoptotic cells) was significantly increased after ATO-G-CSF exposure (FIGURE 10C+D). In addition, the drug combination led to a G2/M phase arrest in U-937 cells (FIGURE 10C) and G0/G1 phase arrest in Kasumi-1 cells (FIGURE 10D). Thus, the combination of ATO and G-CSF was more efficient than ATO alone in inhibiting the cell division of AML cells *in vitro*. Proliferation assay results showed that ATO inhibited significantly the proliferation ability of both cell lines after 72 h of incubation. However, a superior effectiveness of the drug combination was only observed in U-937 cells. In Kasumi-1 cells, the combination appeared to ameliorate the effect of ATO alone (FIGURE 10E+F).

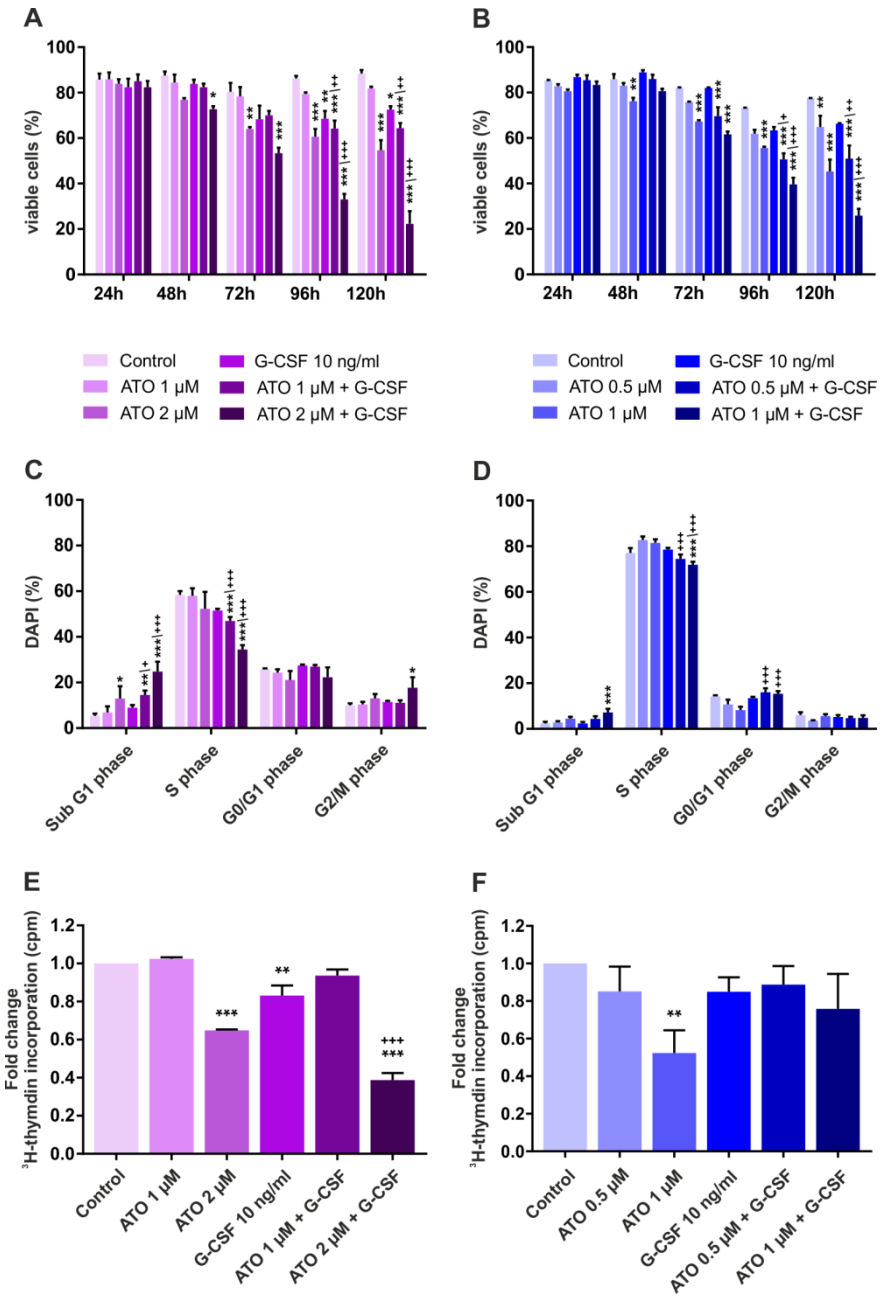

Figure 10: Synergistic anti-leukemic effect of ATO and G-CSF in AML cell lines U-937 and Kasumi-1 *in vitro*.

Viability assays, cell cycle and proliferation analyses of control and ATO-G-CSF-treated U-937 and Kasumi-1 cells. (A) Cell viability of treated AML cells was measured at different time points by FACS analysis using 7-AAD/Annexin V staining. Viable cells are defined as 7-AAD/Annexin V double negative cells. (B) Cell cycle differences of treated AML cells were evaluated by DAPI staining after 72 h of incubation and performed with a NucleoCounter® NC-3000™. (C) Proliferation analyses of treated AML cells using ^{3}H-thymidin incorporation assay were conducted after 72 h of incubation with a MicroBeta LumiJET Microplate Counter. Data are presented as means ± SD, n = 3. * $p < 0.05$, ** $p < 0.01$, *** $p < 0.001$ compared to control; $^{+}$ $p < 0.05$, $^{++}$ $p < 0.01$, $^{+++}$ $p < 0.001$ compared to ATO alone.

6.2.2 G-CSF induces AQP9 expression in AML cells in vitro

To further investigate an AQP9 expression-stimulating effect of G-CSF, which may have resulted in an increased ATO sensitivity and caused the enhanced synergistic anti-leukemic effect of ATO and G-CSF, U-937 and Kasumi-1 cells were primarily screened for the basal AQP9 and G-CSFR protein expression levels by western blot (FIGURE 11A+B) and FACS (FIGURE 11C). As indicated in FIGURE 11, AQP9 protein expression levels were comparable in both cell lines, while the expression level of G-CSFR was multifold higher in Kasumi-1 cells.

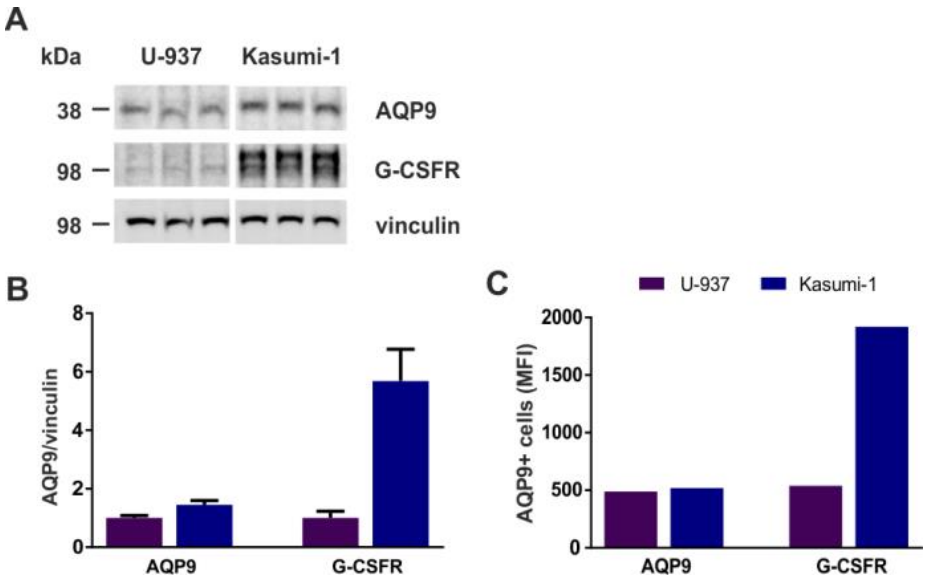

Figure 11: Basic protein expression levels of AQP9 and G-CSFR in U-937 and Kasumi-1 cells. (A+B) AQP9 and G-CSFR protein levels were analyzed by western blot. Protein expression was normalized to vinculin and represents means ± SD, n = 3. (C) AQP9 and G-CSFR expression levels were measured by FACS. Data are presented as mean fluorescence intensity (MFI).

To prove an AQP9 expression-stimulating effect of G-CSF *in vitro*, U-937 and Kasumi-1 cells were cultivated with 0.5 – 2 µM ATO, 10 ng/ml G-CSF and with a combination of both for 24 – 72 h. Cells were subsequently analyzed for AQP9 protein expression by western blot (FIGURE 12A+B) and FACS (FIGURE 12C+D), as well as Kasumi-1 cells for AQP9 mRNA expression by qRT-PCR (FIGURE 13). The analyses demonstrated that G-CSF induced an upregulation of AQP9 protein levels in both cell lines already after 24 h of treatment. However, the response to G-CSF differed between both cell lines. Kasumi-1 cells were much more prone to G-CSF's AQP9-stimulating effect compared to U-937 cells. Kasumi-1 cells showed significant increased AQP9 protein expression levels after 48 h of G-CSF incubation (FIGURE 12B+D). This AQP9 expression-inducing effect of G-CSF was also confirmed for AQP9 mRNA expression levels especially observed in combination with ATO (FIGURE 13).

Conversely, in U-937 cells, G-CSF just slightly increased the AQP9 protein levels after 48 h of incubation. Only G-CSF in combination with the highest ATO dose showed a significant upregulation of AQP9 expression observed in FACS analysis (FIGURE 12A+C).

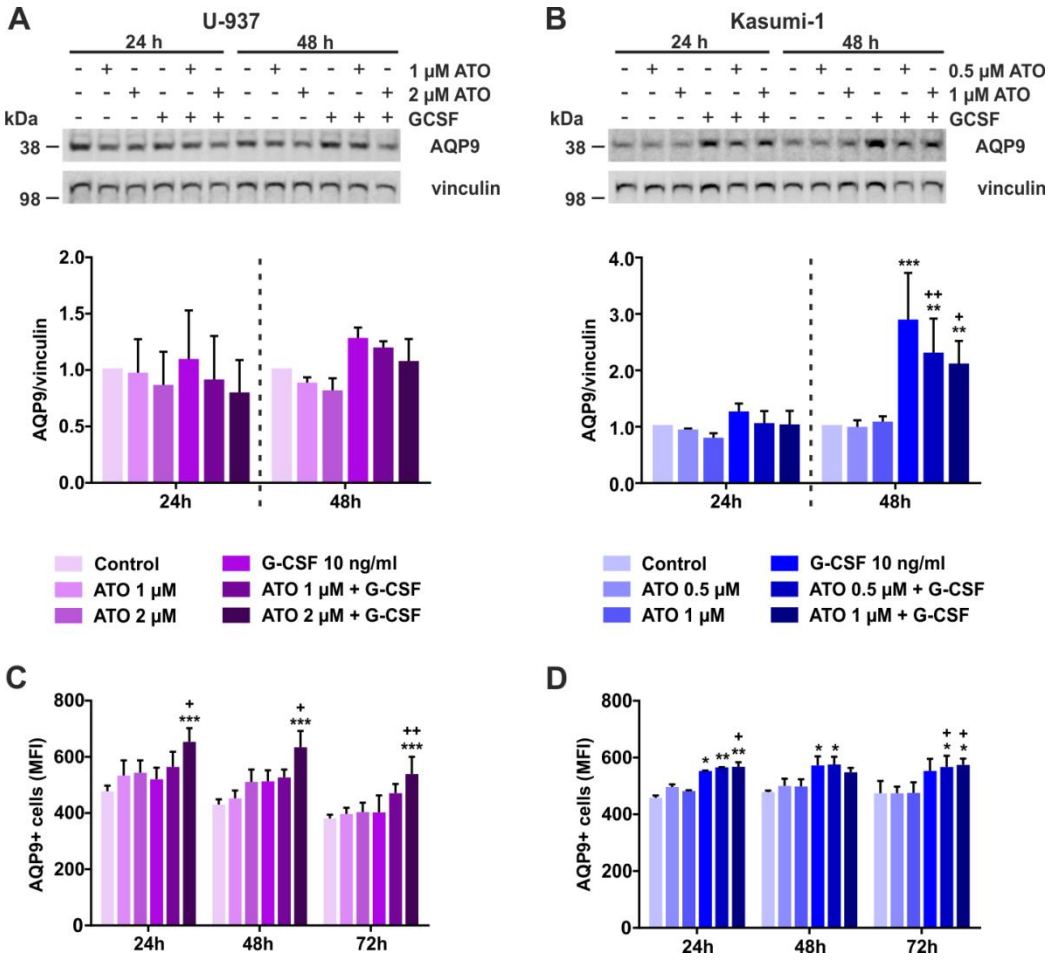

Figure 12: Increased AQP9 protein levels in G-CSF-treated U-937 and Kasumi-1 cells.
Data of U-937 cells is shown in A+C and of Kasumi-1 cells in B+D. (A+B) AQP9 protein levels of ATO-G-CSF-treated AML cells were analyzed by western blot. Protein expression was normalized to vinculin and is presented relative to the control of each time point. (C+D) AQP9 protein levels of ATO-G-CSF-treated AML cells were measured by FACS analysis. Data are presented as mean fluorescence intensity (MFI) and represent means ± SD, n = 3. * $p < 0.05$, ** $p < 0.01$, *** $p < 0.001$ compared to control; $^{+}$ $p < 0.05$, $^{++}$ $p < 0.01$, $^{+++}$ $p < 0.001$ compared to ATO alone.

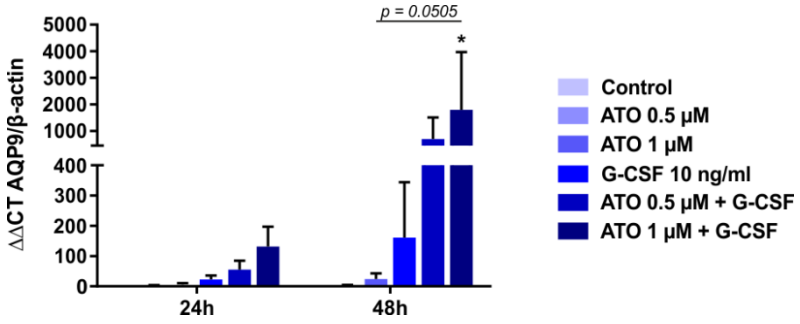

Figure 13: Increased AQP9 mRNA expression levels in ATO-G-CSF-treated Kasumi-1 cells.
AQP9 mRNA expression of ATO-G-CSF-treated Kasumi-1 cells was analyzed by qRT-PCR. AQP9 expression level was normalized to β-actin and analyzed with the ΔΔCT method. Data are presented as means ± SD, n = 3. * $p < 0.05$, ** $p < 0.01$, *** $p < 0.001$ compared to control.

6.2.3 Synergistic anti-leukemic effect of ATO and G-CSF in vivo

The *in vitro* observed synergistic anti-leukemic effect of ATO and G-CSF was also tested *in vivo*. For that, U-937 cells were selected as target cells because of their fast and predictable engraftment kinetics *in vivo*. The dose of 4 mg/kg ATO was designated as a good medication for mice due to previously measured ATO concentrations in murine blood by AAS (paragraph 6.1). 2x 10^6 U-937 cells were injected into unirradiated mice, followed by daily intraperitoneal injections of 4 mg/kg ATO, 250 µg/kg G-CSF or the combination of both for three weeks. Mice were sacrificed, and the bone marrow, peripheral blood and spleen were analyzed for leukemia burden (CD33-positive cells) by FACS (FIGURE 14A-C). The bone marrow was also screened for AQP9 expression levels as well as for the cell death markers α-spectrin and caspase-3 (CASP3) cleavage by western blot (FIGURE 14D-G).

The analysis showed that the combinatorial ATO-G-CSF treatment significantly reduced the number of engrafted CD33-positive leukemia cells in the bone marrow (FIGURE 14A) and in the peripheral blood (FIGURE 14B) compared to control and ATO alone. In the spleen, the combination of both drugs significantly decreased the leukemia burden compared to ATO alone (FIGURE 14C). However, treatment with G-CSF alone also led to diminished numbers of leukemia cells, which was especially evident in the peripheral blood and spleen (FIGURE 14B+C). The anti-leukemic effect of G-CSF was not clearly observed in the bone marrow (FIGURE 14A). In all three organs, the treatment with ATO alone stimulated the leukemia cell growth instead of reducing it (FIGURE 14A-C). The analysis for AQP9 expression in the bone marrow showed that the levels barely varied among the treatment groups (FIGURE 14D+E). Additionally, in the bone marrow, increased apoptotic markers 120 kDa α-spectrin and cleaved CASP3 confirmed the enhanced synergistic anti-leukemic effect of ATO and G-CSF compared to control and to each single drug (FIGURE 14D+F+G). Based on these

observations, the combination of ATO and G-CSF was superior to each single drug in preventing leukemia cell growth *in vivo.*

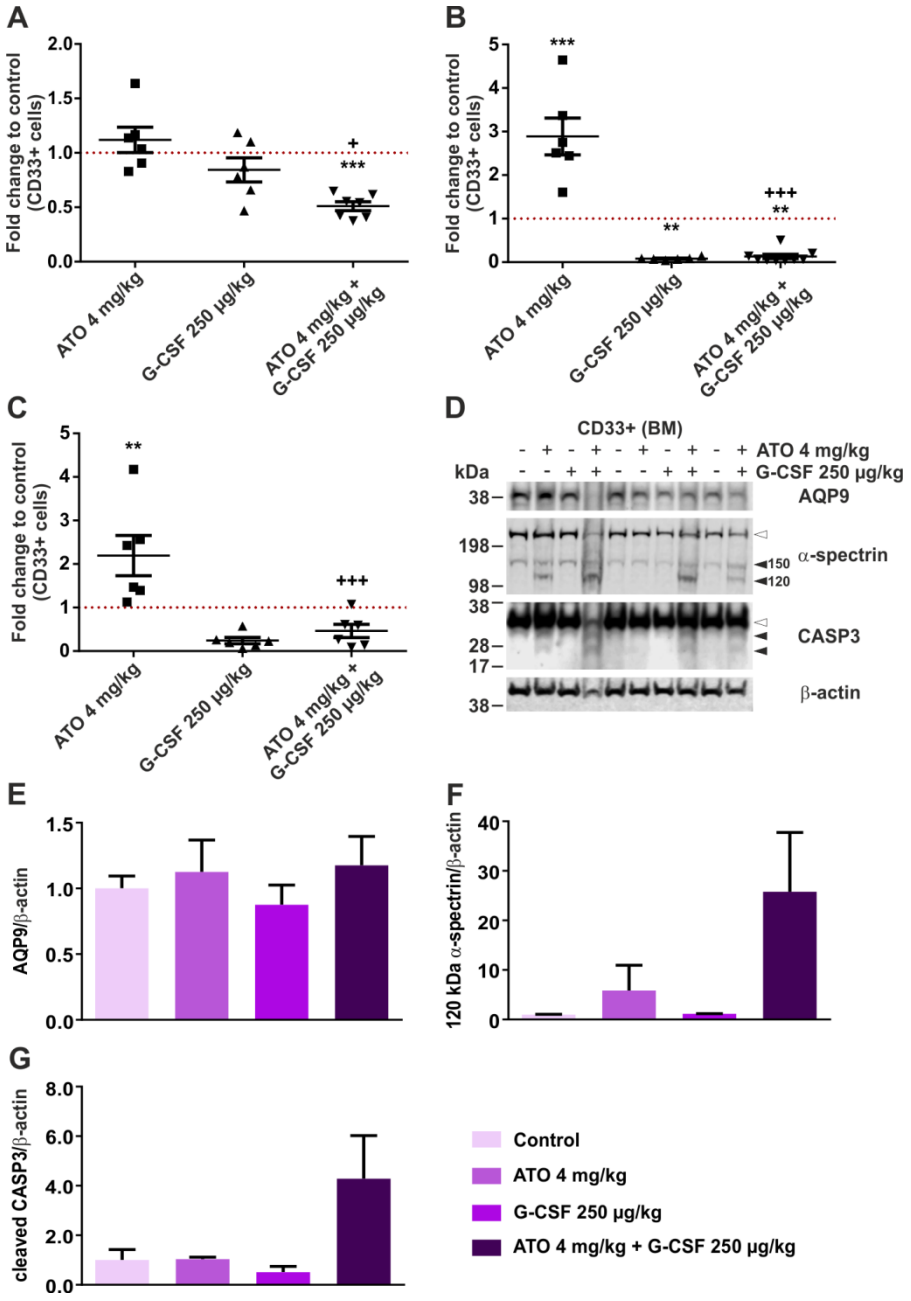

Figure 14: Synergistic effect of ATO and G-CSF inhibits leukemia cell growth *in vivo*.

2x 10^6 U-937 cells were injected intravenously into NSG mice. After four days, treatment with daily intraperitoneal injections of 4 mg/kg ATO, 250 µg/kg G-CSF or the combination of both were started for three weeks. PBS-treated mice served as controls. Mice were euthanized and bone marrow (BM) (A), peripheral blood (B) and spleen (C) were screened for U-937 leukemia cells (CD33-positive) by FACS. (D–G) CD33-positive isolated BM cells were analyzed by western blot for AQP9 expression (D+E), spectrin (full-length, 150 kDa-, 120 kDa-fragment) (D+F) and caspase-3 (CASP3) cleavage (full-length, cleaved 28kDa-fragment) (D+G). Protein expression was normalized to β-actin. (A–C) Data are presented as fold change to control, means ± SEM of n = 6 per group. (D–G) Data represent

pooled BM samples from three mice from two independent experiments. * $p < 0.05$, ** $p < 0.01$, *** $p < 0.001$ compared to control; $^{+}$ $p < 0.05$, $^{++}$ $p < 0.01$, $^{+++}$ $p < 0.001$ compared to ATO alone.

6.2.4 Treatment of AML patient samples with ATO and G-CSF

To prove the synergistic anti-leukemic effect of ATO and G-CSF also on patient-derived AML cells, freshly isolated PBMCs of adult AML patients were cultivated *in vitro* with 1 µM ATO, 10 ng/ml G-CSF and with the combination of both for 72 – 96 h. Harvested cells were subsequently analyzed for the cell count (FIGURE 15A+C+E) and AQP9 expression by FACS (FIGURE 15B+D+F). In only three of six patient samples (FIGURE 15), a slight cell count reduction was observed upon ATO-G-CSF treatment (FIGURE 15A+C+E). Regarding the AQP9 expression levels, no obvious upregulation was detected (FIGURE 15B+D+F).

Owing to the difficulties in growing patient-derived AML cells *in vitro*, previously *in vivo* expanded pediatric patient-derived AML cells were used to test the synergistic effect of ATO and G-CSF *in vivo*. For that, $2x\ 10^6$ P49S AML cells (FAB M5) were injected into unirradiated mice, followed by daily intraperitoneal injections of 4 mg/kg ATO, 250 µg/kg G-CSF or the combination of both for three weeks. Mice were sacrificed, and the bone marrow, peripheral blood and spleen were analyzed for leukemia burden (CD33-positive cells) (FIGURE 16A+B+C) as well as the bone marrow was screened for AQP9 expression levels (FIGURE 16D) by FACS. The results demonstrated a clearly reduced leukemic cell number in the bone marrow (FIGURE 16A), peripheral blood (FIGURE 16B) and spleen (FIGURE 16C) upon treatment with ATO and G-CSF compared to control and ATO alone. ATO alone did not show an anti-leukemic effect. However, G-CSF alone also inhibited the leukemia cell growth in all three organs, similar to that observed in the study with ATO-G-CSF-treated U-937 cells *in vivo* (paragraph 6.2.3; FIGURE 14). The bone marrow analysis revealed increased AQP9 expression levels upon G-CSF and ATO-G-CSF treatment compared to control and ATO alone (FIGURE 16D). Hence, the combination of ATO and G-CSF was capable to decelerate AML patient-derived cell growth *in vivo* while AQP9 was upregulated, but obviously without the need of ATO.

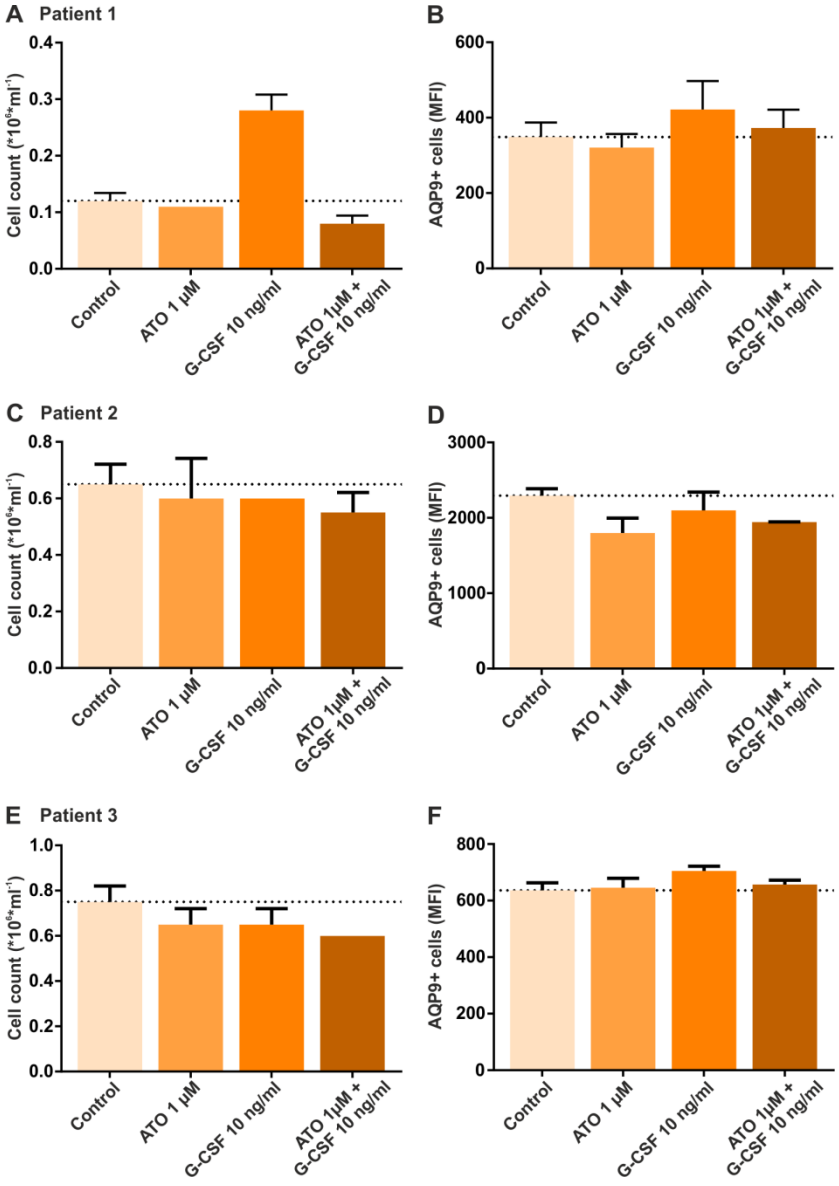

Figure 15: G-CSF tends to increase the toxicity of ATO in AML patient samples *in vitro*.

Cell count and AQP9 protein expression measurements were performed for AML patient samples. Three out of six with promising results are shown (A–F). Each sample was incubated with ATO/G-CSF for 72 h (patient 2 and 3) or 96 h (patient 1). Data are presented as mean ± SD, n = 2 for each patient. (A+C+D) Cell count was performed with trypan blue staining, absolute cell counts are shown. (B+D+F) AQP9 protein level was measured by FACS and is presented as mean fluorescence intensity (MFI).

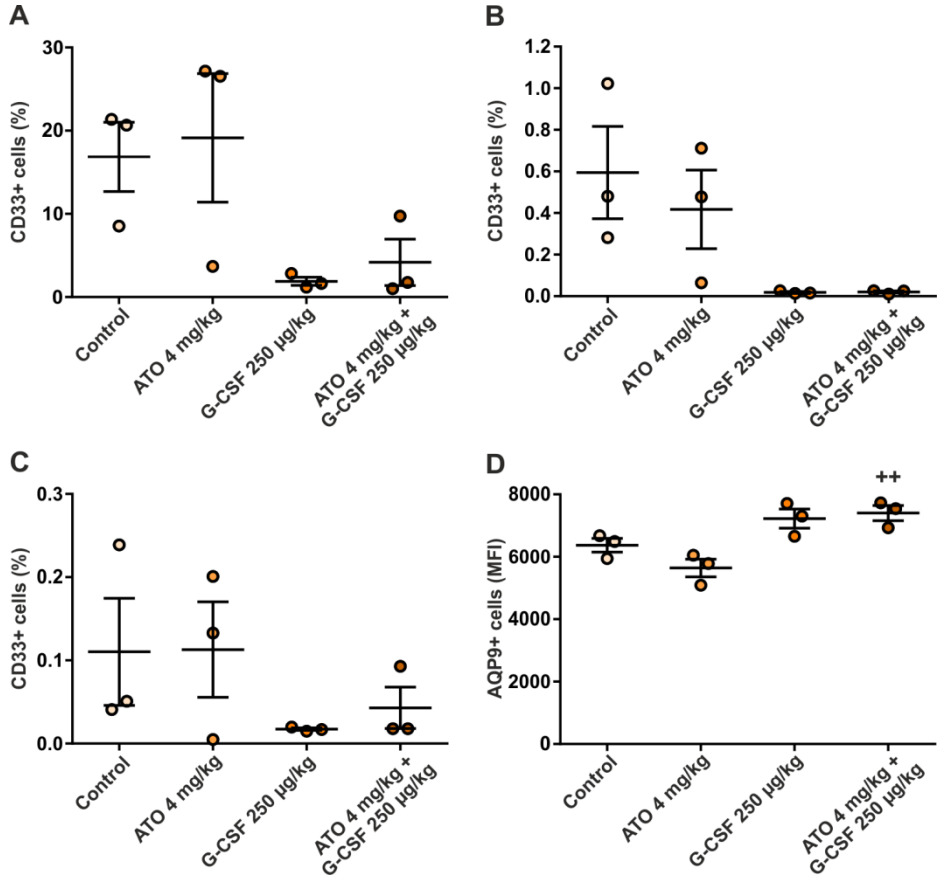

Figure 16: G-CSF inhibits cell growth of the AML patient sample P49S *in vivo*.

2x 10^6 AML patient cells (P49S) (FAB M5) were injected intravenously into NSG mice. After four days, daily intraperitoneal injections of 4 mg/kg ATO, 250 µg/kg G-CSF or the combination of both were started for three weeks. PBS-treated mice served as controls. Mice were euthanized, and bone marrow (A), peripheral blood (B) and spleen (C) were screened for leukemia cells (CD33-positive) by FACS. (D) Bone marrow was also screened for AQP9 expression by FACS and is presented as mean fluorescence intensity (MFI). Data are shown as means ± SEM of n = 3 per group. $^{+}$ $p < 0.05$, $^{++}$ $p < 0.01$, $^{+++}$ $p < 0.001$ compared to ATO alone.

To decrease the anti-leukemic effect of G-CSF as a single agent, the G-CSF medication was reduced from daily injections of 250 µg/kg to 300 µg/kg three times a week in the following mouse experiment. The ATO dosage was also reduced from daily injections of 4 mg/kg to 2.5 mg/kg. 2x 10^6 of patient-derived AML cells P93A (FAB M4) were injected into unirradiated mice, followed by daily intraperitoneal injections of 2.5 mg/kg ATO, 300 µg/kg G-CSF three times a week or the combination of both for three weeks. Mice were sacrificed, and the bone marrow, peripheral blood and spleen were analyzed for leukemia engraftment (CD33-positive cells) (FIGURE 17A+B+C). The bone marrow was screened for AQP9 expression levels by FACS (FIGURE 17D). In addition, bone marrow cells were also analyzed for their immature $CD34^{+}CD38^{-}$ immunophenotype (FIGURE 17E). The results show that the combination of ATO and G-CSF reduced the leukemia burden in the bone marrow (FIGURE

17A), peripheral blood (FIGURE 17B) and spleen (FIGURE 17C). The lower ATO dose resulted in a stimulation of leukemia growth in all three organs. Whereas, even a reduced dose of G-CSF also decreased the leukemia burden in all examined organs (FIGURE 17A+B+C) as observed in the study with ATO-G-CSF-treated P49S cell *in vivo* (FIGURE 16). The AQP9 expression level in the bone marrow was also significantly increased upon G-CSF and ATO-G-CSF treatment in comparison to control and ATO alone (FIGURE 17D). The analysis of bone marrow cells for the immunophenotype demonstrated that immature $CD34^+CD38^-$ cells were obviously reduced upon G-CSF and ATO-G-CSF treatment, while $CD34^-CD38^+$ cells were increased, and $CD34^+CD38^+$ slightly decreased compared to control and ATO alone groups (FIGURE 17E). Taken together, for the treatment of AML patient-derived cells, G-CSF alone was capable to decrease the leukemia growth *in vivo* while AQP9 expression was induced.

6.2.5 G-CSF modifies AQP9 expression in human and murine cells

To test whether the previously observed AQP9-stimulating effect of G-CSF on leukemia cells is generally applicable to non-cancerous human cells, healthy volunteers were treated with 5 µg/kg/day G-CSF for three days (FIGURE 18A) or healthy donor PBMCs were cultured in the presence of 10 ng/ml G-CSF *in vitro* for 72 h (FIGURE 18B). CD33-positive cells from peripheral blood of G-CSF-treated and non-treated healthy volunteers were analyzed by microarray analysis and AQP9 mRNA expression was evaluated. Data of G-CSF-treated volunteers were normalized to the untreated ones. Microarray results showed a massive and significant increase of AQP9 mRNA expression upon G-CSF treatment compared to non-treated control samples (FIGURE 18A). However, *in vitro* cultured and G-CSF-treated CD33- and CD34-positive cells of healthy donors did not demonstrate an increase in AQP9 protein expression level as measured by FACS (FIGURE 18B).

Therefore, the AQP9 expression-stimulating effect of G-CSF was further tested *in vivo* using NSG mice. For that, mice were treated with 300 µg/kg G-CSF three times a week for one week. Mice were sacrificed, and mouse CD45-positive bone marrow leukocytes (FIGURE 19A) as well as mouse CD34-positive hematopoietic stem cells were screened for AQP9 expression by FACS (FIGURE 19B). After one week of treatment, mouse CD45- and CD34-positive cells showed a significant increase of the AQP9 expression level upon G-CSF medication.

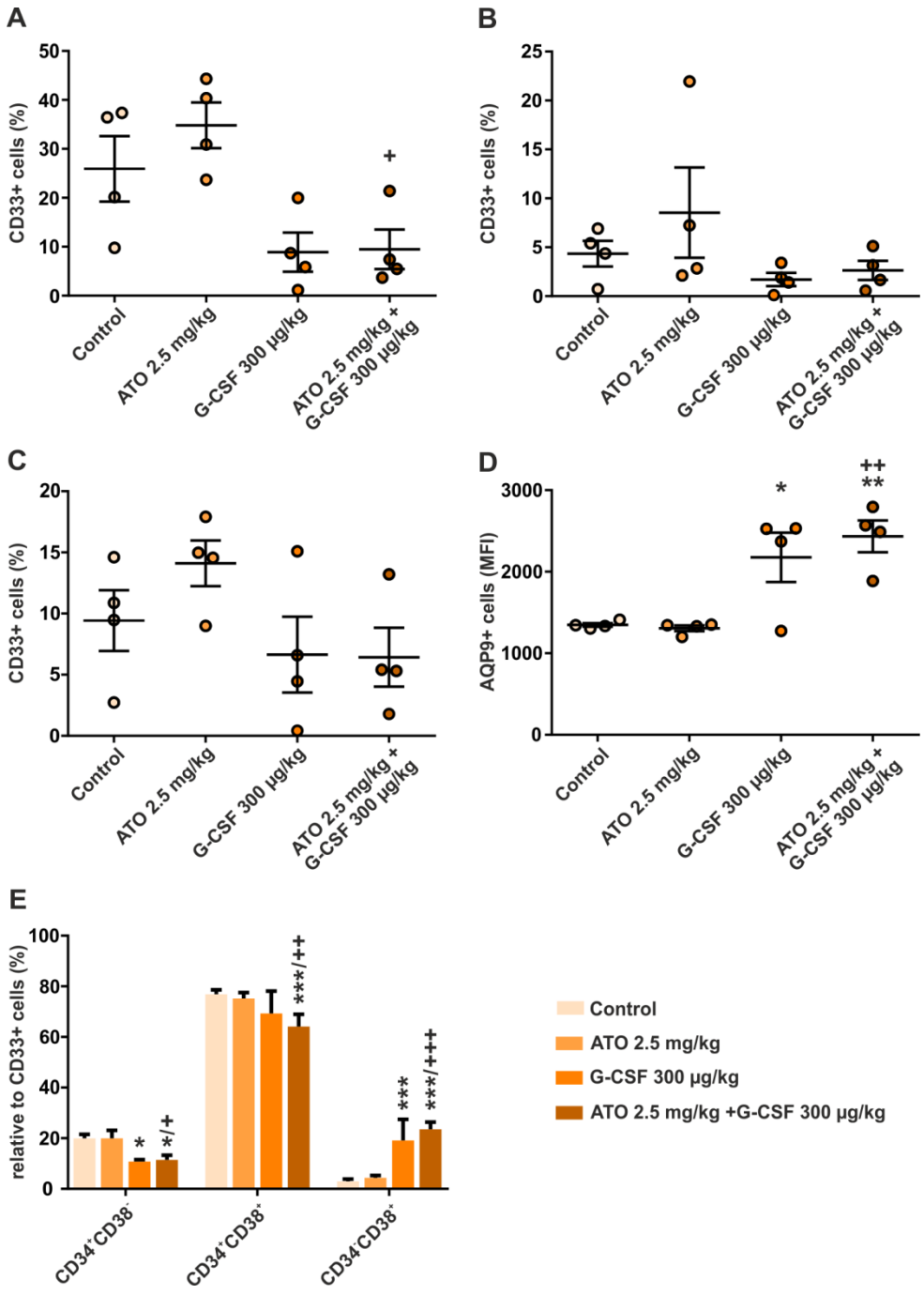

Figure 17: G-CSF inhibits AML patient sample P93A engraftment *in vivo*.

2x 10^6 AML patient cells (P93A) (FAB M4) were injected intravenously into NSG mice. After 14 days, daily intraperitoneal injections of 2.5 mg/kg ATO, three times a week 300 µg/kg G-CSF or the combination of both were started for three weeks. PBS-treated mice served as controls. Mice were euthanized, and bone marrow (A), peripheral blood (B) and spleen (C) were screened for leukemia CD33-positive cells by FACS. (D) Bone marrow was also screened for AQP9 expression by FACS and is presented as mean fluorescence intensity (MFI). Data are shown as means ± SEM of n = 3 per group. * $p < 0.05$, ** $p < 0.01$, *** $p < 0.001$ compared to control; $^{+}$ $p < 0.05$, $^{++}$ $p < 0.01$, $^{+++}$ $p < 0.001$ compared to ATO alone.

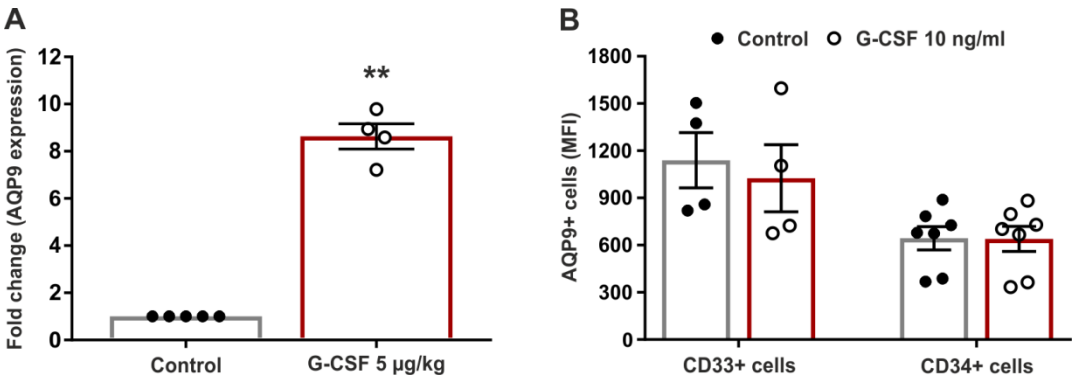

Figure 18: AQP9 expression levels in CD33+ cells of healthy volunteers treated or non-treated with G-CSF.

(A) Microarray analysis of AQP9 mRNA expression from CD33-positive cells of healthy individuals treated with 5 µg/kg/day G-CSF for three days compared to non-treated individuals. AQP9 expression of G-CSF-treated volunteers was normalized to controls without G-CSF treatment and is presented as fold change to control. (B) FACS analysis of AQP9 protein levels from healthy donor CD33- and CD34-positive cells treated daily with 10 ng/ml G-CSF for 72 h compared to control non-treated cells. AQP9 level is shown as mean fluorescence intensity (MFI). Data are presented as means ± SEM of n = 4-7 per group.

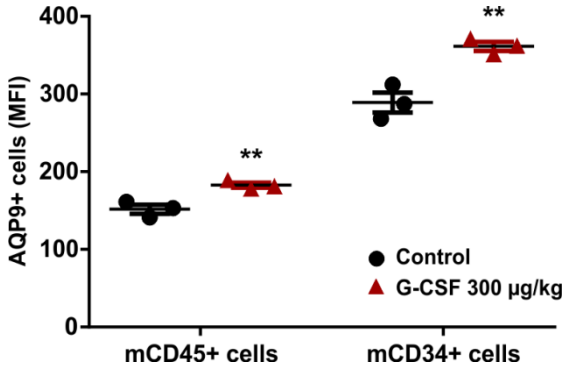

Figure 19: Increased murine AQP9 expression in bone marrow mCD45- and mCD34-positive cells.

NSG mice were injected intraperitoneally with 300 µg/kg G-CSF or PBS (control) three times a week for one week. Mice were euthanized, and bone marrow mouse CD45 (mCD45)-positive and CD34 (mCD34)-positive cells were screened for AQP9 expression by FACS, shown as mean fluorescence intensity (MFI). Data are presented as means ± SEM of n = 3 per group.

6.3 CAR T cell-based therapy of ALL cells

6.3.1 Monospecific anti-CD19 and bispecific anti-CD20-CD19 CAR T cells eradicate CD19-CD20-positive patient-derived B-ALL in vivo

Redirected CAR T cells are a novel highly promising approach for targeted immunotherapy of hematological malignancies, especially for ALL. Because of tumor antigen-loss during treatment, difficulties with heterogeneous tumor antigen patterns and severe therapy-associated complications, further optimization of CAR T cell therapy is absolutely necessary (Davila *et al.*, 2014; Ruella and Maus, 2016). To explore the power of bispecific CAR T cells in controlling leukemia with a heterogeneous antigen pattern, $2x\ 10^6$ of previously *in vivo* expanded pediatric patient-derived ALL cells (P94H) with a $CD19^+CD20^{+/-}$ phenotype were injected into unirradiated mice. Ten days later, $2x\ 10^7$ monospecific anti-CD19, anti-CD20 or bispecific anti-CD20-CD19 CAR T cells were inoculated. Mice injected with CAR T cells of irrelevant specificity and untreated mice served as controls (FIGURE 20+21). Mice were sacrificed after seven weeks, and bone marrow (FIGURE 20A+C) as well as peripheral blood (FIGURE 20B+D) were screened for leukemia burden (CD10-positive cells) and circulating CAR T cells (CD45-CD3-positive cells) by FACS. The results demonstrated that the $CD19^+CD20^{+/-}$ ALL cells were efficiently eliminated by the bispecific anti-CD20-CD19 and monospecific anti-CD19 CAR T cells in the bone marrow (FIGURE 20A) and peripheral blood (FIGURE 20B) compared to controls. In addition, the detection of these CAR T cells also confirmed highly active and circulating CAR T cells in the bone marrow and peripheral blood (FIGURE 20C+D). The monospecific anti-CD20 CAR T cells, however, did not show an anti-leukemic effect (FIGURE 20A+B) neither did they circulate in both tissues (FIGURE 20C+D).
Moreover, paraffin sections of the bone marrow from tibia of the CAR T cell-treated mice were stained with haematoxylin and eosin (H&E) and analyzed for human CD10 by immune histology (FIGURE 21). Bone marrow infiltration was markedly decreased by the bispecific and monospecific anti-CD19 CAR T cells compared to controls, which was also confirmed by FACS analysis (FIGURE 20). An anti-leukemic effect of anti-CD20 CAR T cells was also not observed in bone marrow sections.

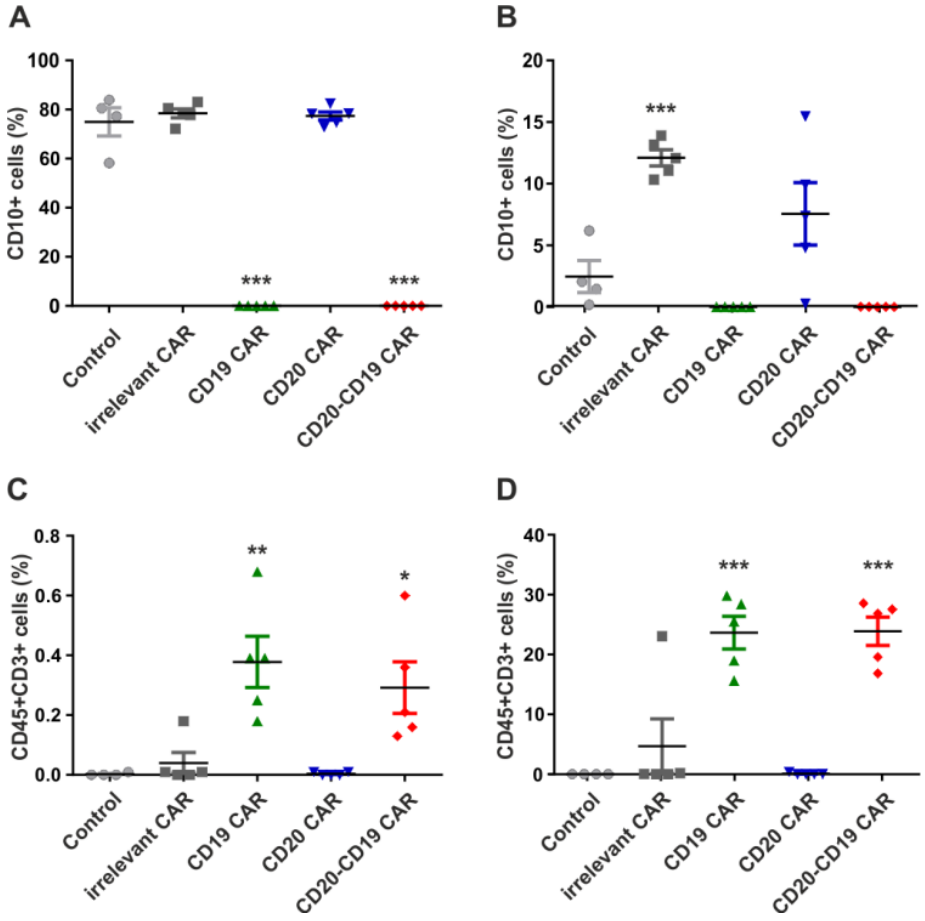

Figure 20: Monospecific anti-CD19 and bispecific anti-CD20-CD19 CAR T cells eradicate CD19-CD20-positive patient-derived ALL cells (P94H) *in vivo*.

NSG mice were transplanted intravenously with 2x 10^6 B-ALL patient cells (P94H). After ten days, 2x 10^7 CAR T cells engineered with an anti-CD19, anti-CD20 or anti-CD20-CD19 CAR construct were injected intravenously. As controls, mice received T cells with a CAR of irrelevant specificity or no T cells. Mice were sacrificed after seven weeks, and the bone marrow (A+C) and peripheral blood (B+D) were analyzed for leukemia cells (CD10-positive) (A+B) and for CAR T cells (CD45-CD3-positive) (C+D) by FACS. Data are presented as means ± SEM of n = 4-5 per group. * $p < 0.05$, ** $p < 0.01$, *** $p < 0.001$ compared to control.

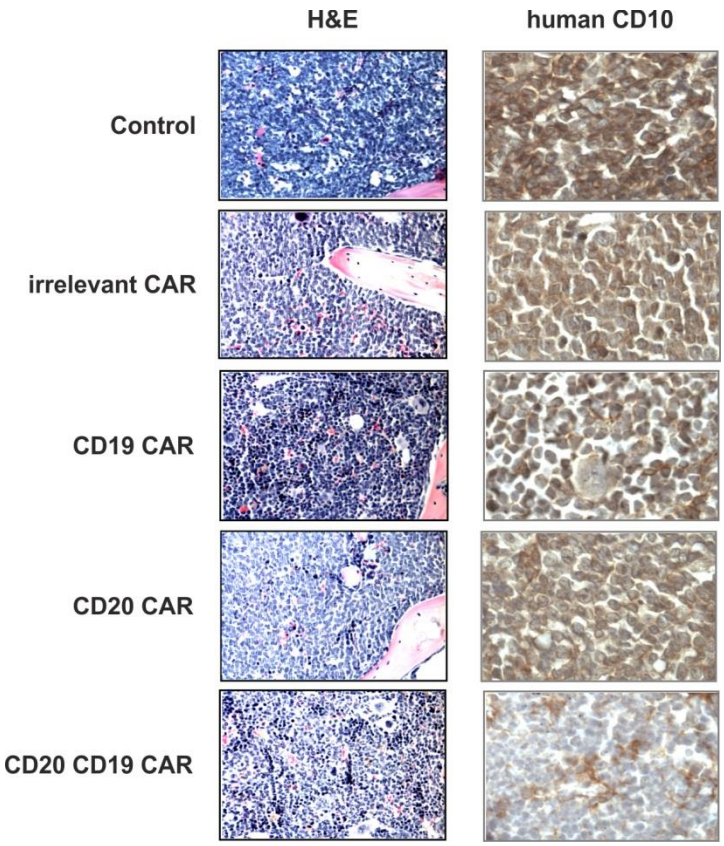

Figure 21: Paraffin sections of bone marrow from tibia.
Histology of the bone marrow of CAR T cell-treated mice transplanted with the human B-ALL P94H. Mice were sacrificed in week seven and paraffin sections of bone marrow from tibia were stained by haematoxylin and eosin stain (H&E) and for human CD10 by immune histology. Microscope magnification for H&E staining is 20-fold, for human CD10 40-fold.

6.3.2 Adapter CAR T cells specifically kill CD19-positive B-ALL cells in the presence of a biotinylated antibody in vitro

To control the CAR T cell intensity and off-tumor toxicities based on a non-lethal 'on-switch' strategy, the generation of universal adapter CAR T cells is a great improvement in optimizing CAR T cell therapy (Kloss *et al.*, 2012; Juillerat *et al.*, 2016). With the herein introduced universal adapter anti-biotin CAR T cells – targeting biotin-conjugated mAbs and mAb fragments – generally all kinds of tumor antigens which are accessible to mAbs can be targeted. Thus, this modularity allows approaching a wide range of tumors. In this study, anti-biotin CAR T cells (60 – 80 % positive for LNGFR as a CAR marker) were primarily tested *in vitro* against the CD19-positive B-ALL cell line Nalm-6 to evaluate the killing efficacy as well as the state of differentiation and exhaustion in the presence or absence of a biotinylated mAb. Moreover, several types of anti-biotin CAR T cells with different spacer length (#7-, #10- and #9 CAR with decreasing spacer lengths) and various forms of anti-CD19 mAbs

(unconjugated/ biotin-conjugated Fc-optimized 4G7SDIE (4G7) anti-CD19 mAb or Fab fragment and biotinylated anti-CD19 mAb clone REA675 (REA)) were tested (FIGURE 22). For that, enhanced firefly luciferase transduced Nalm-6 cells (Nalm-6-effluc-mCherry) were co-cultivated with different types of anti-biotin CAR T cells in a 1:1 E:T cell ratio and with various forms of mAbs for 48 h. A subsequent analysis revealed that #9 CAR T cells with a very short spacer length (spacer domain consists of only a hinge region) (FIGURE 22A) were much more effective in killing Nalm-6 cells in the presence of a biotinylated mAb than #7- and #10 CAR T cells with longer spacer length (#7 CAR spacer domain is composed of hinge-CH2-CH3, #10 CAR spacer consists of hinge-CD8) (FIGURE 22D). #9 CAR T cells efficiently killed the target cells when a biotinylated mAb was added, whereas the power of #7- and #10 CAR T cells was limited. As a consequence, only #9 CAR T cells were further analyzed for exhaustion (PD-1), activation (CD25, CD69) (FIGURE 22B) and differentiation markers (CD62L, CD45RA, CD45RO, CD95) upon co-culture experiments (FIGURE 22C). The analysis for exhaustion showed that PD-1 was upregulated after co-cultivation with biotinylated mAbs and Nalm-6 cells compared to unbiotinylated/ biotinylated mAbs or Nalm-6 cells alone. Based on the obviously increased activation markers CD25 and CD69, #9 CAR T cells were highly active after co-incubation with biotinylated mAbs and Nalm-6 cells. But the incubation with single biotinylated mAbs resulted in a light upregulation of the activation markers as well (FIGURE 22B). The analysis for the differentiation status of #9 anti-biotin CAR T cells showed a markedly decrease of naïve T cells ($CD62L^+CD45RA^+CD45RO^-CD95^-$) and increase of effector T cells ($CD62L^-CD45RA^+CD45RO^-CD95^+$) after co-cultivation with Nalm-6 cells and biotinylated mAbs in comparison to Nalm-6 cells or unbiotinylated/ biotinylated mAbs alone. The number of effector memory T cells ($CD62L^-CD45RA^-CD45RO^+$ $CD95^+$) increased upon cultivation with Nalm-6 cells independently of an absence or presence of a mAb, whereas central memory T cells ($CD62L^+CD45RA^-CD45RO^+CD95^+$) decreased upon stimulus of biotinylated mAbs and Nalm-6 cells. Number of T memory stem cells ($CD62L^+CD45RA^+$ $CD45RO^-CD95^+$) did not change upon treatment (FIGURE 22C). Taken together, #9 anti-biotin CAR T cells showed an efficient killing capability *in vitro* in the presence of biotinylated mAbs, which resulted in increased exhaustion and activation markers as well as in expansion of differentiated effector T cells.

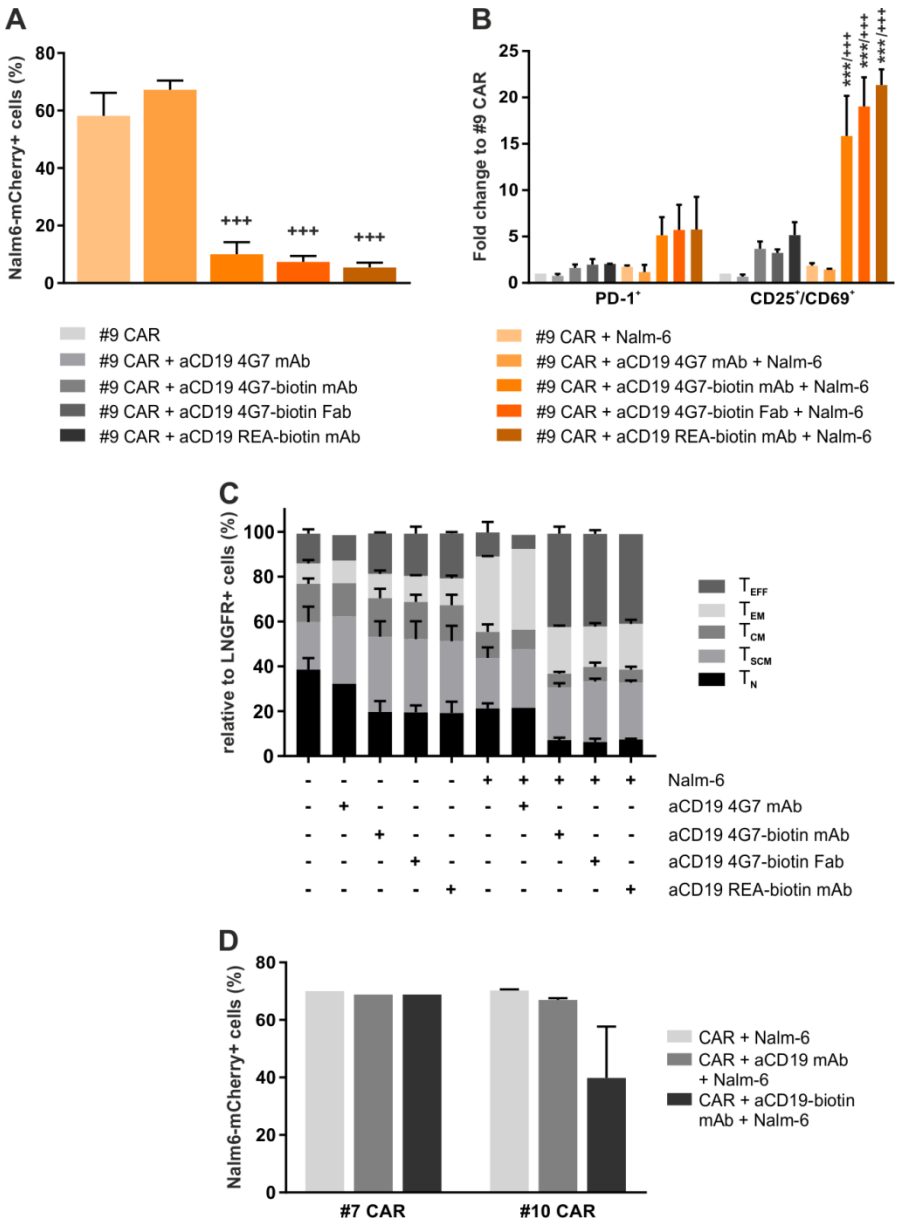

Figure 22: Adapter CAR system for targeting of CD19-positive B-ALL cell line Nalm-6-effluc-mCherry *in vitro*.

#9 CAR T cells were co-cultivated with or without 100 ng/ml of monoclonal antibody (mAb) (anti-CD19 (aCD19) 4G7SDIE (4G7), aCD19 4G7-biotin, aCD19 4G7-biotin Fab fragment, aCD19 REA675 (REA)-biotin) and with or without Nalm-6-mCherry cells for 48 h. (A) *In vitro* killing potency was analyzed by FACS. (B+C) #9 CAR T cells were screened for exhaustion ($PD\text{-}1^+$) and activation ($CD25^+/CD69^+$) (B) as well as for naivety markers (CD45RA, CD45RO, CD62L, CD95) (C) by FACS. Data are shown as means ± SD, n = 3. * $p < 0.05$, ** $p < 0.01$, *** $p < 0.001$ compared to #9 CAR; + $p < 0.05$, ++ $p < 0.01$, +++ $p < 0.001$ compared to CAR + Nalm-6. T_{CM}, central memory T cell ($CD62L^+CD45RA^-CD45RO^+CD95^+$); T_{EFF}, effector T cell ($CD62L^-CD45RA^+CD45RO^-CD95^+$); T_{EM}, effector memory T cell ($CD62L^-CD45RA^-CD45RO^+CD95^+$); T_N, naïve T cell ($CD62L^+CD45RA^+CD45RO^-CD95^-$); T_{SCM}, T memory stem cell ($CD62L^+CD45RA^+CD45RO^-CD95^+$).

6.3.3 Adapter CAR T cells specifically kill CD19-positive B-ALL cells in the presence of a biotinylated antibody in vivo

After validation of the specific killing capability in the presence of a biotinylated mAb *in vitro*, the universal adapter anti-biotin CAR T cells were further tested for their efficacy and specificity against the CD19-positive B-ALL cell line Nalm-6 *in vivo*. Despite not showing a high efficacy *in vitro* (FIGURE 22D), #7- and #10 anti-biotin CAR T cells were included in the *in vivo* experiments. For this purpose, unirradiated NSG mice were inoculated with 0.5x 10^6 Nalm-6-effluc-mCherry cells and six days later injected with 25x 10^6 freshly produced #9, #10 or #7 adapter CAR T cells. In addition, mice were treated with 50 µg/mouse of biotinylated anti-CD19 Fc-optimized 4G7SDIE mAb three times a week. Untreated mice as well as mice which were injected with #9 CAR T cells and additionally treated with a non-biotinylated anti-CD19 4G7SDIE mAb ("mock") served as negative controls. Monospecific CD19 CAR T cell-injected mice were used as positive controls. Three weeks after, mice were analyzed for leukemia burden by bioluminescence imaging prior to euthanization (FIGURE 23A+B). For post-mortem analysis, bone marrow was screened for leukemia cells (Nalm-6-mCherry-positive cells) (FIGURE 23C) and peripheral blood for circulating CAR T cells (LNGFR-positive cells) by FACS (FIGURE 23D). Bioluminescence imaging demonstrated a significantly reduced signal of Nalm-6-effluc-mCherry cells in all CAR T cell injected mice compared to untreated mice, regardless of the previously treatment with a biotinylated or non-biotinylated mAb (FIGURE 23A+B). Likewise, analysis of the bone marrow by FACS confirmed that leukemia was non-specifically eradicated by the adapter CAR T cells in all CAR T cell-transplanted mice (FIGURE 23C). Examining the peripheral blood, circulating CAR T cells were evident in all CAR T cell-inoculated mice, even in the mock mice which were treated with an unbiotinylated mAb. However, the number of #7 CAR T cells in the peripheral blood was reduced in comparison to #9- and #10 CAR T cells. This observation led to an exclusion of #7 CAR T cells in further *in vivo* experiments (FIGURE 23D).

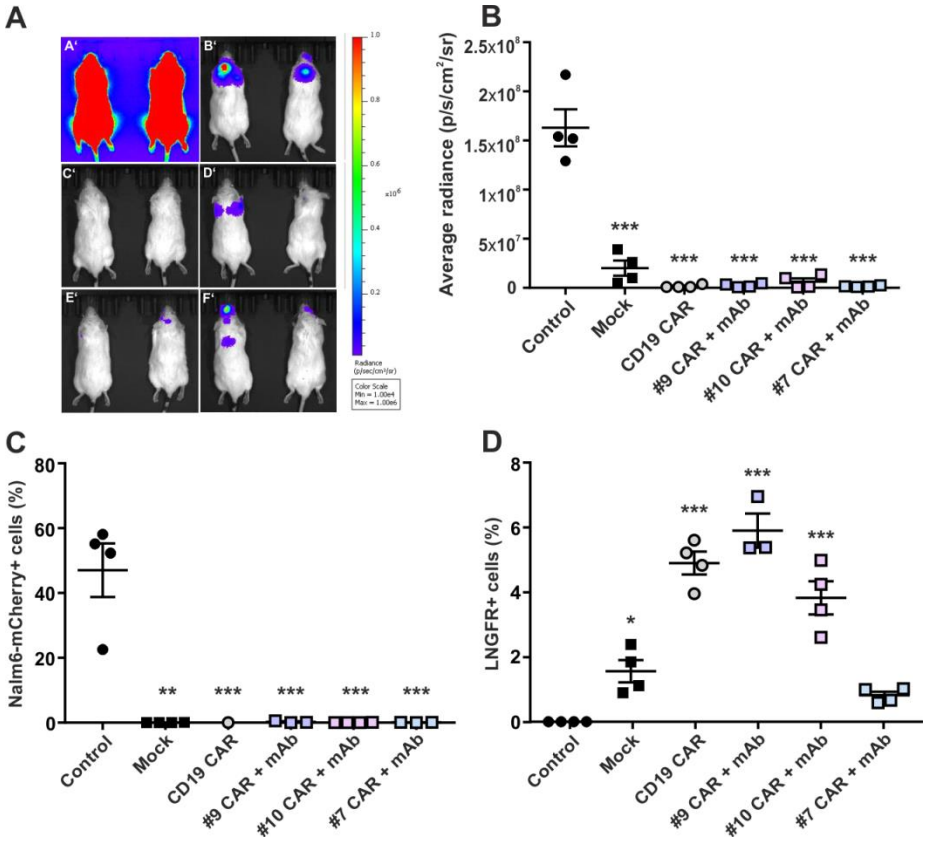

Figure 23: Adapter CAR system for targeting of CD19-positive B-ALL cell line Nalm-6-effluc-mCherry with the mAb anti-CD19 4G7SDIE-biotin *in vivo*.

NSG mice were injected intravenously with 0.5x 10^6 Nalm-6-effluc-mCherry cells. Six days after leukemia inoculation, mice were randomized to the treatment groups, transplanted intravenously with 25x 10^6 CAR T cells or/and injected intraperitoneally with 50 µg/mouse biotinylated CD19 mAb three times a week. Three weeks after CAR T cell transplantation, mice were imaged bioluminescently (A+B) and euthanized to screen for leukemia burden in the bone marrow (C) and for CAR T cell expansion in the peripheral blood (D) by FACS. Data are presented as means ± SEM of n = 3-5 per group. * $p < 0.05$, ** $p < 0.01$, *** $p < 0.001$ compared to control. A' control, B' mock, C' anti-CD19 CAR, D' #9 CAR + mAb, E' #10 CAR + mAb, F' #7 CAR + mAb.

To minimize unspecific CAR T cell activity in the following mouse experiment, the amount of inoculated CAR T cells were markedly reduced from 25x 10^6 to 2x 10^6. In addition, the biotinylated 4G7SDIE Fab antibody was used instead of the prior applied 4G7SDIE mAb to avoid any potential interaction between the Fc domain within the CAR spacer and the Fc receptor-bearing myeloid cells, which might result in a proinflammatory immune response. Like in the preceding *in vivo* experiment, unirradiated NSG mice were injected with 0.5x 10^6 Nalm-6-effluc-mCherry cells and six days later inoculated with 2x 10^6 freshly produced #9- and #10 adapter CAR T cells. In addition, mice were treated daily with 15 µg/mouse biotinylated anti-CD19 4G7SDIE Fab antibody. Untreated mice as well as mice treated only with anti-CD19 4G7SDIE Fab served as controls. Three weeks later, mice were analyzed for

leukemia burden by bioluminescence imaging (FIGURE 24A+B) as well as the bone marrow was screened for leukemia cells (FIGURE 24C) and peripheral blood for CAR T cells (FIGURE 24D). Similar to preceding observations, bioluminescence imaging demonstrated that adapter CAR T cells did not specifically kill the Nalm-6 cells in the presence of a biotinylated Fab. All CAR T cell-transplanted mice showed a reduced leukemia burden, especially mice which were injected with #9 CAR T cells (FIGURE 24A+B). FACS analysis of the bone marrow confirmed the bioluminescence imaging results. CAR T cells alone were able to inhibit leukemia cell growth *in vivo*, regardless of the presence or absence of a biotinylated mAb (FIGURE 24C). Both bioluminescence imaging and FACS indicated that also the biotinylated Fab alone was able to decelerate leukemia cell growth *in vivo* (FIGURE 24A+B+C). Based on FACS results, CAR T cells were evident in the peripheral blood but only in a low amount (FIGURE 24D).

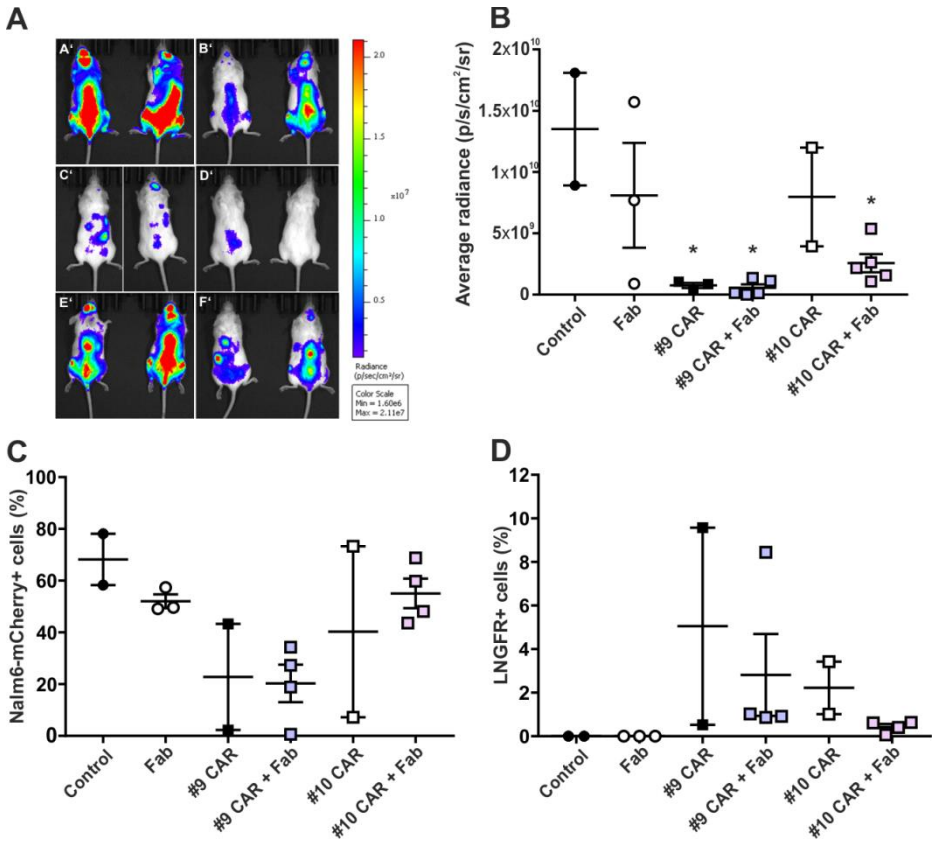

Figure 24: Adapter CAR system for targeting of CD19-positive B-ALL cell line Nalm-6-mCherry with the Fab fragment anti-CD19 4G7SDIE-biotin *in vivo*.

0.5x 10^6 Nalm-6-effluc-mCherry cells were injected intravenously into NSG mice. Six days after leukemia inoculation, mice were randomized to the treatment groups, transplanted intravenously with 2x 10^6 CAR T cells or/and daily injected intraperitoneally with 15 µg/mouse biotinylated anti-CD19 mAb Fab fragment. Three weeks after CAR T cell transplantation, mice were imaged bioluminescently (A+B) and euthanized to screen for leukemia cells in the bone marrow (C) and for CAR T cell

expansion in the peripheral blood (D) by FACS. Data are presented as means ± SEM of n = 3-5 per group. * $p < 0.05$, ** $p < 0.01$, *** $p < 0.001$ compared to control. A' control, B' Fab, C' #9 CAR, D' #9 CAR + Fab, E' #10 CAR, F' #10 CAR + Fab.

To further minimize the non-specific CAR T cell activity and to optimize the *in vivo* experiments, CAR T cell number was reduced from $2x\ 10^6$ to $1x\ 10^6$ per mouse. Instead of using freshly produced CAR T cells, they were firstly frozen and thawed again for attenuating the hyperactivity. To prevent non-specific antibody activity, the Fc-optimized therapeutic 4G7SDIE Fab antibody was replaced by an anti-CD19-biotin mAb (clone REA675), which also displays negligible binding to Fc receptors. Similar to preceding mouse experiments, unirradiated NSG mice were transplanted with $0.5x\ 10^6$ Nalm-6-effluc-mCherry cells and six days later injected with $1x\ 10^6$ previously thawed #9 adapter CAR T cells. Additionally, mice were treated with 50 µg/mouse biotinylated anti-CD19 mAb (clone REA675) three times a week. Untreated, only mAb-injected and CAR T cell-transplanted mice served as controls. Three weeks later, mice were analyzed for leukemia burden by bioluminescence imaging (FIGURE 25A+B) as well as the bone marrow was screened for leukemia cells (FIGURE 25C) and peripheral blood for CAR T cell expansion (FIGURE 25D). The bioluminescence imaging demonstrated that #9 CAR T cells in combination with biotinylated mAb reduced the leukemia burden compared to untreated control mice (FIGURE 25A+B). Once again, mAb alone decreased leukemia burden as observed with 4G7SDIE Fab treated mice (FIGURE 24A+B). The FACS analysis of the bone marrow confirmed the bioluminescence imaging results, but without an obvious anti-leukemic effect of the biotinylated anti-CD19 mAb alone (FIGURE 25C). In contrast to freshly produced CAR T cells in preceding mouse experiments (FIGURE 23+24), thawed CAR T cells showed barely non-specific activity and killed the leukemia cells generally in the presence of a biotinylated mAb. Examination of the peripheral blood demonstrated that circulating CAR T cells were present in all CAR T cell-transplanted mice (FIGURE 25D).

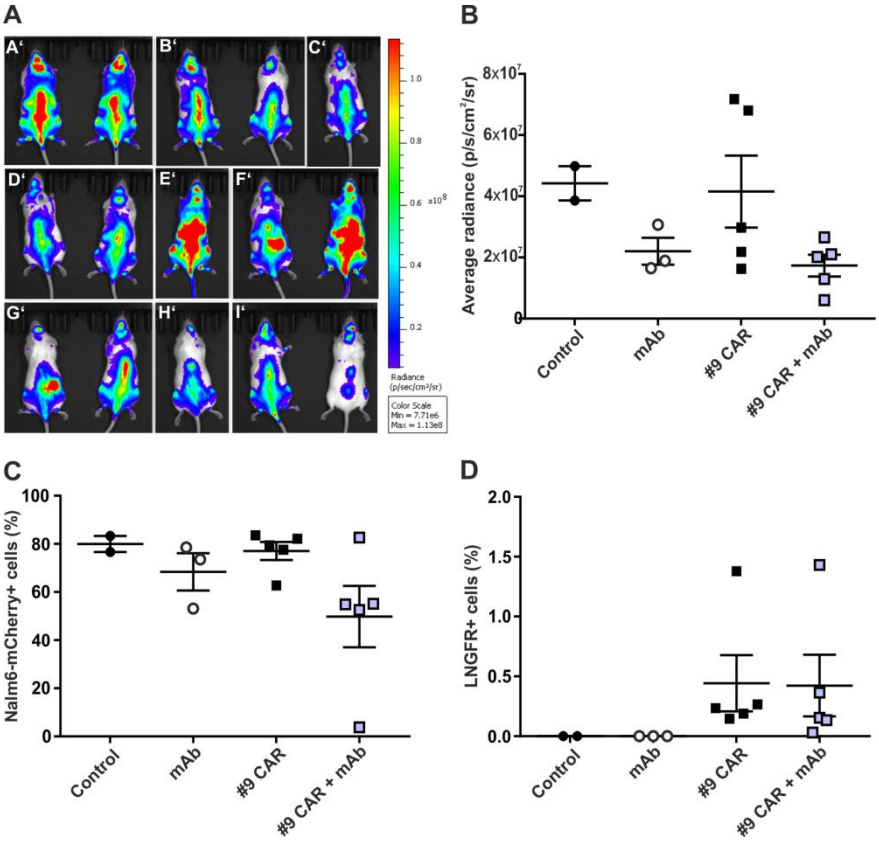

Figure 25: Adapter CAR system for targeting of CD19-positive B-ALL cell line Nalm-6-effluc-mCherry with the mAb anti-CD19 REA675-biotin *in vivo*.

NSG mice were injected intravenously with 0.5x 10^6 Nalm-6-effluc-mCherry cells. Six days after leukemia inoculation, mice were randomized to the treatment groups, transplanted intravenously with thawed 1x 10^6 CAR T cells or/and injected intraperitoneally with 50 µg/mouse biotinylated CD19 mAb (clone REA675) three times a week. Three weeks after CAR T cell transplantation, mice were imaged bioluminescently (A+B) and euthanized to screen for leukemia burden in the bone marrow (C) and for CAR T cell expansion in the peripheral blood (D) by FACS. Data are shown as means ± SEM of n = 3-5 per group. * $p < 0.05$, ** $p < 0.01$, *** $p < 0.001$ compared to control. A' control, B'+C' mAb, D'-F' #9 CAR, G'-I' #9 CAR + mAb.

To achieve a significant decrease of leukemia burden in CAR T cell and biotinylated mAb-injected mice, the cell number of thawed CAR T cells was increased from 1x 10^6 to 2x 10^6 per mouse in the following *in vivo* experiment. To additionally reduce the anti-leukemic effect of the biotinylated anti-CD19 mAb (clone REA675) alone, the mAb application frequency was decreased from three times to once a week. Again, unirradiated mice were inoculated with 0.5x 10^6 Nalm-6-effluc-mCherry cells and six days later injected with 2x 10^6 previously thawed #9 adapter CAR T cells. Mice were treated with 50 µg/mouse biotinylated anti-CD19 mAb (clone REA675) once a week. Untreated, only mAb-injected and CAR T cell-transplanted mice served as controls. Three weeks later, mice were screened for leukemia burden by bioluminescence imaging (FIGURE 26A+B), and the bone marrow was analyzed for

leukemia cells (FIGURE 26C) and the peripheral blood for circulating CAR T cells (FIGURE 26D). Both bioluminescence imaging and FACS demonstrated that #9 CAR T cells in combination with a biotinylated mAb significantly reduced the leukemia burden compared to control untreated mice (FIGURE 26A+B+C). However, also #9 CAR T cell-transplanted mice showed a significant reduction of the leukemia burden analyzed by FACS (FIGURE 26C). The biotinylated mAb alone did not substantially decrease the leukemia cells (FIGURE 26A+B+C). Nevertheless, the superiority of the combination of CAR T cells with a biotinylated mAb in killing leukemia cells was apparent *in vivo*, when compared to CAR T cells alone. This was also confirmed by an increased level of circulating CAR T cells in the peripheral blood in the presence of a biotinylated mAb (FIGURE 26D).

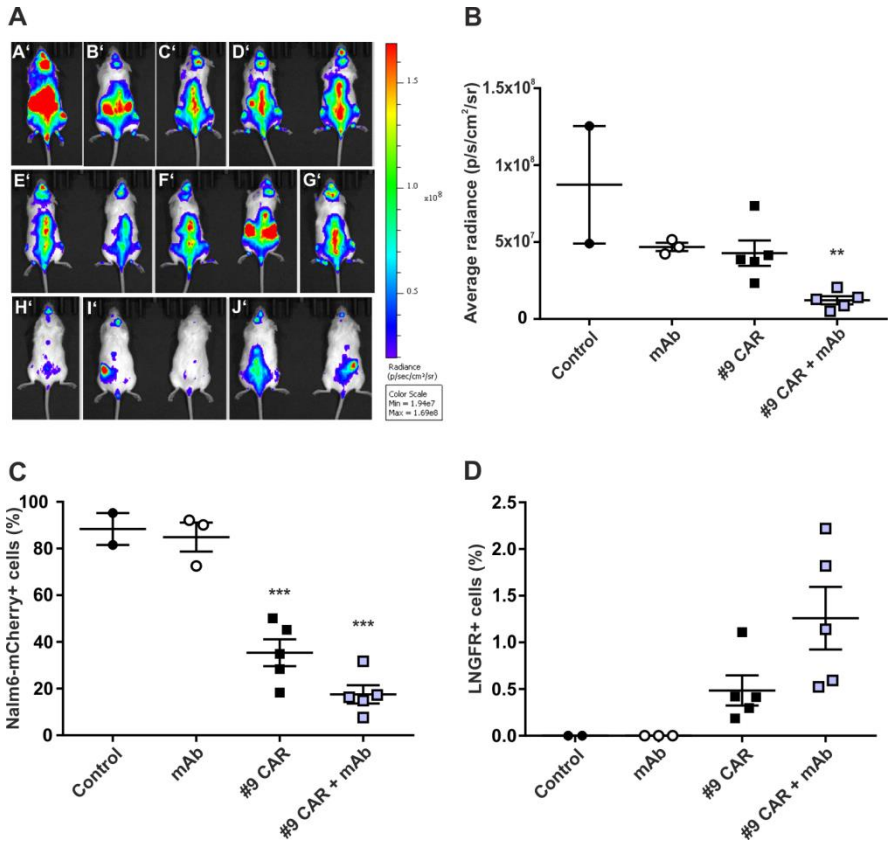

Figure 26: Adapter CAR system for targeting of CD19-positive B-ALL cell line Nalm-6-effluc-mCherry with the mAb anti-CD19 REA675-biotin *in vivo* II.

0.5x 10^6 Nalm-6-effluc-mCherry cells were injected intravenously into NSG mice. Six days after leukemia inoculation, mice were randomized to the treatment groups, transplanted intravenously with thawed 2x 10^6 CAR T cells or/and injected intraperitoneally with 50 µg/mouse biotinylated CD19 mAb (clone REA675) once a week. Three weeks after CAR T cell transplantation, mice were imaged bioluminescently (A+B) and euthanized to screen for leukemia burden in the bone marrow (C) and for CAR T cell expansion in the peripheral blood (D) by FACS. Data are presented as means ± SEM of n = 3-5 per group. * $p < 0.05$, ** $p < 0.01$, *** $p < 0.001$ compared to control. A'+B' control, C'+D' mAb, E'-G' #9 CAR, H'-J' #9 CAR + mAb.

6.3.4 Adapter CAR T cells specifically kill γδ-TCR/ CD231-positive T-ALL cells in the presence of an antibody in vitro

The prognosis for patients with T cell malignancies is still poor due to limited options for targeted therapies. CAR T cell therapy for T-ALL might result in self-targeting and compromising the therapeutic ability due to a shared surface antigen pool between normal and malignant T cells (K. H. Chen *et al.*, 2016; Chen *et al.*, 2017). Instead of using other competent immune cells (for example NK cells), universal adapter CAR T cells could also help to overcome the lack of therapy options, for example by using αβ-TCR-positive CAR T cells to kill γδ-TCR-positive T-ALLs (FIGURE 27A) as well as by targeting only malignant T cell antigens such as CD231 (Talla-1) (FIGURE 27B). To test the modularity and efficacy of universal adapter CAR T cells in targeting T-ALLs *in vitro*, the T cell lines Molt-14-effluc-mCherry (γδ-TCR-positive) and Jurkat-effluc-mCherry (CD231-positive) were co-cultivated with αβ-TCR-positive #9 CAR T cells in E:T ratios of 10:1 – 1:1, with or without the addition of the appropriate biotinylated mAb for 24 h. Cells were finally analyzed by a luciferase activity-based cytotoxicity assay. The results demonstrate that the αβ-TCR-positive CAR T cells significantly killed the γδ-TCR-positive Molt-14 cells in all tested E:T ratios of 5:1 to 1:1 compared to controls without the addition of a biotinylated anti-γδ-TCR mAb (FIGURE 27A). Analysis of the Jurkat cells showed that the universal adapter CAR T cells were also able to kill CD231-positive Jurkat cells but in a much less efficient way. A higher E:T ratio just increased the non-specific activity of the CAR T cells (FIGURE 27B).

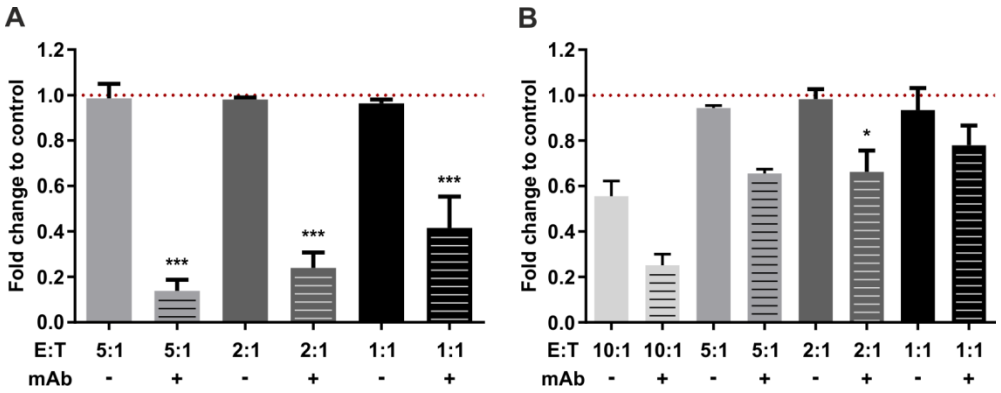

Figure 27: Adapter CAR T cells specifically kill γδ-TCR-/ CD231-positive T-ALLs with the appropriate biotinylated mAb.

Molt-14-effluc-mCherry (A) and Jurkat-effluc-mCherry (B) were co-cultivated with αβ-TCR-positive #9 CAR T cells in different E:T ratios (10:1 – 1:1) for 24 h with or without the addition of 100 ng/ml of an anti-γδ-TCR or anti-CD231 monoclonal antibody (mAb), respectively. *In vitro* killing potency of CAR T cells was analyzed by a luciferase activity-based cytotoxicity assay. Data are shown as means ± SD, n = 3. * $p < 0.05$, ** $p < 0.01$, *** $p < 0.001$ compared to each E:T without mAb.

7. DISCUSSION

7.1 ATO has a dose-dependent impact on AML cells and induces resistant LSCs

AML is a severe blood cell malignancy derived from the myeloid lineage and associated with a poor prognosis because of limited therapy possibilities for the highly heterogeneous AML subtypes (Roboz, 2012; Fernandes *et al.*, 2014). It is proposed, that the quiescent leukemia-initiating LSCs play an important role in the leukemogenic process and are often resistant to chemotherapeutic agents due to for example an overexpression of ABC transporters (Goodell *et al.*, 1996; de Jonge-Peeters *et al.*, 2007). When chemotherapeutics spare LSCs, it is likely that residual cells reinitiate tumor growth which may result in a relapse. The therapeutic agent ATO has been traditionally used in Chinese medicine for chronic leukemia treatment and is nowadays a FDA-approved single drug for the second-line therapy of the FAB M3 AML subtype APL (Zhu *et al.*, 2002; Y. Zhang *et al.*, 2016). Since then, many studies tried to evaluate an anticancer effect of ATO on other AML subtypes or cancer cell types (Halicka *et al.*, 2002; Kumar *et al.*, 2014; Leung *et al.*, 2017).

To assess ATO's applicability on AML cells, this study investigated firstly the drug's effect on the well-established cell lines KG-1a (described as undifferentiated AML cells) and Kasumi-1 (FAB M2). For that, cells were treated with different doses of ATO *in vitro* and analyzed for cell viability. Higher doses of ATO (1 – 2 µM) induced a significant reduction of viable cells and an increase of apoptotic cells in both cell lines after 72 h of treatment, whereas a low ATO dose (0.5 µM) showed only a limited cytotoxicity (FIGURE 6A). This dose-dependent dual effect of ATO was already observed on APL cells by Chen *et al*. two decades ago, where ATO at concentrations of 0.5 – 2 µM preferentially induced apoptosis, while low concentrations of 0.1 – 0.5 µM rather stimulated partial differentiation (Chen *et al.*, 1997). The pro-apoptotic activity of ATO was also confirmed by Halicka *et al*. in U-937 and HL-60 AML cells, independently of a present PML-RARα fusion protein. U-937 and HL-60 cells showed an increased level of DNA breaks already after 18 h of high dose ATO treatment *in vitro* (Halicka *et al.*, 2002). Akao *et al*. demonstrated an apoptosis-inducing effect of ATO in B-ALL cells as well (Akao *et al.*, 1998). Besides targeting PML-RARα, ATO is also able to antagonize aberrant activation of the Hedgehog signaling pathway by blocking the Gli transcription factors, particularly Gli2. Kim *et al*. and Beauchamp *et al*. showed the ATO cytotoxicity on medulloblastoma allografts is associated with an abnormal Hedgehog signaling pathway activation (Kim *et al.*, 2010; Beauchamp *et al.*, 2011). Kerl *et al*. and Boehme *et al*. also observed that the pro-apoptotic effect of ATO on rhabdoid tumors was mediated by targeting the Hedgehog signaling pathway (Kerl *et al.*, 2014; Boehme *et al.*, 2016). Based on this information, *in vitro* ATO-treated Kasumi-1 cells were also screened for

alterations in mRNA expression levels of the transcriptions factors Gli1 (FIGURE 6C) and Gli2 (FIGURE 6D) by qRT-PCR. The results confirmed the preceding observations: ATO treatment reduced the mRNA expression levels of Gli1 and Gli2, especially for Gli2.

To validate the cytotoxicity of ATO on AML cells *in vivo*, patient-derived cells (P84D and P17R) were injected into unirradiated mice and treated with different doses of ATO (0.15 mg/kg, 2.5 mg/kg and 5 mg/kg) for three weeks (FIGURE 7, 9). The analysis of bone marrow and spleen revealed again a dose-dependent effect of ATO comparable to the *in vitro* studies (FIGURE 6). Low doses of ATO did not inhibit AML cell growth (FIGURE 7A+D), only the high dose of 5 mg/kg reduced the leukemia burden *in vivo* (FIGURE 9A). Similar observations were made by Kim *et al*. with the ATO treatment of Hedgehog pathway-dependent medulloblastoma allografts in nude mice. ATO treatment inhibited tumor growth in a dose-dependent manner (Kim *et al.*, 2010). However, in this study, the high dose of 5 mg/kg ATO caused severe side effects resulting in local hyperkeratosis at the injection site of the drug (FIGURE 9D). The same toxic effects were observed by Kim *et al*. testing ATO *in vivo* on human cholangiocarcinoma cancer cells (Kim *et al.*, 2014). They validated a dose-dependent pro-apoptotic effect of ATO on tumor cells *in vitro* and on subcutaneous injected tumors *in vivo* as well. But the tumor surface changed during high dose of ATO treatment revealing hardening and black discoloration (Kim *et al.*, 2014). It is known that long-term exposure to high doses of arsenic leads to dermatological changes and affects the gastrointestinal, cardiovascular, neurological and genitourinary systems (Li *et al.*, 2002; Ratnaike, 2003; Soffritti *et al.*, 2006; Mathews *et al.*, 2013; Wang *et al.*, 2015). In addition, Wu *et al*. demonstrated that chronic ATO exposure inhibited osteoblast differentiation in bone marrow stromal cells of rats resulting in an increased bone marrow loss (Wu *et al.*, 2014).
Nevertheless, in this study ATO showed its potency as an anti-leukemic and pro-apoptotic drug *in vitro*. Hence, ATO is a future hope for AML therapy as well as for the treatment of different cancer types like chondrosarcoma, breast cancer or neuroblastoma (Gesundheit *et al.*, 2008; Jiao *et al.*, 2015; S. Zhang *et al.*, 2016; Shi *et al.*, 2017).

Several studies indicated that ATO can deplete cancer stem cells or at least sensitize them to chemotherapy by promoting the dormant cells to enter into the cell cycle or differentiation (Essers and Trumpp, 2010; Tomuleasa *et al.*, 2010; Wu *et al.*, 2013). In this study, a potential LSC-inhibiting effect of ATO was investigated by analyzing the LSCs residing in the so-called side populations (SP 2n/SP 4n). It was observed that ATO increased the diploid and tetraploid side populations in a dose-dependent manner in the KG-1a cell line *in vitro*. High dose ATO led to a significant increase of the side populations, while low dose of 0.5 µM ATO slightly stimulated them (FIGURE 6B). Although high dose ATO obviously decreased the

cell viability of AML cells (FIGURE 6A), it also initiated an accumulation of LSCs indicating that LSCs were resistant to ATO and had a survival selection advantage. The *in vivo* experiments with patient-derived AML cells displayed results similar to the *in vitro* observations (FIGURE 6). LSCs, which reside in the side-populations, appeared to be resistant to ATO, but to a lower extent (FIGURE 7, 9). The patient-derived sample P84D did not respond to ATO with a decreased cell viability or decelerated growth (FIGURE 7A+D), but the diploid and tetraploid side populations in the spleen were stimulated upon daily ATO injections (FIGURE 7E+F). The patient sample P17R however, responded to the high dose of 5 mg/kg ATO with a reduced leukemia burden (FIGURE 9A), while the LSCs remained resistant (FIGURE 9B+C).
Similar results were described by Tokar *et al*. for ATO-treated non-cancerous prostate epithelial cells. ATO reduced significantly the cell viability of mature prostate epithelial cells, whereas the prostate stem cells appeared to be resistant to ATO and started to over-accumulate due to a higher expression of several anti-apoptotic factors (BCL2 and MT1), stress-related factors (including NF-E2–related factor-2 and superoxide dismutase-1) and arsenic efflux-related genes (for example *ABCC1*) as well as a lower expression of pro-apoptotic factors (like BAX and caspases 3) (Tokar *et al.*, 2010). Based on overexpression experiments with AML cells, Martelli *et al*. and Tabellini *et al*. hypothesized that the PI3K/Akt signaling pathway is involved in the resistance of LSCs to ATO-induced apoptosis (Martelli *et al.*, 2005; Tabellini *et al.*, 2005). Roszak *et al*. also confirmed the ATO resistance of human T cell leukemia stem cell clones (Jurkat cells) due to a predominantly active PI3K/Akt signaling pathway (Roszak *et al.*, 2013).

In conclusion, ATO as a monotherapy displayed an anti-leukemic effect on AML cells, but without depleting LSCs *in vitro* and *in vivo*. Nevertheless, ATO in combination with other cell cycle promoting agents might bring LSCs into the cell cycle and by this increase the treatment efficacy and avoid relapse of future AML patients.

7.2 G-CSF potentiates cytotoxicity of ATO on AML cells potentially by inducing AQP9 expression

ATO in combination with other agents has been proven to be an efficient drug for the treatment of different cancer cell types. For example, the most noted and already FDA-approved combination of ATO and ATRA shows a superior efficacy in APL therapy compared with either single agent. ATO improved notably the clinical outcome of APL patients by inducing the degradation of the PML-RARα protein (Niu *et al.*, 1999; Zhang *et al.*, 2010). ATO can also be potentiated in its pro-apoptotic function on AML cells by several agents such as vitamin D3 (Rogers *et al.*, 2014), the demethylating agent azacytidine (Chau *et al.*, 2015), the antifungal drug itraconazole (Wu *et al.*, 2017) or the naturally occurring substance curcumin (Fan *et al.*, 2014). In this study, G-CSF, which is a hematopoietic cytokine, was tested as a candidate for potentiating the ATO treatment efficacy on AML cells. For that, the AML cell lines U-937 (FAB M5) and Kasumi-1 (FAB M2) were treated *in vitro* with different doses of ATO (0.5 – 2 µM) and G-CSF (10 ng/ml) and analyzed for cell viability, cell cycle and proliferation arrest (FIGURE 10). Cell viability analyses of long-term treatments revealed that the combination of ATO and G-CSF was superior in decreasing the number of viable cells in both cell lines compared to either single agent and to control (FIGURE 10A+B). Likewise, many groups termed ATO as a pro-apoptotic drug for AML cells (Halicka *et al.*, 2002; Kumar *et al.*, 2014) and APL cells (Iriyama *et al.*, 2012). Yoshinari *et al*. firstly described G-CSF as a potent pro-apoptotic agent for APL cells based on morphology changes and DNA fragmentation (Yoshinari *et al.*, 1999). Kitagawa *et al*. further confirmed this observation for AML cells by showing a decreased cell viability of U-937 and 32Dcl3 cells as well as an increased level of apoptotic cells upon G-CSF treatment (Kitagawa *et al.*, 2010). Hence, the synergistic anti-leukemic effect of ATO and G-CSF might result from an additive pro-apoptotic effect of both drugs. Contrary to the demonstrated results in this study, Iriyama *et al*. indicated that G-CSF has rather an anti-apoptotic effect on APL cells, which may result in an increased cell viability (Iriyama *et al.*, 2012). In addition, Morris *et al*. demonstrated that inhibition of G-CSF induces a protective tumor immunity in mouse colon cancer by promoting immune cell responses (Morris *et al.*, 2015), rather suggesting an anti-G-CSF treatment as a potential therapeutic approach for cancer.

In this study, cell cycles analyses of ATO and G-CSF-treated AML cells revealed a significant reduction of the S phase accompanied with an increased number of cells in the apoptotic sub-G1 phase (FIGURE 10C+D). In addition, U-937 cells showed a G2/M phase arrest (FIGURE 10C), while Kasumi-1 cells displayed a G0/G1 phase arrest after exposure to the combination of both agents (FIGURE 10D). Comparable results were shown by Halicka *et al*., where ATO induced a G2/M phase arrest in AML cells, which culminated in apoptosis

(Halicka *et al.*, 2002). On the other hand, Kitagawa *et al*. observed that G-CSF mobilized resting AML cells from G0/G1 into S phase. This resulted in an increased number of cells in the S phase, which implicates a cell cycle-promoting effect of G-CSF (Kitagawa *et al.*, 2010). However, this cell cycle promoting-effect of G-CSF could not be confirmed in this study. In fact, G-CSF as a single agent rather reduced the number of U-937 cells in the S phase instead of increasing it (FIGURE 10C). No changes of the S phase were observed in Kasumi-1 cells (FIGURE 10D). The response to G-CSF seemingly differed between the cell lines regarding their proliferation ability. The proliferation capacity of U-937 cells was significantly reduced upon ATO and G-CSF treatment, whereas Kasumi-1 cells did not show a good response (FIGURE 10E+F). U-937 cells appeared to be more sensitive to G-CSF than Kasumi-1 cells regarding cell cycle and proliferation capability, even though U-937 cells showed a lower expression level of G-CSFR than Kasumi-1 cells (FIGURE 11).

G-CSF is also known for its capability to stimulate myeloid differentiation of hematopoietic progenitor cells (Welte *et al.*, 1985; Skokowa *et al.*, 2009; Lachmann *et al.*, 2015). In addition, Weng *et al*. demonstrated that the blocked differentiation in myeloid LSCs can be reinitiated by granulocyte-macrophage colony-stimulating factor (GM-CSF) administration (Weng *et al.*, 2017). The synergistic anti-leukemic effect of ATO and G-CSF might also result from the cell cycle and differentiation promoting-effect of G-CSF by recruiting quiescent AML cells into the cell cycle for further differentiation and, thereby, rendering them more sensitive to ATO. In accordance with this hypothesis, Iriyama *et al*. demonstrated that G-CSF augmented ATO's potential for inducing the differentiation of APL cells, which might result in a higher vulnerability to ATO (Iriyama *et al.*, 2012). Furthermore, Lemarie *et al*. showed that ATO is able to induce apoptosis of human blood monocytes during differentiation of macrophages stimulated by GM-CSF (Lemarie *et al.*, 2006).

Another possible explanation for the synergistic anti-leukemic effect of ATO and G-CSF could be an enhanced AQP9 expression upon G-CSF treatment. AQP9 is the main transporter for arsenic uptake and elimination (Liu *et al.*, 2002; Carbrey *et al.*, 2009). Many studies revealed that an increased AQP9 expression leads to an enhanced sensitivity to ATO and, thereby, accumulation of arsenic within the cells (Bhattacharjee *et al.*, 2004; Lee *et al.*, 2006; Leung *et al.*, 2007; Iriyama *et al.*, 2013). Indeed, the *in vitro* cultivated U-937 and Kasumi-1 cells showed an increased AQP9 protein expression level upon G-CSF stimulation, validated by western blot and FACS (FIGURE 12). Kasumi-1 cells appeared to be more responsive to G-CSF than U-937 cells, resulting in a significant increase of the AQP9 protein (FIGURE 12) and mRNA expression level (FIGURE 13). This was accompanied by the observation that the basic G-CSFR protein level was much higher in Kasumi-1 cells than in

U-937 cells (FIGURE 11). Leung *et al*. observed the same AQP9-stimulating effect of ATRA and Chau *et al*. of azacytidine in AML cell culture experiments (Leung *et al.*, 2007; Chau *et al.*, 2015). In both studies, co-treatment of ATRA or azacytidine with ATO led to an increased ATO level within the cells and decreased cell viability. Iriyama *et al*. already tested G-CSF as a potential AQP9 stimulator for APL cells *in vitro*. They observed that the combination of G-CSF and ATO enhanced the vulnerability of these cells. But, they could not detect an increased AQP9 expression level upon G-CSF stimulation (Iriyama *et al.*, 2012). In this study, however, G-CSF appeared to sensitize AML cells to ATO treatment by upregulation of AQP9 expression *in vitro*.

To test the synergistic anti-leukemic efficacy of ATO and G-CSF on patient-derived AML cells, freshly isolated CD33-positive leukemic cells were treated *in vitro* with 1 µM ATO, 10 ng/ml G-CSF and with the combination of both for 72 – 96 h. However, the combinatorial ATO-G-CSF treatment did not convincingly show a synergistic effect on the cell count (FIGURE 15A+C+E) and AQP9 expression (FIGURE 15B+D+F). In only three of six patient samples, a slight reduction of the cell count was observed. Regarding AQP9 expression levels, no obvious upregulation was detected. Many studies have tried to establish optimal culture conditions for patient-derived AML cells *in vitro*, such as using serum-free media (Bruserud *et al.*, 2000) or co-culturing with mesenchymal stromal cells, which support the growth and long-term maintenance of HSCs and LSCs (Ito *et al.*, 2015). In this study, the optimal *in vitro* culturing of patient-derived AML cells appeared to be problematic. Without the addition of cytokines, AML cells often show a rapid differentiation (Ito *et al.*, 2015).
Therefore, the synergistic anti-leukemic efficacy of ATO and G-CSF was further examined on AML cells *in vivo*. For that, U-937 cells were injected into unirradiated mice and treated daily with the combination of 4 mg/kg ATO and 250 µg/kg G-CSF or with the single agents for three weeks (FIGURE 14). The analysis of bone marrow, peripheral blood and spleen revealed again a synergistic anti-leukemic effect of ATO and G-CSF compared to control and ATO alone (FIGURE 14A-C), comparable to the *in vitro* studies with U-937 and Kasumi-1 cells (FIGURE 10). Furthermore, the detection of increased apoptotic markers (activated CASP3 and cleaved α-spectrin) by western blot confirmed the enhanced anti-leukemic effect of the drug combination in the bone marrow compared to either single agent (FIGURE 14D+F+G). However, G-CSF alone revealed a distinct anti-leukemic effect *in vivo* especially in the peripheral blood and spleen as well, but without upregulation of apoptotic markers (FIGURE 14B+C). The same anti-leukemic efficacy of G-CSF as a single agent was observed in all analyzed organs of mice, which were transplanted with patient-derived AML cells and treated with ATO, G-CSF or with the combination of both for three weeks (FIGURE 16,17). Even a reduced application frequency of G-CSF did not reduce the efficacy of G-CSF as single drug

in inhibiting leukemia cell growth *in vivo* (FIGURE 17). Interestingly, the different ATO doses did not show an impact on both the patient AML (FIGURE 16,17) and on the U-937 cell growth (FIGURE 14) *in vivo*. Bessho *et al*. observed the same leukemia suppressing effect of G-CSF *in vivo*, when treating murine myeloid leukemia cell line-transplanted mice with G-CSF. A preincubation of the murine myeloid leukemia cells with G-CSF for 48 h even prevented the leukemia engraftment in syngeneic mice. *In vitro* experiments elucidated that apoptosis plays a role in the anti-leukemic effect of G-CSF (Bessho *et al.*, 1994), whereas in this study, no increased apoptotic markers could be detected in G-CSF-treated U-937 cells *in vivo* (FIGURE 14D+F+G). In addition, also clinical trials for alternative cancer therapeutic approaches showed occasional tumor regression, when using GM-CSF to enhance immune stimulation and bolster specific T cell and antitumor responses (Baeuerle and Reinhardt, 2009; Marr *et al.*, 2012).

Further analyses of the immunophenotype revealed that G-CSF reduced the $CD34^{+}CD38^{-}$ LSC population, which was accompanied by an increase in $CD34^{-}CD38^{+}$ cells. This indicates a G-CSF-induced differentiation of LSCs *in vivo*. ATO alone did not show any differentiation-promoting effect on LSCs (FIGURE 17E). The ATO resistance of LSCs was already observed in the *in vitro* studies with KG-1a cells (FIGURE 6B). The results of the *in vivo* studies suggest that G-CSF might promote the differentiation of dormant LSCs leading to a deceleration of the leukemia cell growth independently of ATO administration.

In the *in vivo* experiment with U-937 cells, G-CSF treatment did not result in increased AQP9 levels (FIGURE 14D). However, the patient-derived AML cells were susceptible to G-CSF resulting in a significant increase of AQP9 expression (FIGURE 16,17). In the *in vivo* study with the P49S patient-derived AML cells, G-CSF even restored AQP9 levels, which were decreased upon ATO treatment (FIGURE 16). U-937 cells appeared to have an attenuated response to G-CSF compared to patient-derived cells in regard to their AQP9 expression levels. The same trend was observed in the *in vitro* experiments, where the AQP9 expression was only slightly increased in U-937 cells treated with G-CSF or ATO-G-CSF. In contrast, Kasumi-1 cells responded with a highly AQP9 upregulation (FIGURE 12). Nevertheless, the combination of ATO and G-CSF was superior to each single agent in decelerating the leukemia cell growth *in vivo*.

All these observations led to the assumption that the synergistic anti-leukemic effect of ATO and G-CSF might be a multifactorial effect, in which the pro-apoptotic, differentiation-promoting and AQP9-stimulating features of G-CSF play an interactive role for the treatment of AML cells. Although most AML cells express G-CSFR, some AML subtypes are not

responsive to G-CSF (Kitagawa *et al.*, 2010). Therefore, prior analysis for the AQP9 and G-CSFR status of AML patients can help to predict the response to ATO and G-CSF.

7.3 G-CSF stimulates AQP9 expression in healthy human and murine hematopoietic precursor cells

G-CSF is known to stimulate the bone marrow to produce and to induce a release of mature neutrophils (Welte *et al.*, 1985; Semerad *et al.*, 2002). AQP9 is expressed on many tissues such as spleen, liver and brain as well as on hematopoietic cells and neutrophils (Tsukaguchi *et al.*, 1999; Moniaga *et al.*, 2015). To validate an AQP9-stimulating effect of G-CSF on non-cancerous human hematopoietic cells, healthy donor CD33- and CD34-positive cells were tested for AQP9 expression upon G-CSF treatment (FIGURE 18). CD33-positive cells from healthy volunteers, which were treated daily with G-CSF for three days, were analyzed for AQP9 mRNA expression by microarray analysis. The results revealed a significant increase of AQP9 mRNA expression in cells of G-CSF-treated volunteers compared to cells of non-treated controls (FIGURE 18A). However, *in vitro* G-CSF-treated CD33- and CD34-positive cells from healthy donors showed no difference in the AQP9 protein expression level in comparison to the non-treated cells (FIGURE 18B).

Similar to the results of the *in vitro* cultivated patient-derived AML cells (FIGURE 15), an AQP9-inducing effect could not be observed for *in vitro* cultured healthy donor cells. It is known that G-CSFR is mainly expressed on myeloid precursor cells, which start to differentiate into mature myeloid cells upon G-CSF stimulation (Tsuji and Ebihara, 2001; Marino and Roguin, 2008). It might be that the *in vitro* cultured healthy CD33- and CD34-positive cells started to differentiate into mature myeloid cells due to cytokine starvation and suboptimal culture conditions as it was observed by Ito *et al.* for LSCs (Ito *et al.*, 2015). Consequently, they might not appropriately express G-CSFR and react to G-CSF stimuli any more resulting in a non-increased AQP9 expression level.

Therefore, to further examine an AQP9-inducing effect of G-CSF on healthy hematopoietic cells *in vivo*, NSG mice were treated with G-CSF for one week. After euthanization, murine CD45- and CD34-positive bone marrow cells were analyzed for AQP9 protein expression levels. Both cell types showed a significant increase in AQP9 expression levels after one week of G-CSF application (FIGURE 19).

These results indicated that G-CSF has also an AQP9-stimulating effect on healthy hematopoietic cells comparable to its effect on immature myeloid leukemia cells (FIGURE 12).

7.4 Hypothetical network between G-CSF and AQP9

In this study, the combination of ATO and G-CSF showed a synergistic anti-leukemic effect on AML cell lines *in vitro* (FIGURE 10) and *in vivo* (FIGURE 14). This was potentially mediated via an increased AQP9 expression triggered by G-CSF stimulation (FIGURE 12). Myeloid leukemia cells are usually resistant to ATO treatment due to a modest AQP9 expression level. But using this AQP9 expression-inducing effect of G-CSF, combinatorial ATO-G-CSF treatment might lead to a better ATO uptake and, hence, better targeting of acute myeloid leukemia cells (FIGURE 28).

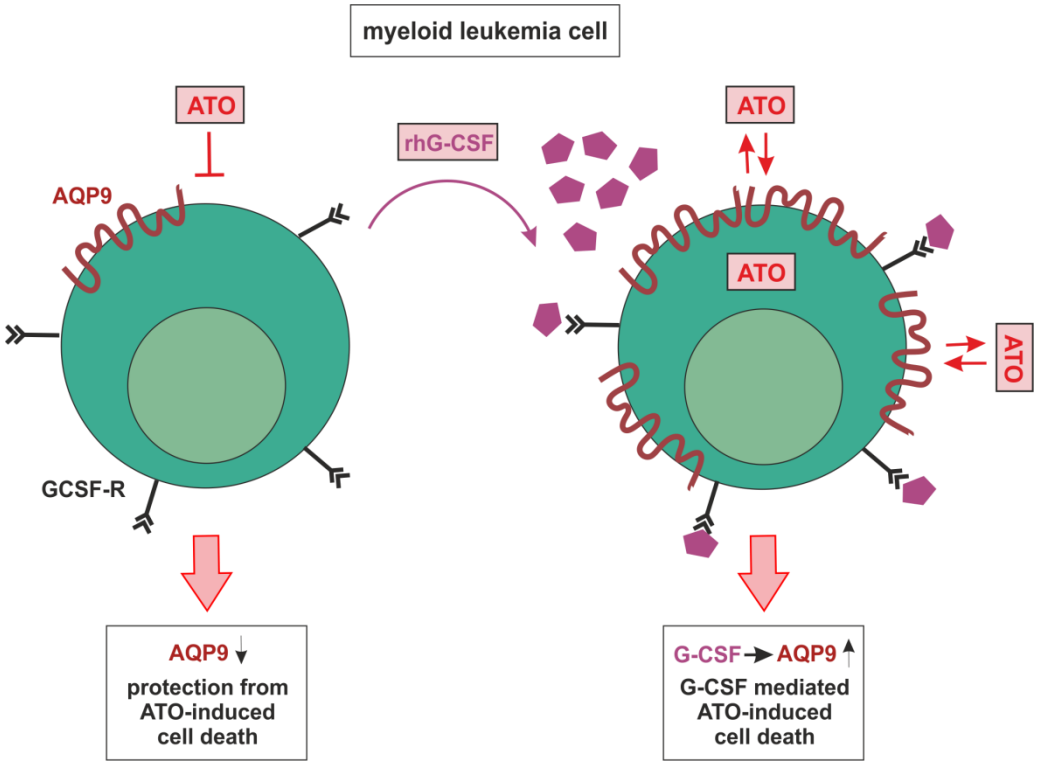

Figure 28: G-CSF-mediated ATO-induced cell death of AML cells.
Myeloid leukemia cells are usually resistant to ATO-induced cell death due to the low expression level of the main arsenic transporter AQP9. Administration of rhG-CSF could lead to an enhanced expression of AQP9 channels and, thus, to a better uptake of ATO by myeloid leukemia cells. This might result in G-CSF-mediated ATO-induced cell death.

The questions why G-CSF leads to an upregulation of AQP9 and whether it is a direct or indirect effect still need to be answered. A potential link could be via the enzyme nicotinamide phosphoribosyltransferase (NAMPT), which is known to be a rate-limiting factor in the biosynthesis of the oxidized form of nicotinamide adenine dinucleotide (NAD+) and to mediate G-CSF-triggered granulopoiesis in healthy individuals and in CN patients (Rongvaux *et al.*, 2002; Revollo *et al.*, 2004; Skokowa *et al.*, 2009). Furthermore, G-CSF increases the

intracellular NAMPT and NAD+ amounts in myeloid cells to induce differentiation (Skokowa *et al.*, 2009). Increased amounts of NAMPT were also observed in ATRA-induced granulocytic differentiation of the AML cell line HL-60 (Jia *et al.*, 2004), rending NAMPT essential for differentiation. Moreover, J. Skokowa and colleagues showed that the administration of NAMPT alone also induces myeloid differentiation of HL-60 cells (Skokowa *et al.*, 2009). In this study, G-CSF triggered AQP9 expression to potentially induce differentiation of the leukemia cells. Like AQP9 via its expression on neutrophils, NAMPT is also involved in response to inflammatory stimuli and inflammatory diseases (Jia *et al.*, 2004; Mesko *et al.*, 2010; Moniaga *et al.*, 2015). This suggests a potential role of AQP9 in differentiation of precursor neutrophils into mature neutrophils under participation of NAMPT and G-CSF. Another co-factor might be IL-1β (and possibly its processing enzyme caspase-1) which also induces NAMPT expression (Jia *et al.*, 2004; Kendal and Bryant-Greenwood, 2007). NAMPT occurs both as an extracellular and intracellular enzyme, converting nicotinamide (NAM) to nicotinamide mononucleotide (NMN) in both spaces (Revollo *et al.*, 2007; Bogan and Brenner, 2008; Ratajczak *et al.*, 2016). These metabolites can be excreted and taken up by cells, which might be also mediated by channel proteins like AQP9. AQP9 allows the passage of several non-charged solutes, including carbamides, purines and pyrimidines, whereas amino acids and cyclic sugars are excluded (Tsukaguchi *et al.*, 1998). In conclusion, G-CSF might upregulate NAMPT and AQP9 to trigger NAD+ biosynthesis and, thereby, to initiate differentiation of immature myeloid cells (FIGURE 29).

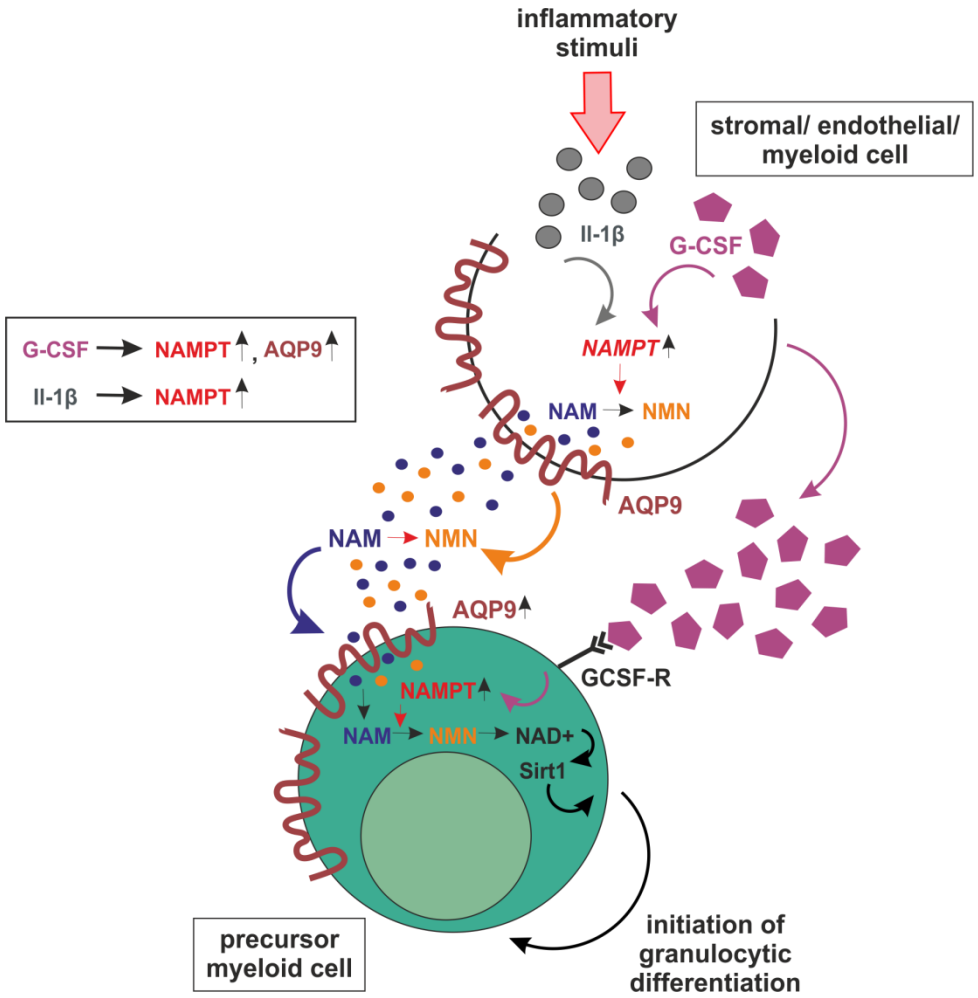

Figure 29: Hypothetical network between G-CSF and AQP9 in granulopoiesis.

Stimulated by inflammatory and extrinsic signals like IL-1β and G-CSF stromal/ endothelial/ myeloid cells induce expression of nicotinamide phosphoribosyltransferase (NAMPT), which is an important enzyme for the nicotinamide adenine dinucleotide (NAD^+) biosynthesis and mediates G-CSF-triggered granulopoiesis. NAMPT's substrate nicotinamide (NAM) and its product nicotinamide mono-nucleotide (NMN) might pass the membranes via the G-CSF upregulated AQP9 channels. Within precursor myeloid cells, intracellular NAMPT triggers NAD^+-dependent sirtuin-1 (Sirt1) activation to further induce granulocytic differentiation of immature myeloid cells.

7.5 Bispecific CAR T cell therapy for prevention of leukemia antigen-loss

Due to a massive progress in targeted therapy strategies for ALL patients over the last years, the prognosis of refractory and relapsed ALL patients has improved significantly. Particularly noteworthy are the newly FDA-approved CAR T cell therapies for BCP-ALL and B cell lymphoma (U.S. Food & Drug Administration, 2017). Nevertheless, CAR T cell therapy needs further optimization because of severe therapy-associated complications and antigen-loss as observed upon therapy with therapeutic antibodies (Davis *et al.*, 1999; Ruella and Maus, 2016). To reduce the 'on-target off-tumor' toxicities of CAR T cell therapy and to overcome the large heterogeneity of antigen patterns, one strategy is targeting two leukemic blast antigens simultaneously with a bispecific CAR. In this study, a bispecific CAR with a $(glycin_4serin)_4$ linker between anti-CD19 and anti-CD20 scFvs was tested for its superiority to monospecific CARs in eradicating a $CD19^+CD20^{+/-}$ heterogeneous patient-derived B-ALL *in vivo* (FIGURE 20,21). The analysis of the bone marrow and peripheral blood of the transplanted mice revealed that both the bispecific and the anti-CD19 CAR T cells eradicated completely the leukemia burden (FIGURE 20A+B), while they further circulated in both organs (FIGURE 20C+D). Comparable results were observed by Zah *et al.* that a bispecific CAR, specific for CD19 and CD20, was able to control both wildtype $CD19^+CD20^+$ and mutant $CD19^-CD20^+$ B cell lymphomas with equal efficacy *in vivo* (Zah *et al.*, 2016). Also other studies examined successfully bispecific CAR T cells in terms of treating cancer, such as Qin *et al.* for targeting CD19- and CD22-positive B-ALL as well as Schneider *et al.* for targeting CD19- and CD20-positive B cell lymphoma (Qin *et al.*, 2015; Schneider *et al.*, 2017). Schneider *et al.* further proved bispecific CAR T cells both more effective and less toxic than an admixture of two monospecific CAR T cell populations (Schneider *et al.*, 2017).

In this study, the monospecific anti-CD20 CAR T cells did not demonstrate an anti-leukemic effect *in vivo* (FIGURE 20A+B), neither did they circulate in bone marrow and peripheral blood (FIGURE 20C+D). *In vitro* analysis of the bispecific, anti-CD19 and anti-CD20 CAR T cells, however, showed equal killing effectiveness as well as antigen specificity (data shown in published paper, Martyniszyn *et al.*, 2017). Anti-CD19 CAR T cells are already well explored in their efficacy and tolerability for BCP-ALL patient therapy (Gill and June, 2015; U.S. Food & Drug Administration, 2017). Many studies have also been performed to investigate anti-CD20 CAR T cells for B cell malignancy treatment (Wang *et al.*, 2014; Chen *et al.*, 2015; Watanabe *et al.*, 2015; Rufener *et al.*, 2016). But the design of the optimal anti-CD20 CAR is challenging due to the complex nature of the multi-pass transmembrane CD20 protein (Einfeld *et al.*, 1988). It is necessary to achieve the right conjugation distance between the T cell and its target antigen and to match the size of the antigen (Marr *et al.*, 2012). Moreover, Long *et al.* revealed that CAR T cells often mediate potent *in vitro* cytolysis, but

show limited expansion, persistence and antitumor efficacy *in vivo* as a result of T cell exhaustion. They further showed that the CD28 co-stimulation domain promotes exhaustion of CAR T cells by inducing a persistent CAR signaling (Long *et al.*, 2015). Thus, the CAR design with a scFv-Fc-CD28-CD3ζ cassette, used in this study, might have triggered exhaustion of the anti-CD20 CAR T cells. Furthermore, the CD20 antigen density might have been suboptimal for the recognition, compromising the effectiveness of the anti-CD20 CAR T cells *in vivo*. Similar results were also observed by Watanabe *et al.* who reported that a low antigen density can cause an insufficient efficacy of CAR T cells (Watanabe *et al.*, 2015). It is also known that the extracellular spacer length plays an important role in enabling robust T cell-mediated response to tumor antigens (Almåsbak *et al.*, 2015; Hudecek *et al.*, 2015). Taken together, the anti-CD20 CAR construct was probably not appropriately designed for the CD20 target antigen and, thus, could not demonstrate an anti-leukemic effectiveness *in vivo*, while the bispecific CAR T cells proved their capability in successfully killing leukemia cells. In conclusion, bispecific CAR T cells appear to be superior to monospecific CAR T cells, demonstrating an effective and clinically applicable tool to prevent antigen escape and to further optimize the efficacy of CAR T cell therapy for cancer.

7.6 Short-spacer adapter CAR T cells specifically kill B cell leukemia in the presence of a biotinylated mAb

Another strategy to decrease 'on-target off-tumor' toxicities of CAR T cell therapy is to use universal adapter CAR T cells, which can be functionally controlled by an integration of an 'on-switch' mechanism. This non-lethal control of CAR T cells allows T cell activation via the addition of a switch molecule. The modularity of this approach enables universal CAR T cells to target a wide range of tumor antigens (Kloss *et al.*, 2012; Wu *et al.*, 2015). In this study, universal adapter anti-biotin CAR T cells with different spacer lengths (#7-, #10- and #9 CAR with decreasing spacer lengths) were tested for their effectiveness in controlling the CD19-positive B-ALL cell line Nalm-6 *in vitro* (FIGURE 22) and *in vivo* (FIGURE 23-26). The *in vitro* results demonstrated that #9 CAR T cells with a very short spacer domain, consisting of only a hinge region, were much more superior in killing leukemia cells in the presence of a biotinylated mAb compared to #7- and #10 CAR T cells with longer spacer domains (FIGURE 22A+D). Further analysis of #9 CAR T cells revealed a high expression of activation (CD25/CD69) and exhaustion markers (PD-1) (FIGURE 22B) as well as a decrease of naïve T cells ($CD62L^+CD45RA^+CD45RO^-CD95^-$) and increase of effector T cells ($CD62L^-CD45RA^+CD45RO^-CD95^+$) (FIGURE 22C) upon co-cultivation with Nalm-6 cells and a biotinylated mAb. The activation and differentiation status of the CAR T cells confirmed the power of #9 CAR T cells in killing leukemia cells in the presence of a biotinylated mAb *in*

vitro. Similar results were observed by Ma *et al.* and Cao *et al.* showing that universal adapter CAR T cells are able to target CD19- and CD22-positive B cell malignancies (Ma *et al.*, 2016) and HER2/neu-positive breast cancer cells (Cao *et al.*, 2016) *in vitro* and *in vivo* by adding FITC-conjugated tumor-targeting antibodies.

In contrast to the *in vitro* results, all three CAR constructs appeared to have comparable power in controlling leukemia cell growth in the first *in vivo* experiment (FIGURE 23). However, also the control mock mice, which were injected only with #9 CAR T cells and an unbiotinylated mAb, revealed a significant decrease of the leukemia burden by bioluminescence imaging (FIGURE 23A+B) and FACS analysis (FIGURE 23C). These results indicated that the leukemia cells were eradicated, either from a non-specific effect of the adapter CAR T cells and/ or from the anti-CD19 4G7SDIE therapeutic mAb alone. Seidel *et al.* already proved the Fc-optimized anti-CD19 4G7SDIE mAb a potent therapeutic with an enhanced ADCC against leukemic blasts in 14 pediatric patients with refractory and relapsed B-ALL at the stage of MRD (Seidel *et al.*, 2016). Further Fc-optimized anti-CD19 mAbs, MEDI-551, MOR208 and CD19-DE, have revealed their effectiveness in B-ALL therapy by an increased ADCC and recruitment of proinflammatory immune cells as well (Kellner *et al.*, 2013; Matlawska-Wasowska *et al.*, 2013; Schewe *et al.*, 2017).
Additionally, in the first *in vivo* study, #7 CAR T cells did not circulate and accumulate properly within the peripheral blood upon stimulus with a biotinylated mAb (FIGURE 23D), whereas the leukemia burden in the bone marrow was eradicated (FIGURE 23A+B+C). This observation supported the theory that the anti-CD19 4G7SDIE mAb alone was also responsible for the inhibition of leukemia cell growth in all CAR T cell transplanted mice. But most importantly, these results indicated a disadvantage of CAR T cells with a longer spacer length *in vivo*. Hudecek *et al.* and Almåsbak *et al.* already observed that CAR T cells with a short spacer length are superior to CAR T cells with a long spacer length regarding T cell function and proliferation. CAR T cells with long spacer domains show *in vitro* but no *in vivo* antitumor activity due to an interaction between the Fc domain within the spacer and the Fc receptor-bearing myeloid cells. This results in an activation-induced T cell death (Almåsbak *et al.*, 2015; Hudecek *et al.*, 2015). Also Hombach *et al.* observed a unintended initiation of an innate immune response due to interaction between the Fc domain within the CAR spacer and the IgG Fc gamma receptors of innate immune cells (Hombach *et al.*, 2010). Therefore, it is highly probable that an interaction between the Fc domain within the #7 CAR spacer domain and the Fc receptor-sustaining murine myeloid cells could have led to an activation-induced death of #7 CAR T cells.

Many studies showed that the use of liposomal clodronate leads to a depletion of Fc receptor-bearing murine monocytes and macrophages in various organs (van Rooijen and Hendrikx, 2010; Hayden *et al.*, 2014; Hanna *et al.*, 2016). In this study, leukemia and CAR T cell-transplanted mice were also treated with liposomal clodronate to prevent the recruitment of proinflammatory immune cells and activation-induced CAR T cell death (data not shown). But almost all mice died immediately after liposomal clodronate injection or within the next days, emphasizing the toxicity of monocytes depletion in immunodeficient mice. Comparable observations were also described by Fraser *et al.* and Hu *et al.* that NSG mice are highly sensitive to the toxicity of clodronate (Fraser *et al.*, 1995; Hu *et al.*, 2011).

To elucidate the specificity of the adapter CAR system and to avoid unintended initiation of an innate immune response in the following mouse experiment, the cell number of CAR T cells was markedly reduced and only #9 and #10 CAR T cells with short spacer lengths were used. To prevent ADCC, a biotinylated Fab fragment of the anti-CD19 4G7SDIE mAb was added as a switch molecule (FIGURE 24). However, the #9 and #10 adapter CAR T cells still demonstrated a non-specific antibody-independent effect *in vivo* (FIGURE 24A-C) while circulating in the peripheral blood (FIGURE 24D). Based on these results, the assumption emerged that the Nalm-6 cell line might not be an appropriate target because of its sensitivity to any kind of cell response. Other groups have also shown that the Nalm-6 cell line are extremely sensitive to cytokine- and cell-mediated cytotoxicity (Schneider *et al.*, 2017). However, it was more likely that the CAR T cells were overstimulated and, therefore, hyperactive. CAR T cells are usually cultured with the cytokines IL-2, IL-7 or IL-15 (Ma *et al.*, 2006). Some studies have shown that culturing with IL-7 and IL-15 is superior to IL-2 regarding CAR T cell expansion, persistence and *in vivo* engraftment (Caserta *et al.*, 2010; Xu *et al.*, 2014). In this study, *in vitro* culturing of CAR T cells with IL-7 and IL-15 could have led to an overstimulation of the cells and later to a non-specific anti-leukemic effectiveness *in vivo*.

For further optimization in the following mouse experiment, the anti-CD19 biotinylated mAb clone REA675 was used as a switch molecule, instead of the anti-CD19 4G7SDIE mAb or Fab, due to its negligible binding to Fc receptors to exclude non-specific antibody activity (FIGURE 25). Furthermore, it exhibits a longer half-life than Fab fragments, which persists only for a few hours in the system (Flanagan and Jones, 2004; Adams *et al.*, 2016). Additionally, CAR T cells were attenuated in their activity prior to use by a freeze-thawing step. With a further reduction of the CAR T cell number and under the optimized conditions, CAR T cells showed barely non-specific activity and were able to kill the leukemia cells in the presence of the biotinylated mAb *in vivo* (FIGURE 25A-C), while they circulated in the

peripheral blood (FIGURE 25D). However, the anti-CD19 biotinylated mAb clone REA675 also revealed a slightly anti-leukemic effect on its own.
By a further reduction of the mAb application frequency from three times to once a week, CAR T cells showed an improved capability for inhibiting the leukemia cell growth in the presence of the biotinylated mAb *in vivo* (FIGURE 26A-C). These results demonstrated the ability and potency of an adapter-CAR T cell system to further reduce 'on-target off-tumor' toxicities of CAR T cell therapy, as recently shown by Cao *et al*. and Ma *et al*. (Cao *et al.*, 2016; Ma *et al.*, 2016).

7.7 Short-spacer adapter CAR T cells for treatment of T cell malignancies

The capability of the adapter CAR T cell system in killing the CD19-positive B-ALL cell line Nalm-6 was discussed in the previous paragraph. The modularity to target different types of tumors, however, needed to be elucidated. Since CAR T cell therapy for T-ALLs is still difficult due to the shared surface markers between normal and malignant T cells, other immune competent cells can be used such as CAR NK cells (K. H. Chen *et al.*, 2016; Chen *et al.*, 2017) or CAR T cells targeting tumor-specific antigens. Typical markers confined to malignant T cells are CD7 (Gomes-Silva *et al.*, 2017), CD231 (Talla-1) and overexpressed antigens like chemokine receptor CCR4 (Perera *et al.*, 2017). Also, universal adapter CAR T cells targeting T cell subset-specific or tumor-associated antigens could be used for future CAR T cell therapy of T cell malignancies. *In vitro* co-culture experiments showed that the adapter anti-biotin #9 CAR T cells were able to kill γδ-TCR-positive Molt-14 T-ALL cells as well as CD231-positive Jurkat T-ALL cells in the presence of a biotinylated tumor-specific mAb (FIGURE 27). These results emphasize the modular concept of the universal adapter CAR T cells in targeting different kind of tumors. However, targeting common T cell antigens like CD3 or CD5 would probably result in self-targeting and autolysis, and would finally compromise the efficacy of the CAR T cell therapy or even lead to T cell aplasia in the human system (Chen *et al.*, 2017; Gomes-Silva *et al.*, 2017). The best way to circumvent self-targeting and to improve the adapter system would be a knockout of the T cell receptor complex in CAR T cells without destroying the CAR construct.

In general, universal adapter CAR T cells are capable of targeting a wide range of tumors accompanied with a decrease of 'on-target off-tumor' toxicities. For that reason, they will play an important role in future CAR T cell therapy.

7.8 Conclusion and outlook

Within this study, two different therapeutic approaches were pursued, a pharmaceutical-based therapy for AML and a CAR T cell-based treatment approach for B-/ T-ALL. Since AML is a widely heterogeneous disorder with many subtypes, a predominant malignant antigen is not clearly given. Targeting a common antigen might also interfere with the normal blood cell formation. Therefore, a new pharmaceutical approach with ATO and G-CSF was tested and proven an effective drug combination for AML therapy. Even G-CSF as a single agent displayed an anti-leukemic effectiveness *in vivo*. With its observed AQP9-stimulating effect, G-CSF might play a more important role in future AML therapy, not only for handling neutropenia and reducing the incidence of infections, but also as an anti-leukemic drug. Furthermore, the AQP9-stimulating effect of G-CSF could be used for several other tumors in which AQP9 is involved, such as hepatocellular carcinomas and prostate cancer (Q. Chen *et al.*, 2016; W. guang Zhang *et al.*, 2016). Also, alternative small molecules might enhance AQP9 expression rendering AQP9 a novel therapeutic target for several cancers.

The predominant antigens of B-ALL CD19, CD20 and CD22 are highly qualified for CAR T cell-based therapy. To reduce 'on-target off-tumor' toxicities of CAR T cell therapy approaches, two strategies were proposed: bispecific CAR T cells and universal adapter CAR T cells. Both demonstrated good effectiveness *in vitro* and *in vivo*. Bispecific CAR T cells are a good tool to prevent specific escape strategies of leukemic blasts like antigen loss. Furthermore, the modularity of the adapter CAR T cells enables targeting of several antigens at the same time as well as many different cancer cell types. Any antigen recognized by an antibody can be detected by this 'on-switch' mechanism. Using adapter CAR T cells, each tumor patient could be individually treated by their antigen profile, which represents a further step towards a personalized medicine (Van 't Veer and Bernards, 2008). CAR T cell therapy could even be the treatment of choice for T cell malignancies if autolysis of CAR T cells could be prevented, which might be facilitated by knocking out the T cell receptor complex of CAR T cells.

In conclusion, two treatment approaches for two types of acute leukemia resulted in a therapeutic success in respective ways. The heterogeneity among acute leukemia is high and, therefore, demands a development of a wide spectrum of treatment possibilities.

8. REFERENCES

Van ’t Veer LJ, Bernards R. Enabling personalized cancer medicine through analysis of gene-expression patterns. Nature 2008; 452: 564–570.

Adams R, Griffin L, Compson JE, Jairaj M, Baker T, Ceska T, et al. Extending the half-life of a fab fragment through generation of a humanized anti-human serum albumin Fv domain: An investigation into the correlation between affinity and serum half-life. MAbs 2016; 8: 1336–1346.

Akao Y, Mizoguchi H, Kojima S, Naoe T, Ohishi N, Yagi K. Arsenic induces apoptosis in B-cell leukaemic cell lines in vitro: Activation of caspases and down-regulation of Bcl-2 protein. Br. J. Haematol. 1998; 102: 1055–1060.

Alatrash G, Daver N, Mittendorf EA. Targeting Immune Checkpoints in Hematologic Malignancies. Pharmacol. Rev. 2016; 68: 1014–1025.

Almåsbak H, Walseng E, Kristian A, Myhre MR, Suso EM, Munthe LA, et al. Inclusion of an IgG1-Fc spacer abrogates efficacy of CD19 CAR T cells in a xenograft mouse model. Gene Ther. 2015; 22: 391–403.

Anurathapan U, Chan RC, Hindi HF, Mucharla R, Bajgain P, Hayes BC, et al. Kinetics of Tumor Destruction by Chimeric Antigen Receptor-modified T Cells. Mol. Ther. 2014; 22: 623–633.

Armstrong SA, Kung AL, Mabon ME, Silverman LB, Stam RW, Den Boer ML, et al. Inhibition of FLT3 in MLL: Validation of a therapeutic target identified by gene expression based classification. Cancer Cell 2003; 3: 173–183.

Baba M, Hasegawa H, Nakayabu M, Shimizu N, Suzuki S, Kamada N, et al. Establishment and characteristics of a gastric cancer cell line (HuGC-OOHIRA) producing high levels of G-CSF, GM-CSF, and IL-6: The presence of autocrine growth control by G-CSF. Am. J. Hematol. 1995; 49: 207–215.

Bader P, Kreyenberg H, Von Stackelberg A, Eckert C, Salzmann-Manrique E, Meisel R, et al. Monitoring of minimal residual disease after allogeneic stem-cell transplantation in relapsed childhood acute lymphoblastic leukemia allows for the identification of impending relapse: Results of the all-bfm-sct 2003 trial. J. Clin. Oncol. 2015; 33: 1275–1284.

Baeuerle PA, Reinhardt C. Bispecific T-cell engaging antibodies for cancer therapy. Cancer Res. 2009; 69: 4941–4944.

Barrett DM, Grupp SA, June CH. Chimeric Antigen Receptor– and TCR-Modified T Cells Enter Main Street and Wall Street. J. Immunol. 2015; 195: 755–761.

Barrett DM, Singh N, Liu X, Jiang S, June CH, Grupp SA, et al. Relation of clinical culture method to T-cell memory status and efficacy in xenograft models of adoptive immunotherapy. Cytotherapy 2014; 16: 619–630.

Beauchamp EM, Ringer L, Bulut G, Sajwan KP, Hall MD, Lee YC, et al. Arsenic trioxide inhibits human cancer cell growth and tumor development in mice by blocking Hedgehog/GLI pathway. J. Clin. Invest. 2011; 121: 148–160.

Bennett JM, Catovsky D, Daniel M -T, Flandrin G, Galton DAG, Gralnick HR, et al. Proposals for the Classification of the Acute Leukaemias French-American-British (FAB) Co-operative Group. Br. J. Haematol. 1976; 33: 451–458.

Berger C, Jensen MC, Lansdorp PM, Gough M, Elliott C, Riddell SR. Adoptive transfer of effector CD8+ T cells derived from central memory cells establishes persistent T cell memory in primates. J. Clin. Invest. 2008; 118: 294–305.

Berger R, Rotem-Yehudar R, Slama G, Landes S, Kneller A, Leiba M, et al. Phase i safety and pharmacokinetic study of CT-011, a humanized antibody interacting with PD-1, in patients with advanced hematologic malignancies. Clin. Cancer Res. 2008; 14: 3044–3051.

Bernstein ID. Monoclonal antibodies to the myeloid stem cells: therapeutic implications of CMA-676, a humanized anti-CD33 antibody calicheamicin conjugate. Leuk. Off. J. Leuk. Soc. Am. Leuk. Res. Fund, U.K 2000; 14: 474–5.

Bessho M, Yoshida S, Sakate K, Murohashi I, Jinnai I, Hirashima K. Suppression of the development of murine myeloid leukemia with granulocyte colony-stimulating factor by inducing apoptosis of leukemic cells. Leukemia 1994; 8: 1185–90.

Bhattacharjee H, Carbrey J, Rosen BP, Mukhopadhyay R. Drug uptake and pharmacological modulation of drug sensitivity in leukemia by AQP9. Biochem. Biophys. Res. Commun. 2004; 322: 836–841.

Binder M, Otto F, Mertelsmann R, Veelken H, Trepel M. The epitope recognized by rituximab. Blood 2006; 108: 1975–1978.

Birbrair A, Frenette PS. Niche heterogeneity in the bone marrow. Ann. N. Y. Acad. Sci. 2016; 1370: 82–96.

Boehme KA, Zaborski JJ, Riester R, Schweiss SK, Hopp U, Traub F, et al. Targeting hedgehog signalling by arsenic trioxide reduces cell growth and induces apoptosis in rhabdomyosarcoma. Int. J. Oncol. 2016; 48: 801–812.

Bogan KL, Brenner C. Nicotinic Acid, Nicotinamide, and Nicotinamide Riboside: A Molecular Evaluation of NAD $^{+}$ Precursor Vitamins in Human Nutrition. Annu. Rev. Nutr. 2008; 28: 115–130.

Bomken S, Fišer K, Heidenreich O, Vormoor J. Understanding the cancer stem cell. Br. J. Cancer 2010; 103: 439–445.

Bonnet D, Dick JE. Human acute myeloid leukemia is organized as a hierarchy that originates from a primitive hematopoietic cell. Nat. Med. 1997; 3: 730–737.

Borthakur G, Kantarjian H, Wang X, Plunkett WK, Gandhi V V., Faderl S, et al. Treatment of core-binding-factor in acute myelogenous leukemia with fludarabine, cytarabine, and granulocyte colony-stimulating factor results in improved event-free survival. Cancer 2008; 113: 3181–3185.

Brentjens RJ, Davila ML, Riviere I, Park J, Wang X, Cowell LG, et al. CD19-Targeted T Cells Rapidly Induce Molecular Remissions in Adults with Chemotherapy-Refractory Acute Lymphoblastic Leukemia. Sci. Transl. Med. 2013; 5: 177ra38-177ra38.

Bridgeman JS, Hawkins RE, Hombach AA, Abken H, Gilham DE. Building better chimeric antigen receptors for adoptive T cell therapy. Curr. Gene Ther. 2010; 10: 77–90.

Bruserud Ø, Gjertsen BT, von Volkman HL. In Vitro Culture of Human Acute Myelogenous Leukemia (AML) Cells in Serum-Free Media: Studies of Native AML Blasts and AML Cell Lines. J. Hematother. Stem Cell Res. 2000; 9: 923–932.

Budel LM, Touw IP, Delwel R, Löwenberg B. Granulocyte colony-stimulating factor receptors in human acute myelocytic leukemia. Blood 1989; 74: 2668–73.

Burnett AK, Hills RK, Milligan D, Kjeldsen L, Kell J, Russell NH, et al. Identification of Patients with Acute Myeloblastic Leukemia Who Benefit from the Addition of Gemtuzumab Ozogamicin: Results of the MRC AML15 Trial. J. Clin. Oncol. 2011; 29: 369–377.

Burnett AK, Russell NH, Hills RK, Hunter AE, Kjeldsen L, Yin J, et al. Optimization of chemotherapy for younger patients with acute myeloid leukemia: Results of the medical research council AML15 trial. J. Clin. Oncol. 2013; 31: 3360–3368.

Cao Y, Rodgers DT, Du J, Ahmad I, Hampton EN, Ma JSY, et al. Design of Switchable Chimeric Antigen Receptor T Cells Targeting Breast Cancer. Angew. Chemie - Int. Ed. 2016; 55: 7520–7524.

Carbrey JM, Song L, Zhou Y, Yoshinaga M, Rojek A, Wang Y, et al. Reduced arsenic clearance and increased toxicity in aquaglyceroporin-9-null mice. Proc. Natl. Acad. Sci. 2009; 106: 15956–15960.

Carpenito C, Milone MC, Hassan R, Simonet JC, Lakhal M, Suhoski MM, et al. Control of large, established tumor xenografts with genetically retargeted human T cells containing CD28 and CD137 domains. Proc. Natl. Acad. Sci. 2009; 106: 3360–3365.

Caserta S, Alessi P, Basso V, Mondino A. IL-7 is superior to IL-2 for ex vivo expansion of

tumourspecific CD4 + T cells. Eur. J. Immunol. 2010; 40: 470–479.

Castaigne S, Pautas C, Terré C, Raffoux E, Bordessoule D, Bastie JN, et al. Effect of gemtuzumab ozogamicin on survival of adult patients with de-novo acute myeloid leukaemia (ALFA-0701): A randomised, open-label, phase 3 study. Lancet 2012; 379: 1508–1516.

Challen GA, Boles NC, Chambers SM, Goodell MA. Distinct Hematopoietic Stem Cell Subtypes Are Differentially Regulated by TGF-β1. Cell Stem Cell 2010; 6: 265–278.

Chan WK, Suwannasaen D, Throm RE, Li Y, Eldridge PW, Houston J, et al. Chimeric antigen receptor-redirected CD45RA-negative T cells have potent antileukemia and pathogen memory response without graft-versus-host activity. Leukemia 2015; 29: 387–395.

Chau D, Ng K, Chan TS-Y, Cheng Y-Y, Fong B, Tam S, et al. Azacytidine sensitizes acute myeloid leukemia cells to arsenic trioxide by up-regulating the arsenic transporter aquaglyceroporin 9. J. Hematol. Oncol. 2015; 8: 1–11.

Chen F, Fan C, Gu X, Zhang H, Liu Q, Gao X, et al. Construction of Anti-CD20 Single-Chain Antibody-CD28-CD137-TCRzeta Recombinant Genetic Modified T Cells and its Treatment Effect on B Cell Lymphoma. Med Sci Monit 2015; 21: 2110–2115.

Chen GQ, Shi XG, Tang W, Xiong SM, Zhu J, Cai X, et al. Use of arsenic trioxide (As2O3) in the treatment of acute promyelocytic leukemia (APL): I. As2O3 exerts dose-dependent dual effects on APL cells. Blood 1997; 89: 3345–3353.

Chen KH, Wada M, Firor AE, Pinz KG, Jares A, Liu H, et al. Novel anti-CD3 chimeric antigen receptor targeting of aggressive T cell malignancies. Oncotarget 2016; 7: 56219–56232.

Chen KH, Wada M, Pinz KG, Liu H, Lin K-W, Jares A, et al. Preclinical targeting of aggressive T-cell malignancies using anti-CD5 chimeric antigen receptor. Leukemia 2017

Chen Q, Zhu L, Zheng B, Wang J, Song X, Zheng W, et al. Effect of AQP9 expression in androgen-independent prostate cancer cell PC3. Int. J. Mol. Sci. 2016; 17

Chen SJ, Zhou GB, Zhang XW, Mao JH, De Thé H, Chen Z. From an old remedy to a magic bullet: Molecular mechanisms underlying the therapeutic effects of arsenic in fighting leukemia. Blood 2011; 117: 6425–6437.

Chiaretti S, Foà R. T-cell acute lymphoblastic leukemia. Haematologica 2009; 94: 160–162.

Chmielewski M, Hombach AA, Abken H. Antigen-specific T-cell activation independently of the MHC: Chimeric antigen receptor-redirected T cells. Front. Immunol. 2013; 4

Chung NG, Buxhofer-Ausch V, Radich JP. The detection and significance of minimal residual disease in acute and chronic leukemia. Tissue Antigens 2006; 68: 371–385.

Cooper LJN, Topp MS, Serrano LM, Gonzalez S, Chang WC, Naranjo A, et al. T-cell clones

can be rendered specific for CD19: Toward the selective augmentation of the graft-versus-B-lineage leukemia effect. Blood 2003; 101: 1637–1644.

Cozzio A, Passegué E, Ayton PM, Karsunky H, Cleary ML, Weissman IL. Similar MLL-associated leukemias arising from self-renewing stem cells and short-lived myeloid progenitors. Genes Dev. 2003; 17: 3029–3035.

Crobu D, Spinetti G, Schrepfer R, Tonon G, Jotti GS, Onali P, et al. Preclinical and clinical phase I studies of a new recombinant Filgrastim (BK0023) in comparison with Neupogen®. BMC Pharmacol. Toxicol. 2014; 15: 7.

Dale DC, Bolyard AA, Schwinzer BG, Pracht G, Bonilla MA, Boxer L, et al. The Severe Chronic Neutropenia International Registry: 10-Year Follow-up Report. Support. Cancer Ther. 2006; 3: 220–231.

van Dalen EC, Raphaël MF, Caron HN, Kremer LCM. Treatment including anthracyclines versus treatment not including anthracyclines for childhood cancer. In: van Dalen EC, editor(s). The Cochrane database of systematic reviews. Chichester, UK: John Wiley & Sons, Ltd; 2014. p. CD006647.

Davila ML, Riviere I, Wang X, Bartido S, Park J, Curran K, et al. Efficacy and Toxicity Management of 19-28z CAR T Cell Therapy in B Cell Acute Lymphoblastic Leukemia. Sci. Transl. Med. 2014; 6: 224ra25-224ra25.

Davis TA, Czerwinski DK, Levy R. Therapy of B-cell lymphoma with anti-CD20 antibodies can result in the loss of CD20 antigen expression. Clin. Cancer Res. 1999; 5: 611–615.

Dean M, Fojo T, Bates S. Tumour stem cells and drug resistance. Nat. Rev. Cancer 2005; 5: 275–284.

Deindl E, Zaruba MM, Brunner S, Huber B, Mehl U, Assmann G, et al. G-CSF administration after myocardial infarction in mice attenuates late ischemic cardiomyopathy by enhanced arteriogenesis. FASEB J. 2006; 20: 956–958.

Deniger DC, Switzer K, Mi T, Maiti S, Hurton L, Singh H, et al. Bispecific T-cells Expressing Polyclonal Repertoire of Endogenous γδ T-cell Receptors and Introduced CD19-specific Chimeric Antigen Receptor. Mol. Ther. 2013; 21: 638–647.

DiJoseph JF, Armellino DC, Boghaert ER, Khandke K, Dougher MM, Sridharan L, et al. Antibody-targeted chemotherapy with CMC-544: A CD22-targeted immunoconjugate of calicheamicin for the treatment of B-lymphoid malignancies. Blood 2004; 103: 1807–1814.

Döhner H, Lübbert M, Fiedler W, Fouillard L, Haaland A, Brandwein JM, et al. Randomized, phase 2 trial of low-dose cytarabine with or without volasertib in AML patients not suitable for induction therapy. Blood 2014; 124: 1426–1433.

Dworzak MN, Schumich A, Printz D, Pötschger U, Husak Z, Attarbaschi A, et al. CD20 up-regulation in pediatric B-cell precursor acute lymphoblastic leukemia during induction treatment: setting the stage for anti-CD20 directed immunotherapy. Blood 2008; 112: 3982–3988.

Ebinger M, Witte KE, Ahlers J, Schäfer I, André M, Kerst G, et al. High frequency of immature cells at diagnosis predicts high minimal residual disease level in childhood acute lymphoblastic leukemia. Leuk. Res. 2010; 34: 1139–1142.

Einfeld DA, Brown JP, Valentine MA, Clark EA, Ledbetter JA. Molecular cloning of the human B cell CD20 receptor predicts a hydrophobic protein with multiple transmembrane domains. EMBO J. 1988; 7: 711–7.

Elkjær M-L, Vajda Z, Nejsum LN, Kwon T-H, Jensen UB, Amiry-Moghaddam M, et al. Immunolocalization of AQP9 in Liver, Epididymis, Testis, Spleen, and Brain. Biochem. Biophys. Res. Commun. 2000; 276: 1118–1128.

Ellison RR, Holland JF, Weil M, Jacquillat C, Boiron M, Bernard J, et al. Arabinosyl cytosine: a useful agent in the treatment of acute leukemia in adults. Blood 1968; 32: 507–23.

Elter T, Gercheva-Kyuchukova L, Pylylpenko H, Robak T, Jaksic B, Rekhtman G, et al. Fludarabine plus alemtuzumab versus fludarabine alone in patients with previously treated chronic lymphocytic leukaemia: A randomised phase 3 trial. Lancet Oncol. 2011; 12: 1204–1213.

Eppert K, Takenaka K, Lechman ER, Waldron L, Nilsson B, van Galen P, et al. Stem cell gene expression programs influence clinical outcome in human leukemia. Nat. Med. 2011; 17: 1086–1093.

Essers MAG, Trumpp A. Targeting leukemic stem cells by breaking their dormancy. Mol. Oncol. 2010; 4: 443–450.

Fan J-X, Zeng Y-J, Wu J-W, Li Z-Q, Li Y-M, Zheng R, et al. [Synergistic killing effect of arsenic trioxide combined with curcumin on KG1a cells]. Zhongguo shi yan xue ye xue za zhi 2014; 22: 1267–1272.

Fenaux P, Wang ZZ, Degos L. Treatment of acute promyelocytic leukemia by retinoids. Curr. Top. Microbiol. Immunol. 2007; 313: 101–28.

Fernandes Â, Azevedo MM, Pereira O, Sampaio- B, Paiva A, Correia-neves M, et al. Proteolytic systems and AMP-activated protein kinase are critical targets of acute myeloid leukemia therapeutic approaches. Oncotarget 2014; 6: 31428–31440.

Feucht J, Kayser S, Gorodezki D, Hamieh M, Döring M, Blaeschke F, et al. T-cell responses against CD19+ pediatric acute lymphoblastic leukemia mediated by bispecific T-cell engager

(BiTE) are regulated contrarily by PD-L1 and CD80/CD86 on leukemic blasts. Oncotarget 2016; 7: 76902–76919.

Figueroa ME, Abdel-Wahab O, Lu C, Ward PS, Patel J, Shih A, et al. Leukemic IDH1 and IDH2 Mutations Result in a Hypermethylation Phenotype, Disrupt TET2 Function, and Impair Hematopoietic Differentiation. Cancer Cell 2010; 18: 553–567.

Finney HM, Lawson AD, Bebbington CR, Weir AN. Chimeric receptors providing both primary and costimulatory signaling in T cells from a single gene product. J. Immunol. 1998; 161: 2791–2797.

Flanagan RJ, Jones AL. Fab antibody fragments: some applications in clinical toxicology. Drug Saf. 2004; 27: 1115–33.

Fraser CC, Chen BP, Webb S, van Rooijen N, Kraal G. Circulation of human hematopoietic cells in severe combined immunodeficient mice after Cl2MDP-liposome-mediated macrophage depletion. Blood 1995; 86: 183–192.

Friend BD, Schiller GJ. Closing the gap: Novel therapies in treating acute lymphoblastic leukemia in adolescents and young adults. 2017

Frigault MJ, Lee J, Basil MC, Carpenito C, Motohashi S, Scholler J, et al. Identification of Chimeric Antigen Receptors That Mediate Constitutive or Inducible Proliferation of T Cells. Cancer Immunol. Res. 2015; 3: 356–367.

Fröhling S, Schlenk RF, Breitruck J, Benner A, Kreitmeier S, Tobis K, et al. Prognostic significance of activating FLT3 mutations in younger adults (16 to 60 years) with acute myeloid leukemia and normal cytogenetics: A study of the AML study group Ulm. Blood 2002; 100: 4372–4380.

Gaipa G, Basso G, Maglia O, Leoni V, Faini A, Cazzaniga G, et al. Drug-induced immunophenotypic modulation in childhood ALL: implications for minimal residual disease detection. Leukemia 2005; 19: 49–56.

Gargett T, Brown MP. The inducible caspase-9 suicide gene system as a ‘safety switch’ to limit on-target, off-tumor toxicities of chimeric antigen receptor T-cells. Front. Pharmacol. 2014; 5: 235.

Gesundheit B, Malach L, Or R, Hahn T. Neuroblastoma cell death is induced by inorganic arsenic trioxide (As(2)O(3)) and inhibited by a normal human bone marrow cell-derived factor. Cancer Microenviron. 2008; 1: 153–7.

Ghelli Luserna Di Rorà A, Iacobucci I, Imbrogno E, Papayannidis C, Derenzini E, Ferrari A, et al. Prexasertib, a Chk1/Chk2 inhibitor, increases the effectiveness of conventional therapy in B-/T- cell progenitor acute lymphoblastic leukemia. Oncotarget 2016; 7: 53377–53391.

Ghosh A, Smith M, James SE, Davila ML, Velardi E, Argyropoulos K V, et al. Donor CD19 CAR T cells exert potent graft-versus-lymphoma activity with diminished graft-versus-host activity. Nat. Med. 2017; 23: 242–249.

Gill S, June CH. Going viral: chimeric antigen receptor T-cell therapy for hematological malignancies. Immunol. Rev. 2015; 263: 68–89.

Gjertsen BT, Schöffski P. Discovery and development of the Polo-like kinase inhibitor volasertib in cancer therapy. Leukemia 2015; 29: 11–19.

Gomes-Silva D, Srinivasan M, Sharma S, Lee CM, Wagner DL, Davis TH, et al. CD7-edited T cells expressing a CD7-specific CAR for the therapy of T-cell malignancies. Blood 2017; 130: 285–296.

Goodell MA, Brose K, Paradis G, Conner AS, Mulligan RC. Isolation and functional properties of murine hematopoietic stem cells that are replicating in vivo. J.Exp.Med. 1996; 183: 1797–1806.

Gorin N-C, Isnard F, Garderet L, Ikhlef S, Corm S, Quesnel B, et al. Administration of alemtuzumab and G-CSF to adults with relapsed or refractory acute lymphoblastic leukemia: results of a phase II study. Eur. J. Haematol. 2013: n/a-n/a.

Gramatges MM, Rabin KR. The adolescent and young adult with cancer: State of the art - Acute leukemias. Curr. Oncol. Rep. 2013; 15: 317–324.

Greaves M. Infection, immune responses and the aetiology of childhood leukaemia. Nat. Rev. Cancer 2006; 6: 193–203.

Griffin TC, Weitzman S, Weinstein H, Chang M, Cairo M, Hutchison R, et al. A study of rituximab and ifosfamide, carboplatin, and etoposide chemotherapy in children with recurrent/refractory B-cell (CD20+) non-Hodgkin lymphoma and mature B-cell acute lymphoblastic leukemia: A report from the Children's Oncology Group. Pediatr. Blood Cancer 2009; 52: 177–181.

Gupta K, Kuznetsova I, Klimenkova O, Klimiankou M, Meyer J, Moore MAS, et al. Bortezomib inhibits STAT5-dependent degradation of LEF-1, inducing granulocytic differentiation in congenital neutropenia CD34+ cells. Blood 2014; 123: 2550–2561.

Hale G, Waldmann H. From Laboratory to Clinic: The Story of CAMPATH-1. In: Diagnostic and Therapeutic Antibodies. New Jersey: Humana Press; 2000. p. 243–266.

Halicka HD, Smolewski P, Darzynkiewicz Z, Dai W, Traganos F. Arsenic trioxide arrests cells early in mitosis leading to apoptosis. Cell Cycle 2002; 1: 201–209.

Haller JS. Therapeutic mule: the use of arsenic in the nineteenth century materia medica. Pharm. Hist. 1975; 17: 87–100.

Hamann PR, Hinman LM, Hollander I, Beyer CF, Lindh D, Holcomb R, et al. Gemtuzumab ozogamicin, a potent and selective anti-CD33 antibody - Calicheamicin conjugate for treatment of acute myeloid leukemia. Bioconjug. Chem. 2002; 13: 47–58.

Handgretinger R, Zugmaier G, Henze G, Kreyenberg H, Lang P, von Stackelberg A. Complete remission after blinatumomab-induced donor T-cell activation in three pediatric patients with post-transplant relapsed acute lymphoblastic leukemia. Leukemia 2011; 25: 181–184.

Hanna BS, Mcclanahan F, Yazdanparast H, Zaborsky N, Kalter V, Rößner PM, et al. Depletion of CLL-associated patrolling monocytes and macrophages controls disease development and repairs immune dysfunction in vivo. Leukemia 2016; 30: 570–579.

Harrington KH, Gudgeon CJ, Laszlo GS, Newhall KJ, Sinclair AM, Frankel SR, et al. The broad anti-AML activity of the CD33/CD3 BiTE antibody construct, AMG 330, is impacted by disease stage and risk. PLoS One 2015; 10

Harrison CJ. Cytogenetics of paediatric and adolescent acute lymphoblastic leukaemia. Br. J. Haematol. 2009; 144: 147–156.

Hasle H, Clemmensen IH, Mikkelsen M. Risks of leukaemia and solid tumours in individuals with Down's syndrome. Lancet 2000; 355: 165–169.

Haso W, Lee DW, Shah NN, Stetler-Stevenson M, Yuan CM, Pastan IH, et al. Anti-CD22-chimeric antigen receptors targeting B-cell precursor acute lymphoblastic leukemia. Blood 2013; 121: 1165–1171.

Hayden RS, Vollrath M, Kaplan DL. Effects of clodronate and alendronate on osteoclast and osteoblast co-cultures on silk-hydroxyapatite films. Acta Biomater. 2014; 10: 486–493.

Hegde M, Corder A, Chow KK, Mukherjee M, Ashoori A, Kew Y, et al. Combinational Targeting Offsets Antigen Escape and Enhances Effector Functions of Adoptively Transferred T Cells in Glioblastoma. Mol. Ther. 2013; 21: 2087–2101.

Hoelzer D. Novel Antibody-Based Therapies For Acute Lymphoblastic Leukemia. ASH Educ. Progr. B. 2011; 2011: 243–249.

Hoelzer D, Huettmann A, Kaul F, Irmer S, Jaekel N, Mohren M, et al. Immunochemotherapy with Rituximab Improves Molecular CR Rate and Outcome In CD20+ B-Lineage Standard and High Risk Patients; Results of 263 CD20+ Patients Studied Prospectively In GMALL Study 07/2003. ASH Annu. Meet. Abstr. 2010; 116: 170.

Hombach A, Hombach AA, Abken H. Adoptive immunotherapy with genetically engineered T cells: Modification of the IgG1 Fc spacer domain in the extracellular moiety of chimeric antigen receptors avoids off-target activation and unintended initiation of an innate immune

response. Gene Ther. 2010; 17: 1206–1213.

Hombach A, Kohler H, Rappl G, Abken H. Human CD4+ T Cells Lyse Target Cells via Granzyme/Perforin upon Circumvention of MHC Class II Restriction by an Antibody-Like Immunoreceptor. J. Immunol. 2006; 177: 5668–5675.

Hombach A, Wieczarkowiecz A, Marquardt T, Heuser C, Usai L, Pohl C, et al. Tumor-specific T cell activation by recombinant immunoreceptors: CD3 zeta signaling and CD28 costimulation are simultaneously required for efficient IL-2 secretion and can be integrated into one combined CD28/CD3 zeta signaling receptor molecule. J. Immunol. 2001; 167: 6123–31.

Hu Z, Van Rooijen N, Yang YG. Macrophages prevent human red blood cell reconstitution in immunodeficient mice. Blood 2011; 118: 5938–5946.

Hudecek M, Lupo-Stanghellini MT, Kosasih PL, Sommermeyer D, Jensen MC, Rader C, et al. Receptor affinity and extracellular domain modifications affect tumor recognition by ROR1-specific chimeric antigen receptor T cells. Clin. Cancer Res. 2013; 19: 3153–3164.

Hudecek M, Sommermeyer D, Kosasih PL, Silva-Benedict A, Liu L, Rader C, et al. The Nonsignaling Extracellular Spacer Domain of Chimeric Antigen Receptors Is Decisive for In Vivo Antitumor Activity. Cancer Immunol. Res. 2015; 3: 125–135.

Hunault M, Harousseau JL, Delain M, Truchan-Graczyk M, Cahn JY, Witz F, et al. Better outcome of adult acute lymphoblastic leukemia after early genoidentical allogeneic bone marrow transplantation (BMT) than after late high-dose therapy and autologous BMT: A GOELAMS trial. Blood 2004; 104: 3028–3037.

Hunger SP, Mullighan CG. Redefining ALL classification: Toward detecting high-risk ALL and implementing precision medicine. Blood 2015; 125: 3977–3987.

Huntly BJP, Gilliland DG. Timeline: Leukaemia stem cells and the evolution of cancer-stem-cell research. Nat. Rev. Cancer 2005; 5: 311–321.

Iriyama N, Yuan B, Hatta Y, Horikoshi A, Yoshino Y, Toyoda H, et al. Granulocyte colony-stimulating factor potentiates differentiation induction by all-trans retinoic acid and arsenic trioxide and enhances arsenic uptake in the acute promyelocytic leukemia cell line HT93A. Oncol. Rep. 2012; 28: 1875–82.

Iriyama N, Yuan B, Yoshino Y, Hatta Y, Horikoshi A, Aizawa S, et al. Aquaporin 9, a promising predictor for the cytocidal effects of arsenic trioxide in acute promyelocytic leukemia cell lines and primary blasts. Oncol. Rep. 2013; 29: 2362–8.

Ishibashi K, Morinaga T, Kuwahara M, Sasaki S, Imai M. Cloning and identification of a new member of water channel (AQP10) as an aquaglyceroporin. Biochim. Biophys. Acta-Gene

Struct. Expr. 2002; 1576: 335–340.

Ito S, Barrett AJ, Dutra A, Pak E, Miner S, Keyvanfar K, et al. Long term maintenance of myeloid leukemic stem cells cultured with unrelated human mesenchymal stromal cells. Stem Cell Res. 2015; 14: 95–104.

Jemal A, Bray F, Center MM, Ferlay J, Ward E, Forman D. Global cancer statistics. CA. Cancer J. Clin. 2011; 61: 69–90.

Jia SH, Li Y, Parodo J, Kapus A, Fan L, Rotstein OD, et al. Pre-B cell colony-enhancing factor inhibits neutrophil apoptosis in experimental inflammation and clinical sepsis. J. Clin. Invest. 2004; 113: 1318–27.

Jiao G, Ren T, Guo W, Ren C, Yang K. Arsenic trioxide inhibits growth of human chondrosarcoma cells through G2/M arrest and apoptosis as well as autophagy. Tumor Biol. 2015; 36: 3969–3977.

de Jonge-Peeters SDPWM, Kuipers F, de Vries EGE, Vellenga E. ABC transporter expression in hematopoietic stem cells and the role in AML drug resistance. Crit. Rev. Oncol. Hematol. 2007; 62: 214–226.

Juillerat A, Marechal A, Filhol J-M, Valton J, Duclert A, Poirot L, et al. Design of chimeric antigen receptors with integrated controllable transient functions. Sci. Rep. 2016; 6: 18950.

June CH, Riddell SR, Schumacher TN. Adoptive cellular therapy: A race to the finish line. Sci. Transl. Med. 2015; 7: 280ps7-280ps7.

Kalos M, Frey N V, Grupp S a, Loren AW, Jemision C, Gilmore J, et al. Randomized, Phase II Dose Optimization Study Of Chimeric Antigen Receptor Modified T Cells Directed Against CD19 (CTL019) In Patients With Relapsed, Refractory CLL. Blood 2013; 122: 873.

Kalos M, Levine BL, Porter DL, Katz S, Grupp SA, Bagg A, et al. T cells with chimeric antigen receptors have potent antitumor effects and can establish memory in patients with advanced leukemia. Sci. Transl. Med. 2011; 3: 95ra73.

Kaneko S, Mastaglio S, Bondanza A, Ponzoni M, Sanvito F, Aldrighetti L, et al. IL-7 and IL-15 allow the generation of suicide gene modified alloreactive self-renewing central memory human T lymphocytes. Blood 2009; 113: 1006–1015.

Kantarjian H, Stein A, Gökbuget N, Fielding AK, Schuh AC, Ribera J-M, et al. Blinatumomab versus Chemotherapy for Advanced Acute Lymphoblastic Leukemia. N. Engl. J. Med. 2017; 376: 836–847.

Kantarjian H, Thomas D, Jorgensen J, Jabbour E, Kebriaei P, Rytting M, et al. Inotuzumab ozogamicin, an anti-CD22-calecheamicin conjugate, for refractory and relapsed acute lymphocytic leukaemia: A phase 2 study. Lancet Oncol. 2012; 13: 403–411.

Kantarjian H, Thomas D, Wayne AS, O'Brien S. Monoclonal antibody-based therapies: A new dawn in the treatment of acute lymphoblastic leukemia. J. Clin. Oncol. 2012; 30: 3876–3883.

Kantarjian HM, DeAngelo DJ, Stelljes M, Martinelli G, Liedtke M, Stock W, et al. Inotuzumab Ozogamicin versus Standard Therapy for Acute Lymphoblastic Leukemia. N. Engl. J. Med. 2016; 375: 740–753.

Kawalekar OU, O'Connor RS, Fraietta JA, Guo L, McGettigan SE, Posey AD, et al. Distinct Signaling of Coreceptors Regulates Specific Metabolism Pathways and Impacts Memory Development in CAR T Cells. Immunity 2016; 44: 380–390.

Kellner C, Zhukovsky EA, Pötzke A, Brüggemann M, Schrauder A, Schrappe M, et al. The Fc-engineered CD19 antibody MOR208 (XmAb5574) induces natural killer cell-mediated lysis of acute lymphoblastic leukemia cells from pediatric and adult patients. Leukemia 2013; 27: 1595–8.

Kendal CE, Bryant-Greenwood GD. Pre-B-cell Colony-enhancing Factor (PBEF/Visfatin) Gene Expression is Modulated by NF-κB and AP-1 in Human Amniotic Epithelial Cells. Placenta 2007; 28: 305–314.

Kenderian SS, Ruella M, Shestova O, Klichinsky M, Aikawa V, Morrissette JJD, et al. CD33-specific chimeric antigen receptor T cells exhibit potent preclinical activity against human acute myeloid leukemia. Leukemia 2015; 29: 1637–1647.

Kerl K, Moreno N, Holsten T, Ahlfeld J, Mertins J, Hotfilder M, et al. Arsenic trioxide inhibits tumor cell growth in malignant rhabdoid tumors in vitro and in vivo by targeting overexpressed Gli1. Int. J. Cancer 2014; 135: 989–995.

Kim EY, Lee SS oo, Shin JH oon, Kim SH yun, Shin DH, Baek SY on. Anticancer effect of arsenic trioxide on cholangiocarcinoma: in vitro experiments and in vivo xenograft mouse model. Clin. Exp. Med. 2014; 14: 215–224.

Kim J, Lee JJ, Kim J, Gardner D, Beachy PA. Arsenic antagonizes the Hedgehog pathway by preventing ciliary accumulation and reducing stability of the Gli2 transcriptional effector. Proc. Natl. Acad. Sci. 2010; 107: 13432–13437.

Kita K, Nishii K, Ohishi K, Morita N, Takakura N, Kawakami K, et al. Frequent gene expression of granulocyte colony-stimulating factor (G-CSF) receptor in CD7+ surface CD3- acute lymphoblastic leukaemia. Leukemia 1993; 7: 1184–90.

Kitagawa J, Hara T, Tsurumi H, Kanemura N, Kasahara S, Shimizu M, et al. Cell cycle-dependent priming action of granulocyte colony-stimulating factor (G-CSF) enhances in vitro apoptosis induction by cytarabine and etoposide in leukemia cell lines. J. Clin. Exp.

Hematop. 2010; 50: 99–105.

Klebanoff CA, Gattinoni L, Restifo NP. CD8+ T-cell memory in tumor immunology and immunotherapy. Immunol. Rev. 2006; 211: 214–24.

Klimiankou M, Mellor-Heineke S, Zeidler C, Welte K, Skokowa J. Role of CSF3R mutations in the pathomechanism of congenital neutropenia and secondary acute myeloid leukemia. Ann. N. Y. Acad. Sci. 2016; 1370: 119–125.

Kloss CC, Condomines M, Cartellieri M, Bachmann M, Sadelain M. Combinatorial antigen recognition with balanced signaling promotes selective tumor eradication by engineered T cells. Nat. Biotechnol. 2012; 31: 71–75.

Knaus HA, Kanakry CG, Luznik L, Gojo I. Immunomodulatory Drugs: Immune Checkpoint Agents in Acute Leukemia. Curr. Drug Targets 2017; 18: 315–331.

Kochenderfer JN, Dudley ME, Feldman SA, Wilson WH, Spaner DE, Maric I, et al. B-cell depletion and remissions of malignancy along with cytokine-associated toxicity in a clinical trial of anti-CD19 chimeric-antigen-receptor-transduced T cells. Blood 2012; 119: 2709–20.

Koehler P, Schmidt P, Hombach AA, Hallek M, Abken H. Engineered T cells for the adoptive therapy of B-cell chronic lymphocytic leukaemia. Adv. Hematol. 2012; 2012: 595060.

Kottaridis PD, Gale RE, Frew ME, Harrison G, Langabeer SE, Belton AA, et al. The presence of a FLT3 internal tandem duplication in patients with acute myeloid leukemia (AML) adds important prognostic information to cytogenetic risk group and response to the first cycle of chemotherapy: Analysis of 854 patients from the United King. Blood 2001; 98: 1752–1759.

De Kouchkovsky I, Abdul-Hay M. ‘Acute myeloid leukemia: a comprehensive review and 2016 update’. Blood Cancer J. 2016; 6: e441.

Krupka C, Kufer P, Kischel R, Zugmaier G, Bögeholz J, Köhnke T, et al. CD33 target validation and sustained depletion of AML blasts in long-term cultures by the bispecific T-cell-engaging antibody AMG 330. Blood 2014; 123: 356–365.

Krupka C, Kufer P, Kischel R, Zugmaier G, Lichtenegger FS, Köhnke T, et al. Blockade of the PD-1/PD-L1 axis augments lysis of AML cells by the CD33/CD3 BiTE antibody construct AMG 330: reversing a T-cell-induced immune escape mechanism. Leukemia 2016; 30: 484–491.

Kumar S, Yedjou CG, Tchounwou PB. Arsenic trioxide induces oxidative stress, DNA damage, and mitochondrial pathway of apoptosis in human leukemia (HL-60) cells. J. Exp. Clin. Cancer Res. 2014; 33: 42.

Kunz JB, Rausch T, Bandapalli OR, Eilers J, Pechanska P, Schuessele S, et al. Pediatric T-cell lymphoblastic leukemia evolves into relapse by clonal selection, acquisition of mutations

and promoter hypomethylation. Haematologica 2015; 100: 1442–1450.

Lachmann N, Ackermann M, Frenzel E, Liebhaber S, Brennig S, Happle C, et al. Large-scale hematopoietic differentiation of human induced pluripotent stem cells provides granulocytes or macrophages for cell replacement therapies. Stem Cell Reports 2015; 4: 282–296.

Lagunas-Rangel FA, Chávez-Valencia V. FLT3–ITD and its current role in acute myeloid leukaemia. Med. Oncol. 2017; 34: 114.

Laing AA, Harrison CJ, Gibson BES, Keeshan K. Unlocking the potential of anti-CD33 therapy in adult and childhood acute myeloid leukemia. Exp. Hematol. 2017

Lane SW, Gilliland DG. Leukemia stem cells. Semin. Cancer Biol. 2010; 20: 71–76.

Lang P, Barbin K, Feuchtinger T, Greil J, Peipp M, Zunino SJ, et al. Chimeric CD19 antibody mediates cytotoxic activity against leukemic blasts with effector cells from pediatric patients who received T-cell-depleted allografts. Blood 2004; 103: 3982–3985.

Laszlo GS, Gudgeon CJ, Harrington KH, Dell'Aringa J, Newhall KJ, Means GD, et al. Cellular determinants for preclinical activity of a novel CD33/CD3 bispecific T-cell engager (BiTE) antibody, AMG 330, against human AML. Blood 2014; 123: 554–561.

Lee DW, Gardner R, Porter DL, Louis CU, Ahmed N, Jensen M, et al. Current concepts in the diagnosis and management of cytokine release syndrome. Blood 2014; 124: 188–195.

Lee DW, Kochenderfer JN, Stetler-Stevenson M, Cui YK, Delbrook C, Feldman SA, et al. T cells expressing CD19 chimeric antigen receptors for acute lymphoblastic leukaemia in children and young adults: A phase 1 dose-escalation trial. Lancet 2015; 385: 517–528.

Lee TC, Ho IC, Lu WJ, Huang JD. Enhanced expression of multidrug resistance-associated protein 2 and reduced expression of aquaglyceroporin 3 in an arsenic-resistant human cell line. J Biol Chem 2006; 281: 18401–18407.

Leget GA, Czuczman MS. Use of rituximab, the new FDA-approved antibody. Curr. Opin. Oncol. 1998; 10: 548–551.

Lemarie A, Morzadec C, Me D, Micheau O, Fardel O. Arsenic Trioxide Induces Apoptosis of Human Monocytes during Macrophagic Differentiation through Nuclear Factor- □ B- Related Survival Pathway Down-Regulation. 2006; 316: 304–314.

Leung J, Pang A, Yuen WH, Kwong YL, Tse EWC. Relationship of expression of aquaglyceroporin 9 with arsenic uptake and sensitivity in leukemia cells. Blood 2007; 109: 740–746.

Leung LL, Lam S-K, Li Y-Y, Ho JC-M. Tumour growth-suppressive effect of arsenic trioxide in squamous cell lung carcinoma. Oncol. Lett. 2017; 14: 3748–3754.

Li Y, Sun X, Wang L, Zhou Z, Kang YJ. Myocardial toxicity of arsenic trioxide in a mouse model. Cardiovasc. Toxicol. 2002; 2: 63–73.

Lichtenegger FS, Krupka C, Haubner S, Köhnke T, Subklewe M. Recent developments in immunotherapy of acute myeloid leukemia. J. Hematol. Oncol. 2017; 10: 142.

Von Lilienfeld-Toal M, Hahn-Ast C, Kirchner H, Flieger D, Dölken G, Glasmacher A. A randomized comparison of immediate versus delayed application of G-CSF in induction therapy for patients with acute myeloid leukemia unfit for intensive chemotherapy. Haematologica 2007; 92: 1719–1720.

Lin C-C, Hsu C, Hsu C-H, Hsu W-L, Cheng A-L, Yang C-H. Arsenic trioxide in patients with hepatocellular carcinoma: a phase II trial. Invest. New Drugs 2007; 25: 77–84.

Litzow MR. Arsenic trioxide. Expert Opin. Pharmacother. 2008; 9: 1773–1785.

Liu Z, Shen J, Carbrey JM, Mukhopadhyay R, Agre P, Rosen BP. Arsenite transport by mammalian aquaglyceroporins AQP7 and AQP9. Proc. Natl. Acad. Sci. 2002; 99: 6053–6058.

Loghavi S, Kutok JL, Jorgensen JL. B-acute lymphoblastic leukemia/lymphoblastic lymphoma. Am. J. Clin. Pathol. 2015; 144: 393–410.

Long AH, Haso WM, Shern JF, Wanhainen KM, Murgai M, Ingaramo M, et al. 4-1BB costimulation ameliorates T cell exhaustion induced by tonic signaling of chimeric antigen receptors. Nat. Med. 2015; 21: 581–590.

Ma A, Koka R, Burkett P. DIVERSE FUNCTIONS OF IL-2, IL-15, AND IL-7 IN LYMPHOID HOMEOSTASIS. Annu. Rev. Immunol. 2006; 24: 657–679.

Ma JSY, Kim JY, Kazane SA, Choi S, Yun HY, Kim MS, et al. Versatile strategy for controlling the specificity and activity of engineered T cells. Proc. Natl. Acad. Sci. 2016; 113: E450–E458.

Mahnke YD, Brodie TM, Sallusto F, Roederer M, Lugli E. The who's who of T-cell differentiation: Human memory T-cell subsets. Eur. J. Immunol. 2013; 43: 2797–2809.

Mahon FX. Discontinuation of tyrosine kinase therapy in CML. Ann. Hematol. 2015; 94: 187–193.

Marcus A, Eshhar Z. Allogeneic chimeric antigen receptor-modified cells for adoptive cell therapy of cancer. Expert Opin. Biol. Ther. 2014; 14: 947–954.

Mardiros A, Dos Santos C, McDonald T, Brown CE, Wang X, Budde LE, et al. T cells expressing CD123-specific chimeric antigen receptors exhibit specific cytolytic effector functions and antitumor effects against human acute myeloid leukemia. Blood 2013; 122:

3138–3148.

Marino VJ, Roguin LP. The granulocyte colony stimulating factor (G-CSF) activates Jak/STAT and MAPK pathways in a trophoblastic cell line. J. Cell. Biochem. 2008; 103: 1512–1523.

Marr LA, Gilham DE, Campbell JDM, Fraser AR. Immunology in the clinic review series; focus on cancer: Double trouble for tumours: Bi-functional and redirected T cells as effective cancer immunotherapies. Clin. Exp. Immunol. 2012; 167: 216–225.

Martelli AM, Tabellini G, Bortul R, Tazzari PL, Cappellini A, Billi AM, et al. Involvement of the phosphoinositide 3-kinase/Akt signaling pathway in the resistance to therapeutic treatments of human leukemias. Histol. Histopathol. 2005; 20: 239–252.

Martyniszyn A, Krahl A-C, André MC, Hombach AA, Abken H. CD20-CD19 bispecific CAR T cells for the treatment of B cell malignancies. Hum. Gene Ther. 2017; 28: hum.2017.126.

Mathews V V., Paul M V., Abhilash M, Manju A, Abhilash S, Nair RH. Myocardial toxicity of acute promyelocytic leukaemia drug-arsenic trioxide. Eur. Rev. Med. Pharmacol. Sci. 2013; 17 Suppl 1: 34–38.

Matlawska-Wasowska K, Ward E, Stevens S, Wang Y, Herbst R, Winter SS, et al. Macrophage and NK-mediated killing of precursor-B acute lymphoblastic leukemia cells targeted with a-fucosylated anti-CD19 humanized antibodies. Leukemia 2013; 27: 1263–1274.

Maude SL, Barrett D, Teachey DT, Grupp SA. Managing Cytokine Release Syndrome Associated With Novel T Cell-Engaging Therapies. Cancer J. 2014; 20: 119–122.

Maude SL, Tasian SK, Vincent T, Hall JW, Sheen C, Roberts KG, et al. Targeting JAK1/2 and mTOR in murine xenograft models of Ph-like acute lymphoblastic leukemia. Blood 2012; 120: 3510–3518.

Maus M V, Kovacs B, Kwok WW, Nepom GT, Schlienger K, Riley JL, et al. Extensive replicative capacity of human central memory T cells. J. Immunol. 2004; 172: 6675–83.

Mendoza JF, Cáceres JR, Santiago E, Mora LM, Sánchez L, Corona TM, et al. Evidence that G-CSF is a fibroblast growth factor that induces granulocytes to increase phagocytosis and to present a mature morphology, and that macrophages secrete 45-kd molecules with these activities as well as with G-CSF-like activity. Exp. Hematol. 1990; 18: 903–10.

Mesko B, Poliskal S, Szegedi A, Szekanecz Z, Palatka K, Papp M, et al. Peripheral blood gene expression patterns discriminate among chronic inflammatory diseases and healthy controls and identify novel targets. BMC Med. Genomics 2010; 3: 15.

Milone MC, Fish JD, Carpenito C, Carroll RG, Binder GK, Teachey D, et al. Chimeric

receptors containing CD137 signal transduction domains mediate enhanced survival of T cells and increased antileukemic efficacy in vivo. Mol. Ther. 2009; 17: 1453–1464.

Minotti G. Anthracyclines: Molecular Advances and Pharmacologic Developments in Antitumor Activity and Cardiotoxicity. Pharmacol. Rev. 2004; 56: 185–229.

Moniaga CS, Watanabe S, Honda T, Nielsen S, Hara-Chikuma M. Aquaporin-9-expressing neutrophils are required for the establishment of contact hypersensitivity. Sci. Rep. 2015; 5: 15319.

Morgan RA, Dudley ME, Wunderlich JR, Hughes MS, Yang JC, Sherry RM, et al. Cancer Regression in Patients After Transfer of Genetically Engineered Lymphocytes. Science (80-.). 2006; 314: 126–129.

Morgan RA, Yang JC, Kitano M, Dudley ME, Laurencot CM, Rosenberg SA. Case Report of a Serious Adverse Event Following the Administration of T Cells Transduced With a Chimeric Antigen Receptor Recognizing ERBB2. Mol. Ther. 2010; 18: 843–851.

Morris KT, Castillo EF, Ray AL, Weston LL, Nofchissey RA, Hanson JA, et al. Anti-G-CSF treatment induces protective tumor immunity in mouse colon cancer by promoting protective NK cell, macrophage and T cell responses. Oncotarget 2015; 6: 22338–47.

Müller T, Uherek C, Maki G, Chow KU, Schimpf A, Klingemann HG, et al. Expression of a CD20-specific chimeric antigen receptor enhances cytotoxic activity of NK cells and overcomes NK-resistance of lymphoma and leukemia cells. Cancer Immunol. Immunother. 2008; 57: 411–423.

Mullighan CG, Downing JR. Genome-wide profiling of genetic alterations in acute lymphoblastic leukemia: recent insights and future directions. Leukemia 2009; 23: 1209–1218.

Nagata S, Tsuchiya M, Asano S, Kaziro Y, Yamazaki T, Yamamoto O, et al. Molecular cloning and expression of cDNA for human granulocyte colony-stimulating factor. Nature 1986; 319: 415–418.

Nakayama H, Tomizawa D, Tanaka S, Iwamoto S, Shimada A, Saito AM, et al. Fludarabine, cytarabine, G-CSF and idarubicin for children with relapsed AML. Pediatr. Int. 2017

National Cancer Institute. What You Need To Know About Leukemia. U.S. Dep. Heal. Hum. Serv. 2013

NIH. Leukemia - Cancer Stat Facts [Internet]. 2017[cited 2018 Jan 23] Available from: https://seer.cancer.gov/statfacts/html/leuks.html

Niu C, Yan H, Yu T, Sun HP, Liu JX, Li XS, et al. Studies on treatment of acute promyelocytic leukemia with arsenic trioxide: remission induction, follow-up, and molecular

monitoring in 11 newly diagnosed and 47 relapsed acute promyelocytic leukemia patients. Blood 1999; 94: 3315–24.

Nowell PC. Discovery of the Philadelphia chromosome: A personal perspective. J. Clin. Invest. 2007; 117: 2033–2035.

O'Hear C, Heiber JF, Schubert I, Fey G, Geiger TL. Anti-CD33 chimeric antigen receptor targeting of acute myeloid leukemia. Haematologica 2015; 100: 336–44.

Oberoi P, Wels WS. Arming NK cells with enhanced antitumor activity: CARs and beyond. Oncoimmunology 2013; 2: e25220.

Owen C, Barnett M, Fitzgibbon J. Familial myelodysplasia and acute myeloid leukaemia - A review. Br. J. Haematol. 2008; 140: 123–132.

Park JH, Brentjens RJ. Are all chimeric antigen receptors created equal? J. Clin. Oncol. 2015; 33: 651–653.

Passegué E, Jamieson CHM, Ailles LE, Weissman IL. Normal and leukemic hematopoiesis: are leukemias a stem cell disorder or a reacquisition of stem cell characteristics? Proc. Natl. Acad. Sci. U. S. A. 2003; 100 Suppl: 11842–9.

Perera LP, Zhang M, Nakagawa M, Petrus MN, Maeda M, Kadin ME, et al. Chimeric antigen receptor modified T cells that target chemokine receptor CCR4 as a therapeutic modality for T-cell malignancies. Am. J. Hematol. 2017; 92: 892–901.

Perillat-Menegaux F, Clavel J, MF A, Baruchel A, Leverger G, Nelken B, et al. - Family history of autoimmune thyroid disease and childhood acute leukemia. J Invest Dermatol 2003; 120: 217–223.

Petersdorf SH, Kopecky KJ, Slovak M, Willman C, Nevill T, Brandwein J, et al. A phase 3 study of gemtuzumab ozogamicin during induction and postconsolidation therapy in younger patients with acute myeloid leukemia. Blood 2013; 121: 4854–4860.

Philip LPB, Schiffer-Mannioui C, Le Clerre D, Chion-Sotinel I, Derniame S, Potrel P, et al. Multiplex genome-edited T-cell manufacturing platform for 'off-the-shelf' adoptive T-cell immunotherapies. Cancer Res. 2015; 75: 3853–3864.

Platzbecker U, Avvisati G, Cicconi L, Thiede C, Paoloni F, Vignetti M, et al. Improved outcomes with retinoic acid and arsenic trioxide compared with retinoic acid and chemotherapy in non-high-risk acute promyelocytic leukemia: Final results of the randomized Italian-German APL0406 trial. J. Clin. Oncol. 2017; 35: 605–612.

Pollyea DA, Gutman JA, Gore L, Smith CA, Jordan CT. Targeting acute myeloid leukemia stem cells: A review and principles for the development of clinical trials. Haematologica 2014; 99: 1277–1284.

Porter DL, Levine BL, Kalos M, Bagg A, June CH. Chimeric antigen receptor-modified T cells in chronic lymphoid leukemia. N. Engl. J. Med. 2011; 365: 725–33.

Pui C-H, Evans WE. Treatment of Acute Lymphoblastic Leukemia. N. Engl. J. Med. 2006; 354: 166–178.

Pui CH, Relling M V., Evans WE. Role of pharmacogenomics and pharmacodynamics in the treatment of acute lymphoblastic leukaemia. Best Pract. Res. Clin. Haematol. 2002; 15: 741–756.

Qin H, Haso W, Nguyen SM, Fry TJ. Preclinical Development of Bispecific Chimeric Antigen Receptor Targeting Both CD19 and CD22. Blood 2015; 126: 4427–4427.

Queudeville M, Handgretinger R, Ebinger M. Immunotargeting relapsed or refractory precursor B-cell acute lymphoblastic leukemia - role of blinatumomab. Onco. Targets. Ther. 2017; 10: 3567–3578.

Radivoyevitch T, Sachs RK, Gale RP, Molenaar RJ, Brenner DJ, Hill BT, et al. Defining AML and MDS second cancer risk dynamics after diagnoses of first cancers treated or not with radiation. Leukemia 2015; 30: 285.

Raetz EA, Cairo MS, Borowitz MJ, Blaney SM, Krailo MD, Leil TA, et al. Chemoimmunotherapy reinduction with epratuzumab in children with acute lymphoblastic leukemia in marrow relapse: A children's oncology group pilot study. J. Clin. Oncol. 2008; 26: 3756–3762.

Raponi S, Stefania De Propris M, Intoppa S, Laura Milani M, Vitale A, Elia L, et al. Flow cytometric study of potential target antigens (CD19, CD20, CD22, CD33) for antibody-based immunotherapy in acute lymphoblastic leukemia: analysis of 552 cases. Leuk. Lymphoma 2011; 52: 1098–1107.

Ratajczak J, Joffraud M, Trammell SAJ, Ras R, Canela N, Boutant M, et al. NRK1 controls nicotinamide mononucleotide and nicotinamide riboside metabolism in mammalian cells. Nat. Commun. 2016; 7

Ratnaike RN. Acute and chronic arsenic toxicity. Postgrad. Med. J. 2003; 79: 391–6.

Restifo NP. Big bang theory of stem-like. Blood 2015; 124: 2014–2016.

Revollo JR, Grimm AA, Imai SI. The NAD biosynthesis pathway mediated by nicotinamide phosphoribosyltransferase regulates Sir2 activity in mammalian cells. J. Biol. Chem. 2004; 279: 50754–50763.

Revollo JR, Körner A, Mills KF, Satoh A, Wang T, Garten A, et al. Nampt/PBEF/Visfatin Regulates Insulin Secretion in β Cells as a Systemic NAD Biosynthetic Enzyme. Cell Metab. 2007; 6: 363–375.

Van Rhenen A, Van Dongen GAMS, Kelder A Le, Rombouts EJ, Feller N, Moshaver B, et al. The novel AML stem cell-associated antigen CLL-1 aids in discrimination between normal and leukemic stem cells. Blood 2007; 110: 2659–2666.

Richarson AD, Scott DA, Zagnitko O, Aza-Blanc P, Chang CC, Russler-Germain DA, et al. Registered report: IDH mutation impairs histone demethylation and results in a block to cell differentiation. Elife 2016; 5: 474–8.

Robak T, Dmoszynska A, Solal-Céligny P, Warzocha K, Loscertales J, Catalano J, et al. Rituximab plus fludarabine and cyclophosphamide prolongs progression-free survival compared with fludarabine and cyclophosphamide alone in previously treated chronic lymphocytic leukemia. J. Clin. Oncol. 2010; 28: 1756–65.

Robert Koch-Institut. Krebs in Deutschland | 2013/2014 | Leukämie C91 – C95. 2014

Roberts KG, Morin RD, Zhang J, Hirst M, Zhao Y, Su X, et al. Genetic Alterations Activating Kinase and Cytokine Receptor Signaling in High-Risk Acute Lymphoblastic Leukemia. Cancer Cell 2012; 22: 153–166.

Roboz GJ. Current treatment of acute myeloid leukemia. Curr. Opin. Oncol. 2012; 24: 711–719.

Rodgers DT, Mazagova M, Hampton EN, Cao Y, Ramadoss NS, Hardy IR, et al. Switch-mediated activation and retargeting of CAR-T cells for B-cell malignancies. Proc. Natl. Acad. Sci. 2016; 113: E459–E468.

Rogers CS, Yedjou CG, Sutton DJ, Tchounwou PB. Vitamin D3 potentiates the antitumorigenic effects of arsenic trioxide in human leukemia (HL-60) cells. Exp. Hematol. Oncol. 2014; 3: 9.

Rongvaux A, She RJ, Mulks MH, Gigot D, Urbain J, Leo O, et al. Pre-B-cell colony-enhancing factor, whose expression is up-regulated in activated lymphocytes, is a nicotinamide phosphoribosyltransferase, a cytosolic enzyme involved in NAF biosynthesis. Eur. J. Immunol. 2002; 32: 3225–3234.

de Rooij J, Zwaan C, van den Heuvel-Eibrink M. Pediatric AML: From Biology to Clinical Management. J. Clin. Med. 2015; 4: 127–149.

van Rooijen N, Hendrikx E. Liposomes for specific depletion of macrophages from organs and tissues. In: Methods in molecular biology (Clifton, N.J.). 2010. p. 189–203.

Rosenberg SA, Packard BS, Aebersold PM, Solomon D, Topalian SL, Toy ST, et al. Use of tumor-infiltrating lymphocytes and interleukin-2 in the immunotherapy of patients with metastatic melanoma. N. Engl. J. Med. 1988; 319: 1676–1680.

Roszak J, Smok-Pieniążek A, Nocuń M, Stępnik M. Characterization of arsenic trioxide

resistant clones derived from Jurkat leukemia T cell line: focus on PI3K/Akt signaling pathway. Chem. Biol. Interact. 2013; 205: 198–211.

Ruella M, Maus M V. Catch me if you can: Leukemia Escape after CD19-Directed T Cell Immunotherapies. Comput. Struct. Biotechnol. J. 2016; 14: 357–362.

Rufener GA, Press OW, Olsen P, Lee SY, Jensen MC, Gopal AK, et al. Preserved Activity of CD20-Specific Chimeric Antigen Receptor-Expressing T Cells in the Presence of Rituximab. Cancer Immunol. Res. 2016; 4: 509–519.

Saito Y, Furukawa T, Obata T, Saga T. Molecular Imaging of Aquaglycero-Aquaporins: Its Potential for Cancer Characterization. Biol. Pharm. Bull 1292; 36: 1292–1298.

Schäbitz WR, Schneider A. New targets for established proteins: exploring G-CSF for the treatment of stroke. Trends Pharmacol. Sci. 2007; 28: 157–161.

Schepers K, Campbell TB, Passegué E. Normal and leukemic stem cell niches: Insights and therapeutic opportunities. Cell Stem Cell 2015; 16: 254–267.

Schewe DM, Alsadeq A, Sattler C, Lenk L, Vogiatzi F, Cario G, et al. An Fc-engineered CD19 antibody eradicates MRD in patient-derived *MLL* -rearranged acute lymphoblastic leukemia xenografts. Blood 2017; 130: 1543–1552.

Schneider D, Xiong Y, Wu D, Nölle V, Schmitz S, Haso W, et al. A tandem CD19/CD20 CAR lentiviral vector drives on-target and off-target antigen modulation in leukemia cell lines. J. Immunother. Cancer 2017; 5: 42.

Schrappe M, Reiter A, Ludwig WD, Harbott J, Zimmermann M, Hiddemann W, et al. Improved outcome in childhood acute lymphoblastic leukemia despite reduced use of anthracyclines and cranial radiotherapy: results of trial ALL-BFM 90. German-Austrian-Swiss ALL-BFM Study Group. Blood 2000; 95: 3310–22.

Segeren CM, Van 't Veer MB. The FAB classification for acute myeloid leukaemia-is it outdated? Netherlands J. Med. ELSEVIER Netherlands J. Med. 1996; 49: 126–131.

Seidel UJE, Schlegel P, Grosse-Hovest L, Hofmann M, Aulwurm S, Pyz E, et al. Reduction of Minimal Residual Disease in Pediatric B-lineage Acute Lymphoblastic Leukemia by an Fc-optimized CD19 Antibody. Mol. Ther. 2016; 24: 1634–1643.

Semerad CL, Liu F, Gregory AD, Stumpf K, Link DC. G-CSF is an essential regulator of neutrophil trafficking from the bone marrow to the blood. Immunity 2002; 17: 413–423.

Shackelford D, Kenific C, Blusztajn A, Waxman S, Ren R. Targeted degradation of the AML1/MDS1/EVI1 oncoprotein by arsenic trioxide. Cancer Res. 2006; 66: 11360–11369.

Shen Z-X, Shi Z-Z, Fang J, Gu B-W, Li J-M, Zhu Y-M, et al. All-trans retinoic acid/As2O3

combination yields a high quality remission and survival in newly diagnosed acute promyelocytic leukemia. Proc. Natl. Acad. Sci. 2004; 101: 5328–5335.

Shi Y, Cao T, Huang H, Lian C, Yang Y, Wang Z, et al. Arsenic trioxide inhibits cell growth and motility via up-regulation of let-7a in breast cancer cells. Cell Cycle 2017: 00–00.

Shimauchi T, Kabashima K, Nakashima D, Sugita K, Yamada Y, Hino R, et al. Augmented expression of programmed death-1 in both neoplastic and non-neoplastic CD4+ T-cells in adult T-cell leukemia/lymphoma. Int. J. cancer 2007; 121: 2585–90.

Shlush LI, Mitchell A, Heisler L, Abelson S, Ng SWK, Trotman-Grant A, et al. Tracing the origins of relapse in acute myeloid leukaemia to stem cells. Nature 2017; 547: 104–108.

Singh N, Liu X, Hulitt J, Jiang S, June CH, Grupp SA, et al. Nature of Tumor Control by Permanently and Transiently Modified GD2 Chimeric Antigen Receptor T Cells in Xenograft Models of Neuroblastoma. Cancer Immunol. Res. 2014; 2: 1059–1070.

Skokowa J, Cario G, Uenalan M, Schambach A, Germeshausen M, Battmer K, et al. LEF-1 is crucial for neutrophil granulocytopoiesis and its expression is severely reduced in congenital neutropenia. Nat. Med. 2006; 12: 1191–1197.

Skokowa J, Dale DC, Touw IP, Zeidler C, Welte K. Severe congenital neutropenias. Nat. Rev. Dis. Prim. 2017; 3: 17032.

Skokowa J, Lan D, Thakur BK, Wang F, Gupta K, Cario G, et al. NAMPT is essential for the G-CSF–induced myeloid differentiation via a NAD+–sirtuin-1–dependent pathway. Nat. Med. 2009; 15: 151–158.

Smith MA, Seibel NL, Altekruse SF, Ries LAG, Melbert DL, O'Leary M, et al. Outcomes for children and adolescents with cancer: Challenges for the twenty-first century. J. Clin. Oncol. 2010; 28: 2625–2634.

Soffritti M, Belpoggi F, Degli Esposti D, Lambertini L. Results of a long-term carcinogenicity bioassay on Sprague-Dawley rats exposed to sodium arsenite administered in drinking water. In: Annals of the New York Academy of Sciences. 2006. p. 578–591.

Souza LM, Boone TC, Gabrilove J, Lai PH, Zsebo KM, Murdock DC, et al. Recombinant human granulocyte colony-stimulating factor: effects on normal and leukemic myeloid cells. Science 1986; 232: 61–65.

Stam RW, Den Boer ML, Schneider P, Nollau P, Horstmann M, Beverloo HB, et al. Targeting FLT3 in primary MLL-gene-rearranged infant acute lymphoblastic leukemia. Blood 2005; 106: 2484–2490.

Di Stasi A, Tey S-K, Dotti G, Fujita Y, Kennedy-Nasser A, Martinez C, et al. Inducible apoptosis as a safety switch for adoptive cell therapy. N. Engl. J. Med. 2011; 365: 1673–83.

Stein EM, Altman JK, Collins R, DeAngelo DJ, Fathi AT, Flinn I, et al. AG-221, an Oral, Selective, First-in-Class, Potent Inhibitor of the IDH2 Mutant Metabolic Enzyme, Induces Durable Remissions in a Phase I Study in Patients with IDH2 Mutation Positive Advanced Hematologic Malignancies [Internet]. Blood 2014; 124: 115.[cited 2017 Sep 21] Available from: http://learningcenter.ehaweb.org/eha/2015/20th/100710/eyal.attar.ag-221.an.oral.selective.first-in-class.potent.inhibitor.of.the.html?f=l4269p16m3

Stein EM, Tallman MS. Emerging therapeutic drugs for AML. Blood 2016; 127: 71–78.

Stemberger C, Graef P, Odendahl M, Albrecht J, Dössinger G, Anderl F, et al. Lowest numbers of primary CD8(+) T cells can reconstitute protective immunity upon adoptive immunotherapy. Blood 2014; 124: 628–37.

Stock W, La M, Sanford B, Bloomfield CD, Vardiman JW, Gaynon P, et al. What determines the outcomes for adolescents and young adults with acute lymphoblastic leukemia treated on cooperative group protocols? A comparison of Children's Cancer Group and Cancer and Leukemia Group B studies. Blood 2008; 112: 1646–1654.

Stock W, Sanford B, Lozanski G, Vij R, Byrd JC, Powell BL, et al. Alemtuzumab can be Incorporated Into Front-Line Therapy of Adult Acute Lymphoblastic Leukemia (ALL): Final Phase I Results of a Cancer and Leukemia Group B Study (CALGB 10102). In: Blood. 2009. p. 838 LP-838.

Szczepański T, van der Velden VHJ, van Dongen JJM. Classification systems for acute and chronic leukemias. Best Pract. Res. Clin. Haematol. 2003; 16: 561–582.

Tabellini G, Cappellini A, Tazzari PL, Falà F, Billi AM, Manzoli L, et al. Phosphoinositide 3-kinase/Akt involvement in arsenic trioxide resistance of human leukemia cells. J. Cell. Physiol. 2005; 202: 623–634.

Tanaka H, Tanaka Y, Shinagawa K, Yamagishi Y, Ohtaki K, Asano K. Three Types of Recombinant Human Granulocyte Colony-Stimulating Factor Have Equivalent Biological Activities in Monkeys. Cytokine 1997; 9: 360–369.

Tay J, Levesque JP, Winkler IG. Cellular players of hematopoietic stem cell mobilization in the bone marrow niche. Int. J. Hematol. 2017; 105: 129–140.

Tettamanti S, Magnani CF, Biondi A, Biagi E. Acute myeloid leukemia and novel biological treatments: Monoclonal antibodies and cell-based gene-modified immune effectors. Immunol. Lett. 2013; 155: 43–46.

Textor A, Listopad JJ, Wührmann L Le, Perez C, Kruschinski A, Chmielewski M, et al. Efficacy of CAR T-cell therapy in large tumors relies upon stromal targeting by IFNγ. Cancer Res. 2014; 74: 6796–6805.

Thokala R, Olivares S, Mi T, Maiti S, Deniger D, Huls H, et al. Redirecting specificity of t cells using the Sleeping Beauty system to express chimeric antigen receptors by mix-and-matching of VL and VH domains targeting CD123+ tumors. PLoS One 2016; 11: e0159477.

Thomas AK, Maus M V., Shalaby WS, June CH, Riley JL. A Cell-Based Artificial Antigen-Presenting Cell Coated with Anti-CD3 and CD28 Antibodies Enables Rapid Expansion and Long-Term Growth of CD4 T Lymphocytes. Clin. Immunol. 2002; 105: 259–272.

Thomas DA, O'Brien S, Faderl S, Garcia-Manero G, Ferrajoli A, Wierda W, et al. Chemoimmunotherapy with a modified hyper-CVAD and rituximab regimen improves outcome in de novo Philadelphia chromosome - Negative precursor B-lineage acute lymphoblastic leukemia. J. Clin. Oncol. 2010; 28: 3880–3889.

Till BG, Jensen MC, Wang J, Qian X, Gopal AK, Maloney DG, et al. CD20-specific adoptive immunotherapy for lymphoma using a chimeric antigen receptor with both CD28 and 4-1BB domains: Pilot clinical trial results. Blood 2012; 119: 3940–3950.

To LB, Haylock DN, Simmons PJ, Juttner C a. The biology and clinical uses of blood stem cells. Blood 1997; 89: 2233–2258.

Tokar EJ, Qu W, Liu J, Liu W, Webber MM, Phang JM, et al. Arsenic-specific stem cell selection during malignant transformation. J. Natl. Cancer Inst. 2010; 102: 638–649.

Tomuleasa C, Soritau O, Kacso G, Fischer-Fodor E, Cocis A, Ioani H, et al. Arsenic trioxide sensitizes cancer stem cells to chemoradiotherapy. A new approach in the treatment of inoperable glioblastoma multiforme. J. BUON. 2010; 15: 758–762.

Topp MS, Kufer P, Gökbuget N, Goebeler M, Klinger M, Neumann S, et al. Targeted therapy with the T-cell - Engaging antibody blinatumomab of chemotherapy-refractory minimal residual disease in B-lineage acute lymphoblastic leukemia patients results in high response rate and prolonged leukemia-free survival. J. Clin. Oncol. 2011; 29: 2493–2498.

Torikai H, Reik A, Liu PQ, Zhou Y, Zhang L, Maiti S, et al. A foundation for universal T-cell based immunotherapy: T cells engineered to express a CD19-specific chimeric-antigen-receptor and eliminate expression of endogenous TCR. Blood 2012; 119: 5697–5705.

Tsuji K, Ebihara Y. Expression of G-CSF receptor on myeloid progenitors. Leuk. Lymphoma 2001; 42: 1351–7.

Tsukaguchi H, Shayakul C, Berger U V., Mackenzie B, Devidas S, Guggino WB, et al. Molecular characterization of a broad selectivity neutral solute channel. J. Biol. Chem. 1998; 273: 24737–24743.

Tsukaguchi H, Weremowicz S, Morton CC, Hediger MA. Functional and molecular characterization of the human neutral solute channel aquaporin-9. Am. J. Physiol. Physiol.

1999; 277: F685–F696.

U.S. Food & Drug Administration. Press Announcements - FDA approval brings first gene therapy to the United States [Internet]. 2017[cited 2017 Oct 25] Available from: https://www.fda.gov/NewsEvents/Newsroom/PressAnnouncements/ucm574058.htm

Vardiman JW, Thiele J, Arber DA, Brunning RD, Borowitz MJ, Porwit A, et al. The 2008 revision of the World Health Organization (WHO) classification of myeloid neoplasms and acute leukemia: Rationale and important changes. Blood 2009; 114: 937–951.

Viadiu H, Gonen T, Walz T. Projection Map of Aquaporin-9 at 7???? Resolution. J. Mol. Biol. 2007; 367: 80–88.

Vick B, Rothenberg M, Sandhöfer N, Carlet M, Finkenzeller C, Krupka C, et al. An advanced preclinical mouse model for acute myeloid leukemia using patients' cells of various genetic subgroups and in vivo bioluminescence imaging. PLoS One 2015; 10

Visani G, Tosi P, Zinzani PL, Manfroi S, Ottaviani E, Testoni N, et al. FLAG (fludarabine + high-dose cytarabine + G-CSF): an effective and tolerable protocol for the treatment of 'poor risk' acute myeloid leukemias. Leukemia 1994; 8: 1842–6.

Walter RB, Appelbaum FR, Estey EH, Bernstein ID. Acute myeloid leukemia stem cells and CD33-targeted immunotherapy. Blood 2012; 119: 6198–6208.

Walter RB, Medeiros BC, Gardner KM, Orlowski KF, Gallegos L, Scott BL, et al. Gemtuzumab ozogamicin in combination with vorinostat and azacitidine in older patients with relapsed or refractory acute myeloid leukemia: A phase I/II study. Haematologica 2014; 99: 54–59.

Wang Y, Bai C, Guan H, Chen R, Wang X, Wang B, et al. Subchronic exposure to arsenic induces apoptosis in the hippocampus of the mouse brains through the Bcl-2/Bax pathway. J. Occup. Health 2015; 57: 212–221.

Wang Y, Zhang W ying, Han Q wang, Liu Y, Dai H ren, Guo Y lei, et al. Effective response and delayed toxicities of refractory advanced diffuse large B-cell lymphoma treated by CD20-directed chimeric antigen receptor-modified T cells. Clin. Immunol. 2014; 155: 160–175.

Wang ZY, Chen Z. Acute promyelocytic leukemia: From highly fatal to highly curable. Blood 2008; 111: 2505–2515.

Watanabe K, Terakura S, Martens AC, van Meerten T, Uchiyama S, Imai M, et al. Target Antigen Density Governs the Efficacy of Anti–CD20-CD28-CD3 ζ Chimeric Antigen Receptor–Modified Effector CD8 $^{+}$ T Cells. J. Immunol. 2015; 194: 911–920.

Wei G, Wang J, Huang H, Zhao Y. Novel immunotherapies for adult patients with B-lineage acute lymphoblastic leukemia. J. Hematol. Oncol. 2017; 10: 150.

Welch JS, Ley TJ, Link DC, Miller CA, Larson DE, Koboldt DC, et al. The origin and evolution of mutations in acute myeloid leukemia. Cell 2012; 150: 264–278.

Welte K, Platzer E, Lu L, Gabrilove JL, Levi E, Mertelsmann R, et al. Purification and biochemical characterization of human pluripotent hematopoietic colony-stimulating factor. Proc. Natl. Acad. Sci. U. S. A. 1985; 82: 1526–30.

Welte K, Zeidler C, Dale DC. Severe Congenital Neutropenia. Semin. Hematol. 2006; 43: 189–195.

Weng S, Matsuura S, Mowery CT, Stoner SA, Lam K, Ran D, et al. Restoration of MYC-repressed targets mediates the negative effects of GM-CSF on RUNX1-ETO leukemogenicity. Leukemia 2017; 31: 159–169.

van der Werff ten Bosch J, Suciu S, Thyss A, Bertrand Y, Norton L, Mazingue F, et al. Value of intravenous 6-mercaptopurine during continuation treatment in childhood acute lymphoblastic leukemia and non-Hodgkin's lymphoma: final results of a randomized phase III trial (58881) of the EORTC CLG. Leukemia 2005; 19: 721–726.

Van de Wetering M, De Lau W, Clevers H. Wnt signaling and lymphocyte development. Cell 2002; 109: S13-9.

WHO. WHO _ Cancer. WHO 2017

Wu C-T, Lu T-Y, Chan D-C, Tsai K-S, Yang R-S, Liu S-H. Effects of Arsenic on Osteoblast Differentiation in Vitro and on Bone Mineral Density and Microstructure in Rats. Environ. Health Perspect. 2014

Wu C-Y, Roybal KT, Puchner EM, Onuffer J, Lim WA. Remote control of therapeutic T cells through a small molecule-gated chimeric receptor. Science (80-.). 2015; 350: aab4077-aab4077.

Wu J-W, Xiao W-T, Zeng Y-J, Fan J-X, Ye Y-B, Li Y-M, et al. [Synergistic Killing Effects of Arsenic Trioxide Combined with Itraconazole on KG1a Cells]. Zhongguo shi yan xue ye xue za zhi 2017; 25: 1003–1010.

Wu J, Ji Z, Liu H, Liu Y, Han D, Shi C, et al. Arsenic trioxide depletes cancer stem-like cells and inhibits repopulation of neurosphere derived from glioblastoma by downregulation of Notch pathway. Toxicol. Lett. 2013; 220: 61–69.

Wulf GG, Wang RY, Kuehnle I, Weidner D, Marini F, Brenner MK, et al. A leukemic stem cell with intrinsic drug efflux capacity in acute myeloid leukemia. Blood 2001; 98: 1166–1173.

Xu Y, Zhang M, Ramos CA, Durett A, Liu E, Dakhova O, et al. Closely related T-memory stem cells correlate with in vivo expansion of CAR.CD19-T cells and are preserved by IL-7 and IL-15. Blood 2014; 123: 3750–3759.

Yang H, Bueso-Ramos C, DiNardo C, Estecio MR, Davanlou M, Geng Q-R, et al. Expression of PD-L1, PD-L2, PD-1 and CTLA4 in myelodysplastic syndromes is enhanced by treatment with hypomethylating agents. Leukemia 2014; 28: 1280–1288.

Yoshinari M, Imaizumi M, Sato A, Minegishi M, Fujii K, Suzuki H, et al. G-CSF induces apoptosis of a human acute promyelocytic leukemia cell line, UF-1: possible involvement of Stat3 activation and altered Bax expression. Tohoku J. Exp. Med. 1999; 189: 71–82.

Youngblood B, Hale JS, Ahmed R. T-cell memory differentiation: insights from transcriptional signatures and epigenetics. Immunology 2013; 139: 277–84.

Zah E, Lin M-Y, Silva-Benedict A, Jensen MC, Chen YY. T cells expressing CD19/CD20 bi-specific chimeric antigen receptors prevent antigen escape by malignant B cells HHS Public Access. Cancer Immunol Res 2016; 4: 498–508.

Zakrzewski JL, Suh D, Markley JC, Smith OM, King C, Goldberg GL, et al. Tumor immunotherapy across MHC barriers using allogeneic T-cell precursors. Nat. Biotechnol. 2008; 26: 453–461.

Zhang H, Ye Z, Yuan Z, Luo Z, Jin H, qian Q. New Strategies for the Treatment of Solid Tumors with CAR-T Cells. Int. J. Biol. Sci. 2016; 12: 718–729.

Zhang K-Z, Zhang Q-B, Zhang Q-B, Sun H-C, Ao J-Y, Chai Z-T, et al. Arsenic trioxide induces differentiation of CD133+ hepatocellular carcinoma cells and prolongs posthepatectomy survival by targeting GLI1 expression in a mouse model. J. Hematol. Oncol. 2014; 7: 28.

Zhang Q-Y, Mao J-H, Liu P, Huang Q-H, Lu J, Xie Y-Y, et al. A systems biology understanding of the synergistic effects of arsenic sulfide and Imatinib in BCR/ABL-associated leukemia. Proc. Natl. Acad. Sci. 2009; 106: 3378–3383.

Zhang S, Ma C, Pang H, Zeng F, Cheng L, Fang B, et al. Arsenic trioxide suppresses cell growth and migration via inhibition of miR-27a in breast cancer cells. Biochem. Biophys. Res. Commun. 2016; 469: 55–61.

Zhang W guang, Li C fei, Liu M, Chen X feng, Shuai K, Kong X, et al. Aquaporin 9 is down-regulated in hepatocellular carcinoma and its over-expression suppresses hepatoma cell invasion through inhibiting epithelial-to-mesenchymal transition. Cancer Lett. 2016; 378: 111–119.

Zhang XW, Yan XJ, Zhou ZR, Yang FF, Wu ZY, Sun HB, et al. Arsenic Trioxide Controls the Fate of the PML-RAR Oncoprotein by Directly Binding PML. Science (80-.). 2010; 328: 240–243.

Zhang Y, Wu S, Luo D, Zhou J, Li D. Addition of arsenic trioxide into induction regimens

could not accelerate recovery of abnormality of coagulation and fibrinolysis in patients with acute promyelocytic leukemia. PLoS One 2016; 11: e0147545.

Zheng P-Z, Wang K-K, Zhang Q-Y, Huang Q-H, Du Y-Z, Zhang Q-H, et al. Systems analysis of transcriptome and proteome in retinoic acid/arsenic trioxide-induced cell differentiation/apoptosis of promyelocytic leukemia. Proc. Natl. Acad. Sci. 2005; 102: 7653–7658.

Zhu J, Chen Z, Lallemand-Breitenbach V, de Thé H. Timeline: How acute promyelocytic leukaemia revived arsenic. Nat. Rev. Cancer 2002; 2: 705–714.

Zwaan CM, Reinhardt D, Hitzler J, Vyas P. Acute Leukemias in Children with Down Syndrome. Hematol. Oncol. Clin. North Am. 2010; 24: 19–34.

9. SUPPLEMENT

9.1 FACS gating strategies

9.1.1 Hoechst 33342 staining for detection of stem cell-like side population

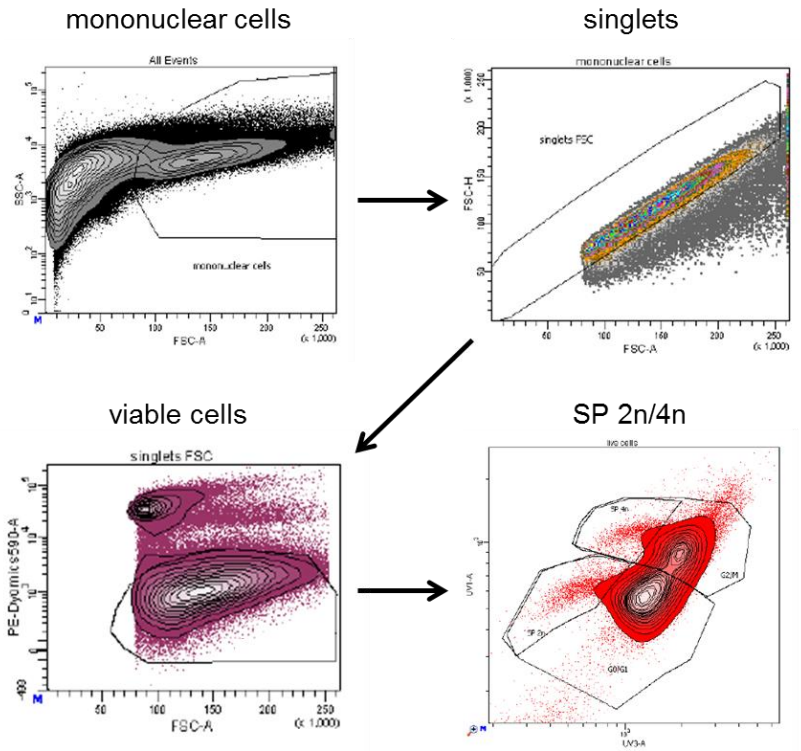

9.1.2 Viability assay – Annexin V staining

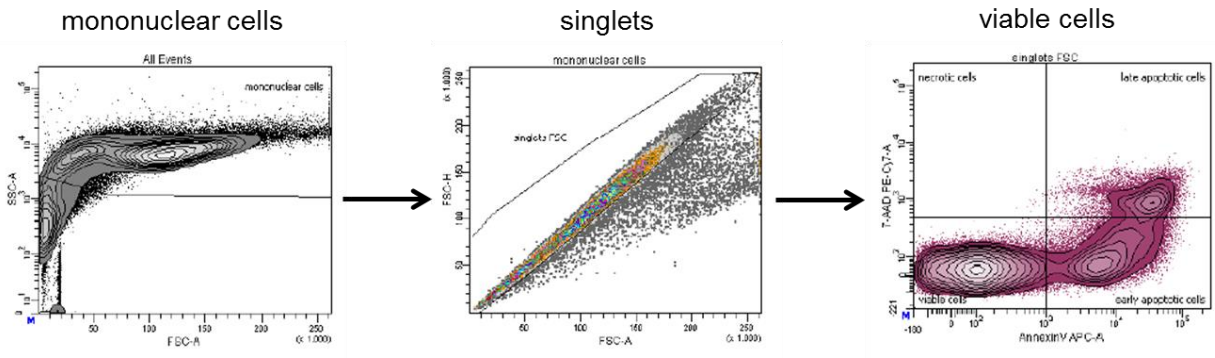

9.1.3 Detection of AQP9 expression level

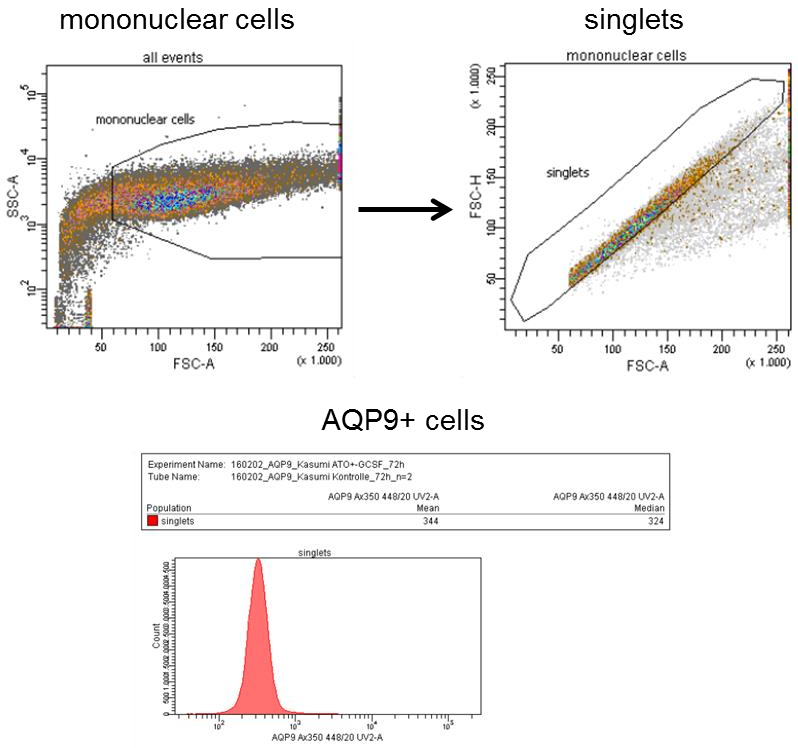

9.1.4 Detection of leukemia in ATO/G-CSF-treated transplanted mice

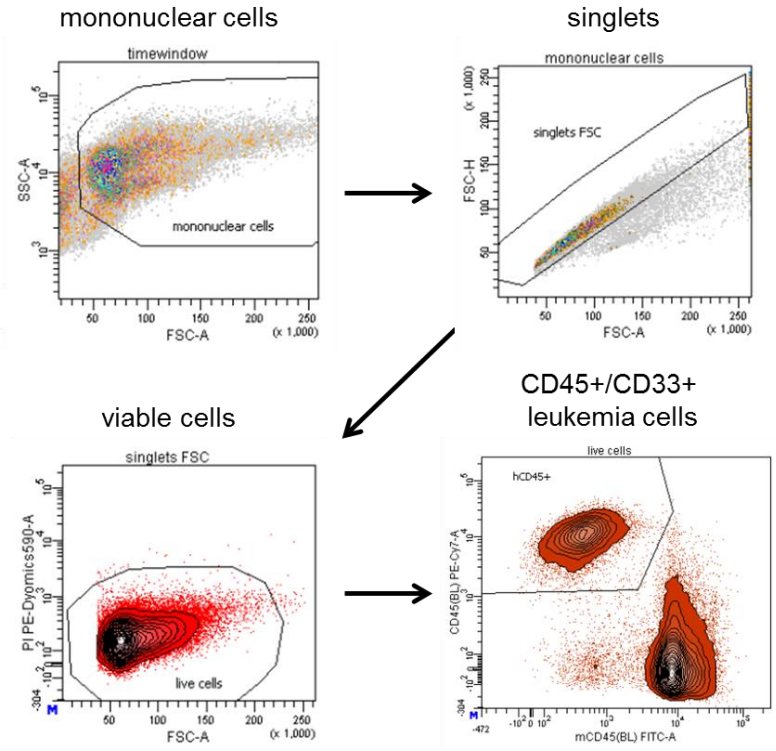

9.1.5 Detection of leukemia and CAR T cells in transplanted mice

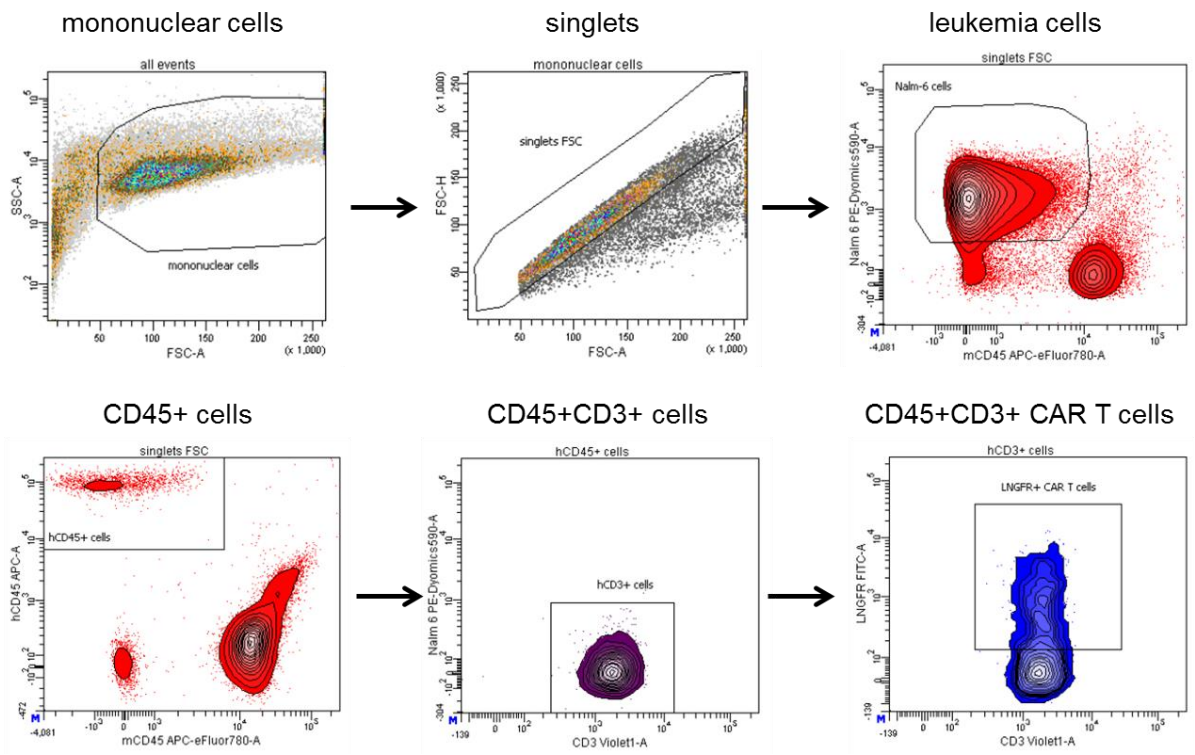

9.2 Abbreviations

7-AAD	7-aminoactinomycin
a-	anti
AAS	atomic absorption spectrometer
ABC	ATP binding cassette
ADCC	antibody-dependent cell-mediated cytotoxicity
AF	Alexa Fluor
ALL	acute lymphoblastic leukemia
AML	acute myeloid leukemia
APC	allophycocyanin
APL	acute promyelocytic leukemia
AQP	aqua(glycero)porin
Ara-C	cytosine arabinoside
ATO	Arsenic trioxide
ATRA	all-*trans* retinoic acid
B-ALL	B cell-ALL
BCP-ALL	B cell precursor-ALL
BCR/ABL	breakpoint cluster region/Abelson murine leukemia viral oncogene homolog 1
BM	bone marrow
BUV	brilliant ultra violet
CAR	chimeric antigen receptor
CASP3	caspase-3
CD	cluster of differentiation
CLL	chronic lymphoblastic leukemia
CML	chronic myeloid leukemia
CN	severe congenital neutropenia
CNS	central nervous system
CRS	cytokine release syndrome
CTLA-4	cytotoxic T lymphocyte-associated antigen 4
DMEM	Dulbecco’s Modified Eagle Medium
DNA	deoxyribonucleic acid
E:T	effector-to-target ratio
effluc	enhanced firefly luciferase
FAB	French-American-British
FACS	fluorescence-activated cell sorting
FCS	fetal bovine serum

FDA	Food and Drug Administration
FITC	fluorescein isothiocyanate
FLAG	fludarabine + high-dose Ara-C + G-CSF
FLT3	Fms-related typrosine kinase 3
Fc	fragment crystallizable
G-CSF	granulocyte-colony stimulating factor
G-CSFR	G-CSF receptor
GM-CSF	granulocyte-macrophage colony-stimulating factor
GO	Gemtuzumab Ozogamicin
GvHD	graft-versus-host disease
H&E	haematoxylin and eosin staining
HD	healthy donor
HRP	horseradish peroxidase
HSC	hematopoietic stem cell
HSCT	allogeneic hematopoietic stem cell transplantation
i.p.	intraperitoneally
i.v.	intravenously
IDH	isocitrate dehydrogenase
IFN	interferon
Ig	immunoglobulin
IL	interleukin
ITD	internal tandem duplication
JAK	Janus tyrosine kinase
LEF-1	enhancer-binding factor 1
LSC	leukemic stem cell
LT-HSC	long-term HSC
mAb	monoclonal antibody
MAPK	mitogen-activated protein kinase
MDS	myelodysplastic syndromes
MHC	major histocompatibility complex
MRD	minimal residual disease
NAD	nicotinamide adenine dinucleotide
NAM	nicotinamide
NAMPT	nicotinamide phosphoribosyltransferase
NK cells	natural killer cells
NMN	nicotinamide mononucleotide
NSG	NOD.Cg-Prkdc^{scid}IL2rg$^{tmWjl/SzJ}$

pAb	polyclonal antibody
PB	peripheral blood
PBMC	peripheral blood mononuclear cells
PBS	Phosphate buffered saline
PCR	polymerase-chain-reaction
PD-1	programmed cell death 1
PE	phycoerythrin
PI3K	phosphoinositide 3-kinase
PLK1	polo-like kinase 1
PML	promyelocytic leukemia
qRT-PCR	quantitative RT-PCR
RARα	retinoic acid receptor α
rhG-CSF	recombinant human G-CSF
RNA	ribonucleic acid
ROR-1	receptor tyrosine kinase-like orphan receptor 1
scFv	single-chain variable fragments
SD	standard deviation
SEM	standard error of the mean
SP	side population
STAT	signal transducer and activator of transcription protein
ST-HSC	short-term subset
T-ALL	T cell-ALL
TBP	TATA box binding protein
TCR	T cell receptor
TIL	tumor-infiltrating lymphocyte
TM	transmembrane
WHO	World Health Organization
Wnt	wingless-related integration site
$\Delta\Delta C_T$ method	comparative C_T method

9.3 Publications

Martyniszyn A, **Krahl AC**, André MC, Hombach AA, Abken H. *CD20-CD19 bispecific CAR T cells for the treatment of B cell malignancies*. Human gene therapy (2017) Dec 5.

Singer E, Walter C, Weber JJ, **Krahl AC**, Mau-Holzmann UA, Rischert N, Riess O, Clemensson LE, Nguyen HP. *Reduced cell size, chromosomal aberration and altered proliferation rates are characteristics and confounding factors in the STHdh cell model of Huntington disease*. Scientific reports (2017) Dec 4;7(1):16880.

Weber JJ, Golla M, Guaitoli G, Wanichawan P, Hayer SN, Hauser S, **Krahl AC**, Nagel M, Samer S, Aronica E, Carlson CR, Schöls L, Riess O, Gloeckner CJ, Nguyen HP, Hübener-Schmid J. *A combinatorial approach to identify calpain cleavage sites in the Machado-Joseph disease protein ataxin-3.* Brain (2017) May 1;140(5):1280-1299.

Pal M, Schwab L, Yermakova A, Mace EM, Claus R, **Krahl AC**, Woiterski J, Hartwig UF, Orange JS, Handgretinger R, André MC. *Tumor-priming converts NK cells to memory-like NK cells.* Oncoimmunology (2017) Apr 18;6(6):e1317411.

9.4 Declaration

The conception of this study and the interpretation of the results were made in cooperation with *PD Dr. Martin Ebinger*, senior physician of the University Children's Hospital Tübingen, Dr. Christian Seitz and Dr. Patrick Schlegel, University Children's Hospital Tübingen, and Prof. Dr. Dr. *Julia Skokowa*, head of the Department of Hematology, Oncology and Clinical Immunology, University Hospital Tübingen.

The experimental work in this study was performed by myself with the following exceptions:

As a part of her master thesis, *Kristina Ruhm* performed viability and cell cycles analyses for U-937 cells (FIGURE 10A+C) and qRT-PCR for Kasumi-1 cells (FIGURE 13) under my guidance.

Jonasz Jeremiasz Weber, Institute of Medical Genetics and Applied Genomics, University Hospital Tübingen, performed western blot analyses in collaboration with me.

Prof. Dr. Hinrich Abken and *Dr. Alexandra Martyniszyn*, Department I for Internal Medicine, University Hospital Cologne, produced the mono- and bispecific CAR T cells for targeting BCP-ALL P94H *in vivo* as well as performed the bone marrow sections from tibia.

Dr. Christian Seitz and *Dr. Patrick Schlegel*, University Children's Hospital Tübingen, cooperated in all *in vivo* experiments for the evaluation of the anti-biotin adapter CAR T cells.

Bioluminescence imaging was done in cooperation with *Prof. Dr. Bernd Pichler* and *Philipp Knopf*, Werner Siemens Imaging Center, Department of Preclinical Imaging and Radiopharmacy, Eberhard Karls University Tübingen.

Atomic absorption spectroscopy measurements were performed by *Dr.* Sibylle *Hildenbrand* and *Anna Glückman*, Institute of Occupational and Social Medicine and Health Services Research, University Hospital Tübingen.

Petra Lehnert collaborated in all mouse experiments under my guidance.

9.5 Danksagung

Mein Dank gilt *Herrn Prof. Dr. Rupert Handgretinger* für das interessante Promotionsthema, sowie für die Betreuung und Begutachtung meiner Doktorarbeit.

Bei *Herrn Prof. Dr. Hans-Georg Rammensee* möchte ich mich vielmals für die Begutachtung meiner Dissertation bedanken.

Ich möchte mich ganz herzlich bei *Herrn PD Dr. Martin Ebinger* für die Aufnahme in seine Arbeitsgruppe, sowie für die Möglichkeit zur Durchführung meiner Doktorarbeit bedanken. Insbesondere möchte ich mich für seine offene Art, herzliche Betreuung und stetige Unterstützung bedanken.

Besonders bedanken möchte ich mich bei *Frau Prof. Dr. Dr. Julia Skokowa* und *Herrn Prof. Dr. Karl Welte*, da sich mich stets unterstützt und in ihre Arbeitsgruppe aufgenommen haben. Vielen Dank für die umfangreiche und herzliche Betreuung, sowie für das Gefühl mich „eurer Laborfamilie“ zugehörig zu fühlen.

Ich möchte mich herzlichst bei *Herrn Dr. Christian Seitz* und *Herrn Dr. Patrick Schlegel* bedanken, die mich freundschaftlich in ihr „CAR-Team“ aufgenommen haben. Vielen Dank für die vielen lehrreichen, wenn auch zum Teil vergeblichen Stunden, im Tierstall. Es war mir eine Freude!

Ich möchte mich von ganzem Herzen bei *Frau Petra Lehnert* bedanken. Als gute Seele unseres Labors hat sie maßgeblich für den Erfolg dieser Arbeit beigetragen. Vielen lieben Dank Petra!!!

Ich danke *Frau Kristina Ruhm*, die ich als Masterstudentin betreuen durfte. Durch ihre tatkräftige Unterstützung konnte das Projekt erst vorangebracht werden.

Ich möchte mich bei allen Kooperationspartnern und Mithelfern bedanken, die alle maßgeblich an dieser Arbeit beteiligt waren.

Ich danke all meinen Laborkollegen aus der Kinderklinik *Darina Siegmund, Marina Schmidt, Karla Baltner, Stefan Grote, Katharina Reinhardt-Heller, Lisa Schwab, Franziska Wiese, Jennifer Rottenberger, Karin Cabanillas-Stanchi, Insa Hirschberger, Caroline Baden* und *Sarah Bühler* für eine schöne, ereignisreiche und lustige Zeit in der Kinderklinik.

Auch danke ich meinen Laborkollegen aus der AG Skokowa *Perihan Mir, Diana Amend, Malte Ritter, Sylwia Stefanczyk, Masoud Nasri, Viktoria Heinrich, Benjamin Dannenmann, Ursula Hermanutz-Klein, Karin Hähnel, Tatsuya Morishima, Regine Bernhard, Ingeborg Steiert* und *Maksim Klimiankou* für ihre tatkräftige Mithilfe und eine schöne Zeit in ihrer Arbeitsgruppe.

Mein besonderer Dank gilt meiner *Familie* und meinen *Freunden*, ohne die ich meine Promotion nicht hätte abschließen können. Vielen Dank Euch allen!

Zuallerletzt möchte ich mich von ganzem Herzen bei meinem Freund und meiner besseren Hälfte *Jonasz Weber* bedanken. Vielen Dank für Deine Mithilfe, Deinen täglichen Antrieb und Ansporn, Deine Geduld und vor allem für Deine Liebe! Ohne Deine Mithilfe wäre es mir nicht möglich gewesen, meine Doktorarbeit fertig zu stellen. Ich liebe Dich!